Spring 4-16-2010

Channel Characterization for Wireless Underground Sensor Networks

Agnelo R. Silva
University of Nebraska at Lincoln, agnelors@gmail.com

CHANNEL CHARACTERIZATION FOR WIRELESS UNDERGROUND SENSOR NETWORKS

by

Agnelo R. Silva

A THESIS

Presented to the Faculty of

The Graduate College at the University of Nebraska

In Partial Fulfillment of the Requirements

For the Degree of Master of Science

Major: Computer Science

Under the Supervision of Professor Mehmet Can Vuran

Lincoln, Nebraska

April, 2010

CHANNEL CHARACTERIZATION FOR WIRELESS UNDERGROUND SENSOR NETWORKS

Agnelo R. Silva, M.S.

Universidade of Nebraska, 2010

Adviser: Mehmet Can Vuran

Wireless Underground Sensor Networks (WUSNs) are natural extensions of the established Wireless Sensor Network (WSN) phenomenon and consist of sensors buried underground which communicate through soil. WUSNs have the potential to impact a wide variety of applications including precision agriculture, environmental monitoring, border patrol, and infrastructure monitoring. The main difference between WUSNs and traditional wireless networks is the communication medium. However, a comprehensive wireless underground channel model for WUSNs has not been developed so far. In this thesis, the Soil Subsurface Wireless Communication (SSWC) channel model is developed based on an extensive empirical study in a large agriculture field. The results of the experiments provide important insights for the model, which have not been available in the wireless communication literature. The SSWC channel model captures the signal attenuation and bit error rate (BER) in underground settings based on five components: (1) The dielectric soil model estimates the soil permittivity based on soil parameters including soil moisture. (2) The direct wave model captures the attenuation of the line-of-sight signal between sender and receiver. (3) The reflected wave model considers the attenuation on the signal which is reflected at the soil surface before reaching the receiver. (4) The lateral wave model estimates the attenuation of a third front of waves that potentially reach the receiver. Due to the fact that

a significant portion of the lateral waves' propagation occurs over-the-air, this form of transmission is an excellent option to extend the communication range without increasing the power consumption. (5) The signal superposition model captures the phase shifting between the mentioned waves, the resulting attenuation, and the bit error rate. The SSWC model is validated through extensive underground experiments. To the best of our knowledge, this is the first channel model for the underground to underground communication in WUSNs with comprehensive set of features. The SSWC channel model is fundamental for the development of cross-layer communication solutions for WUSNs and for the development of underground to aboveground and aboveground to underground channel models for WUSNs.

Acknowledgments

The author wishes to express his appreciation to his advisor, Dr. Mehmet C. Vuran, for his invaluable guidance, support, and encouragement during the course of this research. He also wishes to thank Dr. Lisong Xu and Dr. Byrav Ramamurthy, members of this thesis defense committee, for their advice and suggestions. The author likes to take this opportunity to express his deep gratitude to his wife Monica G. R. Silva and daughter Rebeca G. R. Silva for their continuous support and encouragement during all these years, from the undergraduate studies until to this moment on his academic career.

Table of Contents

List of Figures

Chapter 1

Introduction

Wireless Underground Sensor Networks (WUSNs) are natural extensions of the established Wireless Sensor Network (WSN) phenomenon and consist of sensors buried underground and communicate through soil. WUSNs have the potential to impact a wide variety of applications which are generally classified into four groups: environmental monitoring, infrastructure monitoring, location determination, and security monitoring [1]. The environment monitoring category include applications, such as precision agriculture and landslide monitoring. Infrastructure monitoring applications take care of the existing underground infrastructure, such as the detection of liquid leakage. Location determination applications include solutions to assist the transit of vehicles and people. Moreover, this category of applications include solutions to locate people trapped by a building collapse. Finally, security monitoring applications exploit the concealment of the buried sensors to efficiently detect the movement of people and objects in a protected area, such as the border of a country. Some of these applications are illustrated in Fig. 1.1.

The main difference between WUSNs and traditional wireless networks is the communication medium. In fact, the differences between the propagation of electromagnetic (EM) waves in soil and in air are so significant that communication entirely through soil has been considered not feasible for decades, especially for low-power devices. Nevertheless, the novel research presented in this work present feasible options to realize low-power underground communication. For instance, if a high density of sensor nodes is considered, the necessary communication range would be significantly reduced to distances of the order of meters or dozens of meters.

Due to the challenges for low-power underground communication, a comprehensive wireless underground channel model for WUSNs has not been developed yet. Consequently, the development of protocols for WUSNs is strongly impacted. To this end, a careful analysis of the literature in the wireless underground communication is realized in conjunction with hundreds of hours of very well controlled outdoor experiments [33, 35, 36, 37, 34]. The results of this empirical investigation, realized during a period of 18 months, are summarized in Chapter 3. The following aspects are found to have a strong influence on the communication quality: the soil texture and moisture, the operating frequency, the burial depth, the antenna design, and the irregularity of the soil surface. In other words, the empirical results reveal the strong spatio-temporal environmental dependency of the underground channel. This results in a unique communication phenomenon where both the information, from the viewpoint of many WUSN applications, and the communication media are correlated with the environment parameters. Therefore, an underground channel model for WUSNs must also capture these parameters, besides the operational and deployment aspects.

Accordingly, the second part of this work is related to the development of an underground channel model for WUSNs, called Soil Subsurface Wireless Communication (SSWC), which is presented in Chapter 5. The SSWC model captures the total signal attenuation and the bit error rate (BER) based on five components: the dielectric soil properties prediction model, the direct wave (DW), reflected wave (RW), and lateral wave (LW) factors, and the signal superposition model. The emphasis of the model is in the *propagation problem* and not in the *antenna problem*. In other works, the assumption is the use of a simple insulated dipole as the default antenna. The merit factors, such as the gain due to directivity of special antennas, are also captured in the SSWC model. However, for the sake of the complexity of the model, considering

Figure 1.1: Applications of Wireless Underground Wireless Sensor Networks (WUSNs).

the high number of possible antennas schemes, a deeper consideration of the antenna problem is not included in the model.

Although the in-situ experiments were realized without specific attention to the propagation of lateral waves, the overall empirical results have a good match with the SSWC model validating it for further experiments. The analytical results suggest a significant increase of the communication range, maintaining the same transmit power level, if lateral waves are properly addressed with the use of special antennas. These results have a strong impact on the design of WUSNs. Instead of node topologies with a strong dependency on aboveground devices, there exists a sound theoretical foundation to support multi-hop networking among buried nodes for distances higher than 10 meters. To the best of our knowledge, this is the first comprehensive channel model for the underground-to-underground communication in WUSNs. The SSWC channel model is fundamental for the development of cross-layer modules for WUSNs.

This work is organized as follows: In Chapter 2, the characteristics of WUSNs are presented. In Chapter 3, the development of an outdoor WUSN testbed is discussed. In Chapter 4, the methodology of the underground experiments and the empirical results are discussed. The components of the SSWC channel model for WUSNs are described in Chapter 5. Also, the analytical results are compared with the empirical results. The research challenges and guidelines for the development of cross-layer protocols fro WUSNs are presented in Chapter 6. Finally, the thesis is concluded in Chapter 7.

Chapter 2

Background & Related Work

In this chapter, the characteristics of WUSNs, the differences between WUSNs and Through-The-Earth communication techniques, an introductory discussion about soil properties, and related work are discussed. The characteristics of WUSNs are presented in Section 2.1. The impact of the dielectric properties of the soil on the wireless underground communication is discussed in Section 5.2. A historical overview of wireless communication using buried antennas is provided in Section 2.3. Finally, the related work of WUSNs is discussed in Section 2.4.

2.1 Characteristics of Wireless Underground Sensor Networks (WUSNs)

Wireless Underground Communication Networks (WUCNs) have been investigated in many context recently. Although a novel area, a detailed classification of these networks is necessary since several different scenarios, with distinct challenges and characteristics, are presented under the title *wireless underground communication*. In [1], two possible topologies for WUSNs are presented: the underground topology, where the majority of the nodes are buried, and the hybrid topology, where buried nodes coexist with some nodes deployed above ground. Based on this classification, an extended classification of WUCNs is suggested, as illustrated in Fig. 2.1.

As shown in Fig. 2.1, WUCNs can be mainly classified into two: wireless communication networks for mines and tunnels and wireless underground sensor networks (WUSNs). There exist several solutions that focus on underground communication in mines and/or tunnels [2, 11, 20, 24]. In this context, although the network is located *underground*, the communication takes place *through the air*, i.e., through the voids

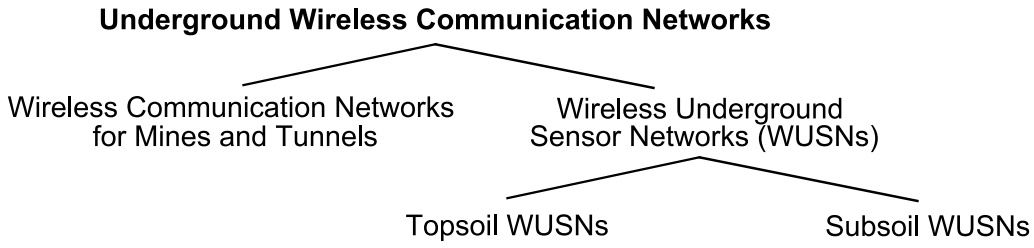

Figure 2.1: Classification of wireless underground communication networks (WUCNs).

that exist underground. Consequently, even though the communication in these voids are more challenging than that in terrestrial WSNs, the channel characteristics exhibit similarities with the terrestrial WSNs.

Although the sensors may be *buried* at different regions of the soil, WUSNs can also be classified into two categories based on the burial depth of the sensors. The recent research on agriculture, environment monitoring, and security mainly focuses on the *soil subsurface*, which is defined as the top few meters of the soil. The soil subsurface is classified into two regions [33]:

- *Topsoil region*, which refers to the first 30cm of soil, or the root growth layer, whichever is shallower.

- *Subsoil region*, which refers to the region below the topsoil, i.e., usually the 30-100cm region.

Accordingly, as shown in Fig. 2.1, *Soil Subsurface WUSNs* can be classified as a function of the deployment region: *Topsoil WUSN*, if the WUSN is deployed in the *topsoil region*, or *Subsoil WUSN*, if deployed in the *subsoil region*. Such classification is necessary because, as will be shown in the Chapters 3 and 5, a difference of 10 or 20cm in the depth of the sensor can cause significant impact on the communication

performance. The underground communication performances for topsoil and subsoil regions differ due to two main reasons:

- ***Soil parameters***. These soil regions may be distinct in terms of soil texture and moisture [16], which are important parameters that affect the wireless communication channel [1, 2, 33]. For instance, after a rainfall or artificial irrigation, the level of the soil moisture at the topsoil region quickly increases, affecting the communication. On the other hand, depending on the soil composition, the changing of the soil moisture at the subsoil region only occurs after hours [44].

- ***Soil surface effects***. When the node is closer to the soil surface, i.e. at the topsoil region, the contributions of reflected [1, 10, 33] and lateral waves [10, 21] are stronger. Therefore, the overall signal attenuation is usually smaller at the topsoil region than at the subsoil region.

Whenever possible, a shallower deployment (topsoil) is preferred due to the smaller length of the soil path and, thus, smaller signal attenuation. However, the WUSN application dictates the soil region where the sensors will be deployed. For instance, for intruder detection and sport field irrigation systems, a burial depth of less than 10cm is expected and better communication channel conditions are possible. On the other hand, the subsoil region is mandatory for many precision agriculture applications. In these systems, non-obstructive approaches are required due to the plowing and similar mechanical activities which occur at the topsoil region. Therefore, burial depths in the root range of crops in the subsoil region, i.e., 40-100cm, are required and more critical communication challenges are associated with these WUSN applications.

Although a WUSN is mainly formed by underground sensor nodes, the network still requires aboveground nodes for additional functionalities such as data retrieval,

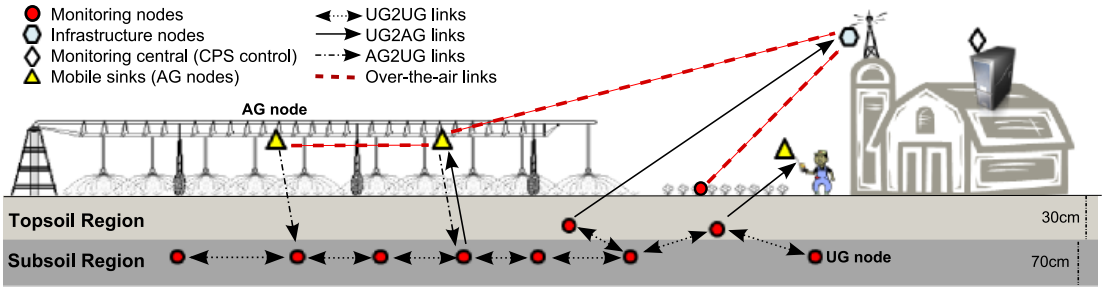

Figure 2.2: Typical WUSN architecture which employs 3 types of communication links: underground-to-underground (UG2UG), underground-to-aboveground (UG2AG), and aboveground-to-underground (AG2UG).

management, and relaying. Therefore, considering the locations of sender and receiver nodes, three different communication links may exist in WUSNs, as shown in Fig. 2.2:

- *Underground-to-underground (UG2UG) Link:* Both the sender and the receiver are buried underground and communicate through soil [33]. This type of communication is employed for multi-hop information delivery and is the main focus of this work.

- *Underground-to-aboveground (UG2AG) Link:* The sender is buried and the receiver is above the ground [35]. Monitoring data is transferred to aboveground relays or sinks through these links.

- *Aboveground-to-underground (AG2UG) Link:* Aboveground sender node sends messages to underground nodes [35]. This link is used for management information delivery to the underground sensors.

A WUSN which intensively uses aboveground nodes in conjunction with the underground nodes is called *Hybrid WUSN* [1]. Therefore, Hybrid WUSNs can potentially use all links: UG2UG, AG2UG, and UG2AG. The main focus of this work is the

Table 2.1: Typical aspects for Through-The-Earth (TTE) and WUSN scenarios.

Aspect	**TTE-based communication**	**WUSN**
Frequency range	VLF / LF	VHF / UHF
Maximum range (soil path)	Up to hundred meters	5cm to dozen meters
Bandwidth	Very small: bps	Small: Kbps
Network topology	One-hop	One-hop and multi-hop
Network density	Sender-receiver or few nodes	Hundred to thousand nodes
Underground channel noise	Very critical aspect	Small impact
Rock penetration	Feasible	Usually not feasible
Soil moisture	Small impact	Very critical aspect
Energy criticality	Relatively small impact	Very critical aspect
Node cost	Relatively high	Small
Communication protocol design	Emphasis on the physical layer	Cross-layer approach

characterization of the UG2UG channel for WUSNs and the provided SSWC channel model can potentially be used as the foundation for the remaining UG2AG and AG2UG channel models which are out of the scope of this thesis.

One kind of underground communication method not represented in Fig. 2.1 is Through-The-Earth (TTE) which provides a way to realize emergency communication to trapped miners in case of disasters [4]. Therefore, TTE is not usually associated with a network and cannot be classified as a kind of WUCN. Although there are similarities between WUSN and TTE solutions, the underground communication challenges for WUSNs and TTE scenarios are significantly different, as shown in Tabel 2.1. For instance, while WUSN nodes are usually deployed at the subsurface region of the soil, a TTE underground device is usually located hundred of meters below the soil surface. The TTE communication had been used for three main applications: miner locating systems (mining disasters), geophysical exploration, and military underground communication (during the nuclear age). Nowadays, the use of TTE systems is mainly related to the former application.

In Table 2.1, a comparison between the typical aspects related to both TTE and WUSNs scenarios is shown. One can observe that the challenges of the TTE-based systems are mainly related to the physical layer, especially techniques to traverse rocks and achieve a longer communication range. On the other hand, WUSNs have lighter soil and communication range constraints. Nevertheless, the underground communication channel is WUSNs is significantly affected by soil moisture changes at the subsoil region [2, 33, 35]. Also, low-power devices are required in WUSNs in order to extend the lifetime of the buried nodes for months or years. Therefore, the design of a WUSN solution requires a non-trivial cross-layer approach [2].

2.2 Dielectric Properties of the Soil

The soil is a *dielectric material*, characterized by a specific *relative permittivity* or dielectric constant. The propagation of electromagnetic (EM) waves is directly affected by the permittivity of the material. More specifically, a smaller value for the relative permittivity basically implies better conditions for the propagation of EM waves. The soil medium behaves as a dielectric mixed material composed of air, *bound* water, *free* water, and bulk soil. If the soil presents small density and high porosity, the conditions for the propagation of EM waves are better due to the high quantity of air in the medium. However, the presence of water in soil has an adverse effect on the communication. The quantity of water in the soil, e.g., the volumetric water content (VWC), is the main attenuation factor for the propagation of EM waves in soil [1, 2, 33, 35].

The soil permittivity varies, besides other factors, as a function of the soil components [28]. The soil texture is generally classified in terms of fractions of sand, clay, and silt particles, as shown in Fig. 2.3. Depending on the amount of clay, silt, and

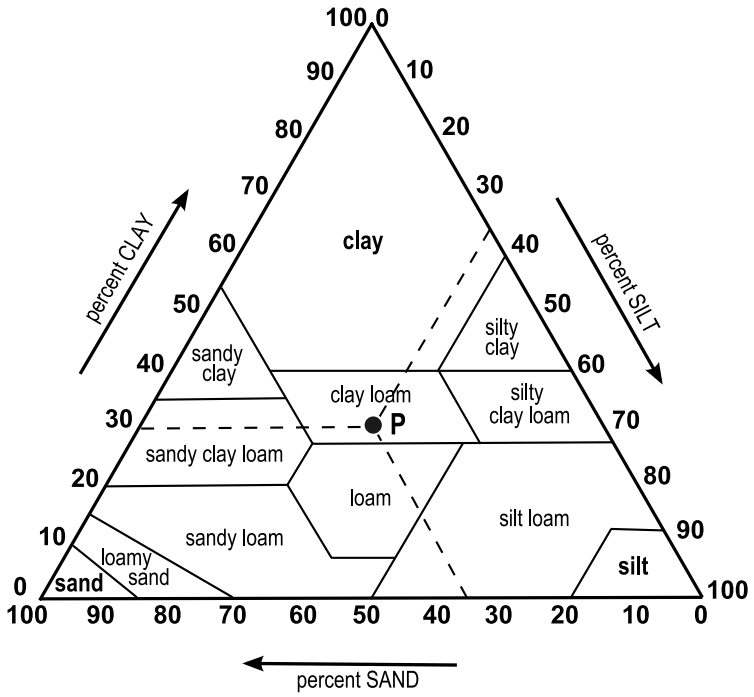

Figure 2.3: Soil texture triangle showing the United States Department of Agriculture (USDA) classification system based on grain size (clay: <0.002mm, silt: 0.002-0.050mm, sand: 0.050-2.0mm).

sand, the soil texture receives a particular name or classification [16]. For instance, the point P in Fig. 2.3 represents a soil texture with a homogeneous mixture of clay, silt, and sand, and it is classified as *clay loam*.

Besides clay, silt, and sand, the soil also contains water. The VWC of the soil represents the fraction of water in the soil. However, the water can be classified into two: the *bound water*, which corresponds to water molecules tightly held to the surface of the soil particles, and the *free water*, which corresponds to water molecules *free* of action of soil particles [6, 13]. Therefore, for the same VWC value, a soil sample can contain more free water than other sample due to differences on the soil texture of the samples. More specifically, the quantity and also the type of clay determine the amount of bounded water in the soil [6, 16]. As will be explained later in Section

5.2, the dielectric properties of the bounded water are different from the free water. Therefore, the attenuation of the EM waves and also the change in the signal velocity (phase shift) vary as a function of the amount of bounded water and the amount of free water. In this way, it is clear that the VWC parameter alone is not sufficient to characterize the attenuation of EM waves propagating in soil. More specifically, the parameters related to the soil texture are also necessary to complement the VWC information to characterize the dielectric properties of the soil and the associated signal attenuation.

Besides the VWC, the frequency of the signal also affects the relative permittivity and, thus, the level of attenuation of EM waves. The soil permittivity is a non-linear function of the frequency [6, 13]. Moreover, depending on the frequency of the waves, the soil *conductivity* dominates the attenuation function. Therefore, contrary to the general belief, a smaller frequency is not always related to a smaller signal attenuation. In other words, even when all soil parameters are known, including the VWC, there is no direct way to precisely calculate the value of the soil permittivity for different frequencies [6, 28]. Consequently, without the value for the soil permittivity, further estimation of the signal attenuation is not possible.

Therefore, many studies were performed, for different frequency ranges, in order to provide a practical way to estimate the value of the soil permittivity for a specific range of frequencies. It is reported that frequency values around 1GHz present reasonable soil permittivity values for practical use of wireless communication and microwave remote sensing applications [2, 18, 28]. Frequency values smaller than 300MHz can result in even smaller attenuation values for the EM signal. However, when the frequency decreases, its wavelength increases and the size of antenna also increases. Hence, usually the use of frequency values smaller than 300MHz for WUSN scenarios is not practical. This latter aspect must be highlighted because the majority of the

theoretical and experimental work for wireless underground communication is related to military applications and long range communication, i.e. higher than 10Km. In these scenarios, the HF to LF frequency bands are typically employed associated with very huge antennas and power consumption. One of the goals of this work is to show that the UHF band (300MHz-3GHz), and more specifically from 300MHz to 1GHz is the optimal frequency band for WUSNs in terms of soil attenuation and practical sizes of antennas [33].

2.3 Buried Antennas

The first studies related to radio frequency (RF) underground waves propagation began in 1909, with the work of Sommerfeld analyzing the problem of vertical electric Hertzian dipole radiation in the presence of a dissipative half-space [38]. In 1926, Sommerfeld published a work considering all four types of elementary dipole: electric or magnetic, vertical or horizontal [39]. In these studies, the dipoles sources are in air, although just above the soil surface [42]. However, the radiation of a Hertzian dipole *immersed in the conducting medium*, such as the soil, is first investigated by Tai, in 1947 [41]. From that moment, many other researchers studied the same topic. The classic work of Banos (1966) [5] is of special interest because it includes a complete characterization of the electromagnetic field components for points in the dissipative medium or above it, e.g., points at the air or inside the water. The Banos' approximate formulas are only valid for conducting medium, such as the sea water, and low frequencies. Also, the antenna problem is not included in these works which considered only elementary source dipoles.

In order to effectively characterize the wireless underground communication, two problems must be solved: the propagation problem, as previously mentioned, and the

antenna problem. More recently, King (1980) [21] addressed the antenna problem for lossy medium, including soil, by analytical, numerical, and empirical means. For underground communication purposes, only an insulated antenna can be considered [21, 42]. However, due to the complexity of the task, only some important classes of embedded insulated antennas are considered in [21]: dipole, loop, and terminated monopole (travelling wave antenna). For all cases, the subsurface is the soil region of choice. However, for very-high power solutions, deeper installations are also feasible. This former work constitutes the foundation for the lateral wave (LW) factor model developed in Chapter 5. The mathematical and physical justifications for the existence of lateral waves and their use for radio communication is provided in [10].

Buried/immersed antennas and lateral waves propagation were mainly studied on the 1940-80's period due to two main application scenarios: a) communication with submarines and b) protection of the communication system of a country in case of a nuclear attack. Probably, the lack of potential applications explains very few research work in the area of wireless underground communication during the last decades. In this work, the continuation of these original studies are realized by extending and adapting them to the WUSN scenario which involves low-power devices and relatively small communication ranges (due to the high density of nodes).

2.4 Related Work

In this section, some recent developments related to wireless communication for the underground environment are presented. The first part of the related work is not actually examples of work in the area of WUSN. However, the discussion of these studies provides an overall vision about the challenges in the underground settings and

also present potential application scenarios for WUSNs. The second part of the work presented in this section is the *state-of-the-art* in the area of WUSNs.

Wireless sensor networks have been used to monitor underground mines to guarantee the safety of mine workers [12, 20]. Similarly, the characteristics of the wireless channel in tunnels have been investigated [2]. As mentioned in Section 2.1, although the mine is underground, the communication among the sensors is through the air in the mine or tunnel.

A shallow depth WSN was used for predicting landslides [32]. This network consists of Mica2 motes [54] which are interfaced with stain gauges and can operate at low depths (25-30cms). In this design, although the sensors are located underground, the communication takes place over the air. Another similar example is a sensor network that is constructed to detect the volcano activities. In this case, the antenna of the sensors is placed above the soil surface to create reliable links [51].

Structural health monitoring (SHM) is another application that has gained interest in wireless sensor networks community. Two examples of such WSN application is Wisden, a data acquisition system for SHM [26, 52] and Duranode [27]. Although underground systems such as sewers also require structural monitoring, these approaches only work with communication through air techniques.

The largest residential water management project in Europe uses sensors to gather information for inspection and cleaning systems in the Emscher sewer system [15]. Similarly, a sensor network is used in other sewer system where the manhole cover is converted into the slot antenna and the *underground* sensors can communicate with the above ground nodes through radiation from it [24]. Again, although the system resides *underground*, the communication between the sensors is performed *through air*. These cases exemplify how the expression *underground network* has been over-utilized and may not be associated with wireless underground communication channel.

A glacier monitoring network, based on a sensor network, was deployed in Norway [23]. This system aims to measure the parameters of ice caps and glaciers using sensors beneath the glaciers. To avoid wet ice, the base stations are connected to two wired transceivers 30m below the surface. Using relatively high transmit power levels (100mW), these under*ice* sensors can finally communicate with the sensors that are placed at deeper locations (up to 80m from the surface). This application is not a typical underground scenario, however it presents challenges similar to the ones for WUSNs.

In addition to these applications, several experimental work focusing on the EM wave propagation through soil and rock are also reported. As part of the recent studies regarding wireless communication through soil, the electromagnetic field of a vertical electric dipole in a conducting half-space is analyzed for the 1-10MHz frequency range [49]. Moreover, experiments using ground-penetrating radars were performed [14, 25, 49, 50]. This specific research area is called *Microwave Remote Sensing* [6, 13] and part of the theoretical model presented in Section 5.2 is based on the results from this research area [28].

As an example of the use of the principles of the surface-penetrating radar, a 100MHz experiment is realized for determining the attenuation and relative permittivity values of various materials, including soil, in [14]. A typical Microwave Remote Sensing application is the detection of landmines based on differences between the permittivity values for soil and landmine. For instance, it is shown that the soil composition has significant effects on the Ground Penetrating Radar (GPR) detection of landmines [25]. Similarly, the investigation of EM propagation in soil in the presence of landmines is reported in [50]. Accordingly, experiments for the 1-2GHz band are realized and a propagation model for landmine detection is provided.

Related to the use of lateral waves for underground communication, a comprehensive study is presented in [10, 21]. Additionally, empirical results of lateral waves communication are reported in [19, 21, 48]. In the latter two works, a special antenna, called eccentrically insulated travelling-wave (EITW) antenna, is adopted for the buried node. A signal generator operating at 144MHz and +30dBm transmit power level is used for a typical UG2AG experiment. The underground node is buried at 40cm and the aboveground receiving antenna is placed 55cm above the soil surface. Communication ranges of more than 50m are achieved, validating the model presented in these works, which are essentially the same reported in [21].

Although significant insight in EM wave propagation through soil can be gathered from these works, none of the existing work provides a complete characterization of the underground communication, especially for the communication between low-power underground devices located at the soil subsurface, the typical WUSN scenario. On the other hand, the following related work are WUSN studies or more closely WUSN-related scenarios.

An overview of the challenges related to the WUSNs was provided in [1]. The challenges for realizing outdoor WUSN experiments are discussed and guidelines are provided in [37]. A theoretical model specifically for wireless UG2UG communication is proposed in [2], but without empirical results to validate the model. UG2UG experiments using Mica2 [54] motes at 433MHz are reported in [33] and the results show a good agreement with the model proposed in [2], especially for high burial depths. These results are also presented in Chapter 3. The mismatches between the model and empirical results for low burial depths suggests the existence of a missing factor not considered in the model provided in [2]. This fact motivates further theoretical investigation which culminates in the SSWC model presented in Chapter 5.

Terrestrial commodity sensors MicaZ [54] motes, operating at 2.4GHz and 0dBm of transmit power level, are tested for UG2AG and the empirical results are reported in [40]. Both received signal strength (RSS) and packet error rate (PER) are evaluated in a typical sender-receiver scenario. Two sets of tests are realized: one considering that the receiver node is located at the soil surface and the other one with the receiver elevated 1m above the soil surface. For these experiments, three burial depths for the sender node are used: 0, 6, and 13 cm. The 0-cm burial depth case is used to establish a baseline for comparisons. The maximum horizontal inter-node distances achieved, with PER <10%, are 2.5 and 7m for 13 and 6cm-burial depths, respectively. These results exemplify the criticality of the soil path attenuation. In the same empirical work, UG2UG experiments are realized. However, such communication link is reported as not feasible for that specific testbed scenario.

A unidirectional UG2AG communication model is proposed in [9]. The model predicts the signal attenuation due to the dielectric loss of the soil and the effects of reflection of the soil surface. Moreover, laboratory experiments are realized to validate the model. The received signal strength is evaluated with a spectrum analyzer. The sensor node used in the experiments is a customized device called *SoilNet* which operates at 2.44GHz and +19dBm of transmit power level. The burial depth of the SoilNet device typically varies from 5 to 9cm. The experimental results with a soil probe shows a signal attenuation increase of 25dB when the width of the soil layer varies from 1 to 7cm. Moreover, a variation of 10dB in the signal attenuation is associated with the VWC increase from 0 to 35%. Finally, the empirical results show that the bulk density and bulk electrical conductivity cause small impacts on the signal attenuation, at least for the investigated pure sand/water mixture. These results agree with the experimental and analytical results shown in Chapters 3 and 5. The UG2AG model

proposed in [9] assumes that the receiving antenna is located very far from the buried node.

Another unidirectional UG2AG communication model is proposed in [46] to support the use of a customized sensor node called *Soil Scout* which operates at 869MHz and +10dBm of transmit power level. To this end, an ultra wideband elliptical antenna [29] is proposed for the underground communication [45]. This antenna is used for the experiments to validate the model which predicts the signal attenuation due to a) the dielectric loss of the soil, b) the effects of reflection of the soil surface, and c) the effects of the refraction of some EM waves at the soil surface (angular defocusing). The results show an adequate radiation efficiency (>90%) of this wideband antenna in different soil textures and moisture levels. Communication ranges of 30 and 150m are reported for the burial depths of 40cm and 25cm, respectively. However, only long-range (>20m), one-hop, UG2AG communication links are considered.

UG2AG and AG2UG experiments using customized sensor nodes are reported in [31]. A maximum communication range of more than 60m is achieved for the nodes operating at 868MHz, +10dBm of transmit power level and burial depths smaller than 10cm. In [35], UG2AG and AG2UG experiments using Mica2 motes operating at 433MHz and +10dBm of transmit power level are realized. Due to the adoption of a novel antenna scheme involving an ultrawide band antenna [29], significant extension of the communication range is achieved. The ranges of 22 and 37m are reported for 35cm and 15cm-burial depths, respectively. In [36], another set of UG2AG and AG2UG experiments using Mica2 motes are realized in a real precision irrigation scenario.

Despite the potential applications of the existing work, a comprehensive characterization of the UG2UG communication channel for different depths at the soil subsurface region has not been provided. In fact, theoretical and empirical examination of UG2UG links are only reported in [2] and [33], respectively. Accordingly, in this thesis,

the characteristics of the UG2UG communication channel for WUSNs located at the soil subsurface region are investigated.

Chapter 3

Development of a WUSN Testbed

Despite the potential of WUSNs, very few field experiments have been realized by the end of 2009, causing delays on the proliferation of WUSN applications. Moreover, recent models for the wireless underground communication channel are also proposed but few field experiments are realized to verify the accuracy of the models [2, 9, 46]. One possible explanation for the lack of a significant number of field experiments for WUSNs is that such experiments proved to be extremely complex and present novel challenges compared to the traditional wireless environment. Moreover, constant changes in the outdoor environment, such as the soil moisture, can contribute to the problems related to the repeatability and comparisons between WUSN experiments.

In this chapter, the details related to the development of an outdoor WUSN testbed are presented in order to improve the accuracy and to reduce the time for WUSN experiments [37]. More specifically, the development of two real WUSN testbeds are described. The first part of the experiments were realized in University of Nebraska-Lincoln City Campus on a field provided by the UNL Landscaping Services during August-November 2008 period. The second part of the experiments were realized in UNL South Central Agricultural Laboratory, Clay Center, NE, during July-October 2009 period. Moreover, the experiments in [33, 35, 36] followed the guidelines described in this work. Based on the experiences acquired from hundreds of hours of WUSN experiments in these testbeds, the details related to the development of an outdoor WUSN testbed are presented [37]. This is the first work that proposes guidelines for the development of a WUSN testbed to improve the accuracy and to reduce the time for WUSN experiments. The recommended practices in this chapter range from radio frequency (RF) measurements using sensor nodes to the use of practical techniques that

significantly reduce the time to install and remove the sensor nodes in the underground setting. The main objective of this work is the proliferation of best practices in the area of WUSNs related to the following goals:

- The time reduction for the realization of WUSN experiments through the use of a WUSN testbed.
- The improvement of the accuracy of the experiments.
- An easier and standardized way to compare results from experiments realized in different WUSN testbeds.
- The establishment of a standard methodology for WUSN measurements.

The rest of this chapter is organized as follows: In Section 3.1, an overview of a WUSN testbed and its physical layout is presented. In Section 3.2, diverse aspects to be controlled in a WUSN experiment, such as the digging process, the soil composition, the soil moisture, the antenna orientation, and the transitional region are discussed. In Section 3.3, detailed guidelines to preserve the quality and accuracy of the experiments, even when sensor nodes are used as RF measurement tools, are presented. The overall architecture of a WUSN testbed and the aspects of its software are provided in Section 3.4.

3.1 WUSN Testbed Architecture

Three different communication links exist in WUSNs based on the locations of the sender and receiver nodes, as shown in Section 2.1 and also illustrated in Fig. 3.1. Accordingly, a WUSN testbed must support experiments in these three communication scenarios. In this section, the testbed architecture for UG2UG experiments is presented

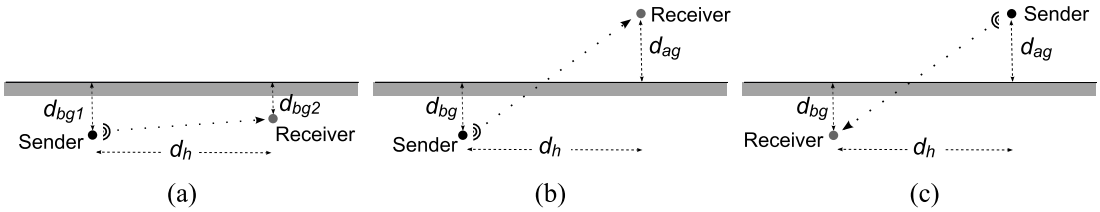

Figure 3.1: The three communication scenarios supported by the WUSN testbed: (a) UG2UG link, (b) UG2AG link, and (c) AG2UG link.

first, followed by guidelines to extend the testbed to support aboveground nodes, i.e., to realize UG2AG and AG2UG experiments.

UG2UG Testbed. A practical WUSN testbed must allow an easy configuration of the physical deployment aspects. As shown in Fig. 3.1, these deployment parameters reflect the location of the sensor nodes. The parameter d_{bg}, also called *burial depth*, is defined as the distance between the center of the antenna of the buried sensor node and the surface of the soil. The distance above the ground d_{ag}, used in the UG2AG and AG2UG scenarios, is the distance between the center of the antenna of the aboveground device and the surface of soil. Finally, the parameter d_h is the horizontal inter-node distance between the sender and the receiver nodes. Therefore, from the communication perspective, the antenna is the element of interest. In fact, the actual locations of the sensor, processor, and transceiver modules are not considered in defining the physical distances of a WUSN testbed experiment, only the antenna. However, preliminary tests show that metallic objects nearby the antenna of a node can significantly impact the results of WUSN experiments. Therefore, the actual position of a node's module, such as a soil moisture sensor, may change the results and this scenario must be avoided or informed in the report of the experiment.

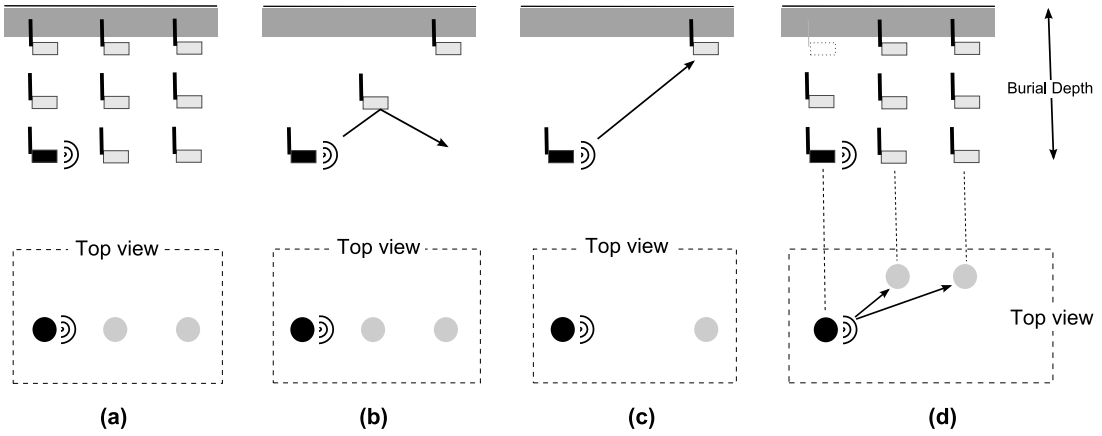

Figure 3.2: (a) The grid concept used to speed up the experiments in a WUSN testbed. (b) A case, where the grid can interfere with the results. (c) Ideal case for experiments and (d) an alternate grid solution.

In Fig. 3.2, the grid concept applied in a WUSN testbed, designed for UG2UG experiments, is illustrated. The *grid* concept is very important in wireless communication testbeds. The basic idea is to perform multiple simultaneous point-to-point (sender-receiver) tests, speeding up the overall time spent in an experiment. As shown in Fig. 3.2(a), one of the sensors temporarily has the role of sender and it broadcasts a sequence of test messages. Only one node can be selected as a sender for each experiment. Therefore, the remaining nodes in Fig. 3.2(a) are potential receivers. After the end of the test, it is possible to verify the results of the experiments consulting each receiver individually.

However, the scheme in Fig. 3.2(a) results in high interference since a node may be on the direct path between two other nodes as shown in Fig. 3.2(b). An alternate solution is to perform experiments individually as shown in Fig. 3.2(c), which eliminates any obstacles between sensor nodes. Therefore, it is clear that the original grid idea must be modified in underground settings to maintain the accuracy of WUSN experiments and also to provide the flexibility of having multiple simultaneous tests. A

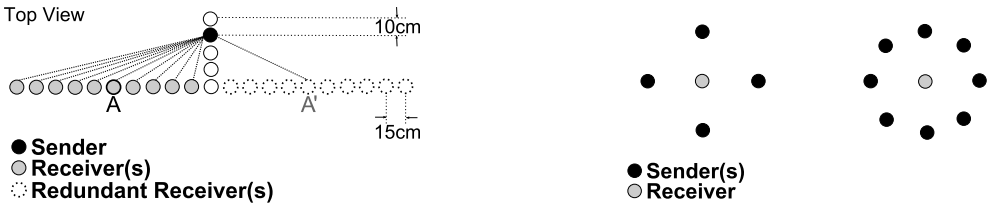

(a) (b)

Figure 3.3: WUSN testbed layouts for UG2UG communication: (a) The layout used to investigate the effects of the inter-node distance and (b) the layout used for transmission contention tests: 4 and 8-sender cases.

simple solution is shown in Fig. 3.2(d). This new scheme proposes a direct line-of-sight (without obstacles) between the hole where the sender is located and the holes where the receivers are located. The difference is more clear when the top views of Figs.3.2(a) and Fig. 3.2(d) are compared. With this new design, the grid imposes two constraints in the WUSN testbed:

- *A hole is designated only for the senders:* The hole, which is used to place the sender node(s), i.e., the sender hole, must have direct line-of-sight with all other holes. In other words, no other hole or obstacle can exist between the sender holes and the other holes. It is possible to have multiple senders in the same sender hole. However, only one sender can be active at a given moment.

- *At the senders hole, no receivers are allowed:* If receivers are placed at the same hole as the sender, one of them can be a potential communication obstacle to the other. For instance, if the nodes Sender A, Receiver 1, and Receiver 2 are buried, in this order, in the same hole, the Receiver 1 will be an obstacle for the propagation of waves from the Sender to the Receiver 2.

Based on the dimensions of the sensor nodes and the communication constraints empirically verified in [33], the physical layout for basic WUSN testbeds are illustrated

in Figs. 3.3. The layouts are presented in a top view, where each circle is a hole. The presented layouts consider the use of 10cm-diameter holes and commodity WSN sensor nodes with a maximum transmit power of +10dBm. Naturally, the distances can be modified if larger and more powerful sensor nodes are used. The first layout in Fig. 3.3(a) is used for inter-node distance experiments. The 5 holes in the center are used by sender nodes and only one of these holes can contain an active sender for an experiment. The horizontal holes in Fig. 3.3(a), with the exception of the central one, are assigned for receiver nodes. Multiple receivers holes can be active in an experiment. The holes at the right side of the central node are used for redundant receivers. As shown in Fig. 3.3(a), the same inter-node distance is used for the receivers A and A', where the latter is used for redundancy in experiments. After the end of the experiment, the results of the receiver A are expected to be very close to the measurements from the sensor A', assuming they have the same burial depth. As shown in Fig. 3.3(a), this first architecture provides:

- Direct line-of-sight between sender and receiver without any artificial obstacle.
- Simultaneous experiments for different inter-node distances and, optionally, different burial depths.
- High accuracy in the results through the redundancy in the measurements.

The use of multiple nodes in the same hole, as suggested in Fig. 3.2(d), deserves special attention. In this case, the testbed would be actually based on a 3D-grid which is a natural option to speed up the experiments. However, the placement of a sensor nearby the antenna of another underground node can interfere with the experiment results. Preliminary tests are necessary to verify if this interference will potentially occur before deciding for the use of a 3D-grid in the underground setting. In the experiments in [33], the use of multiple nodes at the same hole were not possible due to

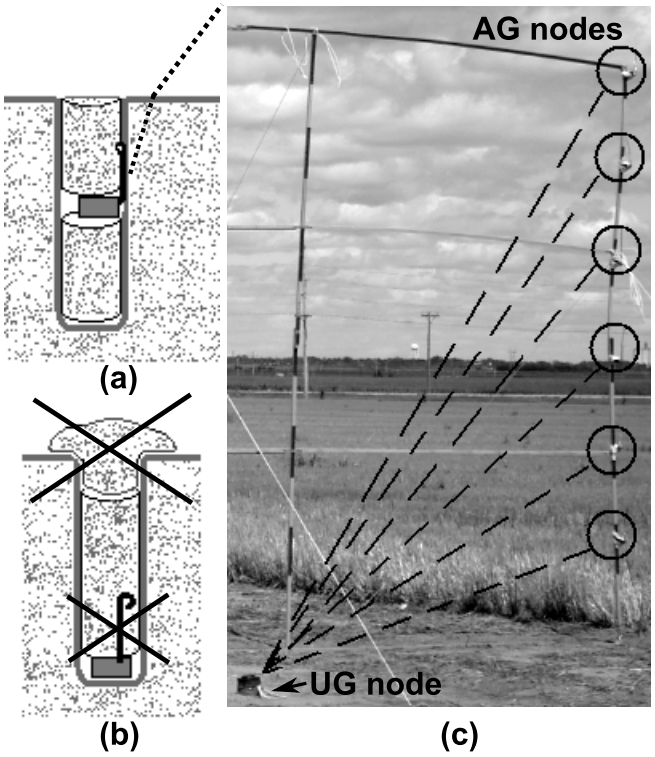

Figure 3.4: UG2AG and AG2UG experiments. (a) The antenna must be positioned in the direction of the aboveground device and without any line-of-sight obstacle. (b) Some aspects allowed for UG2UG experiments are not allowed for aboveground experiments. (c) Grid of aboveground nodes.

the interference issues. Therefore, in that case, every hole in the layout contains only one sensor and the underground part of the testbed was constrained to a 2D-grid.

It is possible to extend the testbed in Fig. 3.3(a) to support multiple senders at different holes. However, the complexity of this new layout can be pretty high and the implementation of a unique and general purpose testbed can be very difficult. One alternate solution is to create additional testbeds for this kind of experiments. One example of application of this new testbed is the transmission contention experiments. In Fig. 3.3(b), the layouts of the 4-sender and 8-sender cases are shown.

UG2AG/AG2UG Testbed. UG2AG and AG2UG links are required for several functionalities of WUSNs, such as network management and data retrieval. Therefore,

the WUSN testbed must also provide support for UG2AG and AG2UG experiments. As shown in Fig. 3.3(a), the UG2UG testbed has 5 special holes for sender nodes and 20 holes for receivers. Extending the WUSN to aboveground experiments implies that the sender (or the receivers) will be located above the soil surface. Accordingly, the grid scheme can be adapted to this new scenario. The following guidelines are provided for extending the WUSN testbed for aboveground experiments:

- The surface of the paper pipe must be aligned with the soil surface, as shown in Fig. 3.4(a).
- The propagation of the antenna cannot be disturbed by the paper pipes filled with soil, as shown in Fig. 3.4(b). The mentioned paper pipes can be used, but the antenna must be positioned in a way that it points to the direction of the aboveground device(s), as shown in Fig. 3.4(a).
- The hole must have a direct line-of-sight (without obstacles) to the aboveground device(s), as shown in Fig. 3.4(c).
- The aboveground nodes devices can be easily installed using a 10cm-length buried 3/4" PVC pipe in conjunction with a wood stake. It also possible to build a grid of aboveground devices, as shown in Fig. 3.4(c).

All the devices and schemes presented in this section speed up the realization of the experiments in [33, 35, 36]. Without these schemes, the same experiments would last more than 3 times longer. At the same time, the accuracy of these experiments is not compromised.

3.2 Factors That Impact Outdoor WUSN Testbeds

In this section, the factors that impact the realization of WUSN experiments are presented. The challenges of burying and unburying sensor nodes are presented and the use of paper and plastic pipes are described. Also, the analysis of the soil texture and soil moisture of the WUSN testbed is included as an essential part of the results of the experiments in the presented guidelines. The errors caused by the antenna orientation and the use of sensor nodes to make RF measurements are also discussed. Finally, the issues related to the transitional region of WUSNs are presented.

3.2.1 The Digging Process

Burying and unburying sensor nodes are very time-consuming tasks in underground settings. For instance, in the experimental testbed developed in [33], almost 2 hours were necessary to dig a single 20cm-diameter, 1m-depth hole, even with the use of an electric power auger. Therefore, an initial consideration about the dimensions of the holes is necessary. Besides the time issue, the larger a hole is, the larger is the modification of the soil density at that area and this parameter affects the signal attenuation caused by the soil [28, 33]. A second aspect is related to the depth of the hole. The majority of the WUSN applications will not require burial depths higher than 1m [1, 2, 33]. Therefore, the WUSN testbed considered in this section assumes a burial depth smaller than 1m, that is, at the subsurface region of soil. The process of digging deeper holes is only feasible with special machines. On the other hand, for shallow holes, there are many simple and manual digging tools available in the market considering that the diameter of the hole is restricted to up 4cm. In the case of our testbed, the required minimum diameter is 7.5cm due to the dimensions of the sensor node. Therefore, 8cm-diameter holes were dug with power augers. The difficulty to bury a sensor node also highlights an important aspect for the success of WUSN

applications: the deployment of hundreds or thousands of these devices needs to be relatively simple. In this sense, sensor nodes with cylindrical form and a tiny diameter (2.5 to 4cm) are required.

Besides the difficulty and the time spent in the process of burying and unburying sensor nodes, the repetition of an experiment is also a challenge. To place a sensor node and its antenna at the same place and orientation in a deeper hole is not an easy task. This issue is aggravated with the use of small holes, such as a 10cm-diameter hole. To address these challenges, the use of paper and plastic (PVC) pipes is required. In the testbed in [33], preliminary tests using Mica2 [54] motes at 433MHz are realized to verify how the adoption of paper and plastic pipes would interfere in the results of the experiments. The comparison between the results with and without paper and plastic pipes, shows an additional attenuation ranging from 2 to 8dB. These values correspond, respectively, to the use of paper pipes and different thicknesses of plastic pipes. These values are still considered small in comparison with the value of the soil attenuation which typically varies from 20 to 50dB [33]. To obtain a smaller attenuation value due to the introduction of the plastic pipe, smaller thicknesses can be used. In Fig. 3.5, the use of a *paper pipe*, made with a 55x70cm poster board, is illustrated. In this case, the variation caused by the paper pipe is smaller than 1.5dB.

The paper/plastic pipe helps to preserve the physical structure of the hole for multiple experiments. However, to perform the experiments, the sensor should also be covered with soil. Therefore, the re-use of a hole for multiple experiments is still a problem. A possible solution for this issue is the use of paper pipes filled with soil. In our testbed, additional 7.5cm-diameter paper pipes are used for this purpose. These new paper pipes contain the same soil which is taken out from the digging process. These pipes, with both ends sealed, can have different lengths, helping to make experiments for different burial depths.

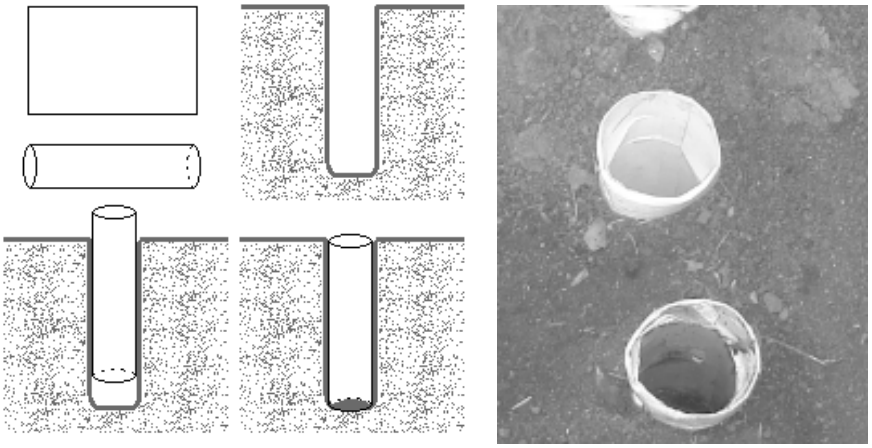

(a) (b)

Figure 3.5: (a) The preparation and installation of paper pipes. (b) Paper pipes used in 10cm-diameter and 90cm-depth holes for a temporary WUSN testbed [33].

Table 3.1: Example of a soil analysis report.

Depth	**Organic Matter**	**Texture**	**%Sand**	**%Silt**	**%Clay**
0-15cm	6.4	Loam	27	45	28
15-30cm	2.6	Clay Loam	31	40	29
30-45cm	1.5	Clay Loam	35	35	30

3.2.2 Soil Texture and Soil Moisture

The soil characteristics have a strong influence on the signal attenuation [1, 2, 28, 33]. As a consequence, WUSN experiments realized without the characterization of the soil are incomplete. In parallel with the preparation of the testbed, soil samples must be collected and sent to a specialized laboratory for soil analysis. The soil texture analysis provided by the laboratory presents very important parameters to be added in all results from the testbed. In Table 3.1, the soil analysis from the testbed in [33] performed by a specialized laboratory [57] is presented as an example.

Besides the soil texture, the water content (WC), or soil moisture, is other parameter to be included in every WUSN experiment report. However, differently from the soil texture, which is very stable for the same site, the WC is dynamic and depends on the environment and the weather. Moreover, the WC also varies as a function of the burial depth [17, 46]. These facts are important because the WC can significantly modify the results of an experiment, as suggested in [2, 22, 33, 46].

There are two basic methods to measure the amount of water in the soil: soil water content and soil water potential measurements [17]. The soil water potential measurement, expressed in bars units, is related to the energy status of the soil water. Tensiometer and electrical resistance sensors are some examples of soil sensors that can be used to gather water potential measurements. This method provides a more realistic measurement of the actual plant water stress and, therefore, has a significant value for irrigation purposes. On the other hand, the soil water content measurement provides an effective measurement of the portion of water in the soil sample. This aspect has a direct relation with the dielectric properties of the soil [28] and, consequently, impacts the underground wireless communication behavior [2, 22, 33, 46].

The soil water content (WC) can be expressed in two forms: gravimetric water content (GWC) and volumetric water content (VWC). A method called *oven drying method* is usually used to calculate the GWC [17]. This method consists of separating and weighing a sample of the soil. Then, this soil sample is completely dry in an oven and it is weighed again. The difference in the weights divided by first measurement represents the VWC in the soil sample, a number varying from 0 to 1. Having the GWC value, the VWC can be obtained by [17]:

$$VWC = \frac{GWC * \rho_{soil}}{\rho_{water}}\ , \tag{3.1}$$

$$\rho_{soil} = \frac{m_{soil}}{V_{soil}} \tag{3.2}$$

where VWC and GWC are the volumetric water content and gravimetric water content of the soil sample, respectively, ρ_{soil} is the soil density in g/cm^3, ρ_{water} is the water density (1g/cm^3 at 4^{o}C), m_{soil} is the mass of the soil sample in g, and V_{soil} is the volume of the soil sample in cm^3.

Despite its simplicity, the direct evaluation of the VWC using the gravimetric method is not practical for the WUSN testbed for three reasons. First, the gravimetric method implies that a soil sample must be regularly removed from the testbed and this continuous process is time-consuming and destructive. Second, the conversion GWC to VWC given by (3.1) depends on the bulk soil density parameter. This density changes for different burial depths and its measurement requires additional attention [17]. As a result, the good accuracy of the GWC measurement can be compromised in the VWC conversion. Finally, it is not possible to have a significant number of measurements of the VWC on a long-term experiment. For instance, if we would like to analyze the effects of the rainfall over the WUSN communication, the presence of a person continuously taking soil samples would be required. Instead, the use of soil moisture sensors that can dynamically take VWC measurements are required in the testbed. Some examples of these sensors are the time domain reflectometer (TDR) and capacitance-based devices [17]. Recent work in WUSN show the successful use a capacitance-based sensor, ECH$_2$O EC-5 [55] sensor [8, 46, 31], for water content measurements.

The WC measurements must be collected frequently to confirm that the same WC value is present during the experiments. This is specially recommended when a set of experiments is partitioned into many different sessions and distinct days. This continuous need of taking WC measurements during a set of experiments, is another reason for the use of soil moisture sensors as part of the testbed infra-structure. The soil texture and the WC must be informed together in the experiments reports. The comparisons between experiments realized in different testbeds are only feasible including with these parameters in the analysis.

3.2.3 Antenna Orientation

Usually, the antenna orientation is not a very critical factor for over-the-air wireless communication experiments. However, considering the extreme attenuation due to the soil propagation, the antenna orientation is an additional constraint to be considered in the deployment of WUSNs, specially for multi-hop underground networks, where the communication range varies based on the antenna orientation. Accordingly, the experiments in a WUSN testbed can be easily compromised if the antenna orientation is not carefully adjusted.

To illustrate the impacts of antenna orientation, experiments are performed by placing a sender and a receiver, both Mica2 motes [54], at different angles as shown in Fig. 3.6(a) [33]. The vertical polarization of the antennas is specifically adopted because preliminary tests proved that it provided the best results for our WUSN testbed environment, however the explanation in this section also applies to other types of antenna polarization.

The original antenna of a Mica2 mote is a standard one-quarter wavelength monopole antenna with 17cm-length. It is well known that the radiation pattern of this type of antenna does not exhibit a perfect omni-directional radiation pattern. Therefore, it

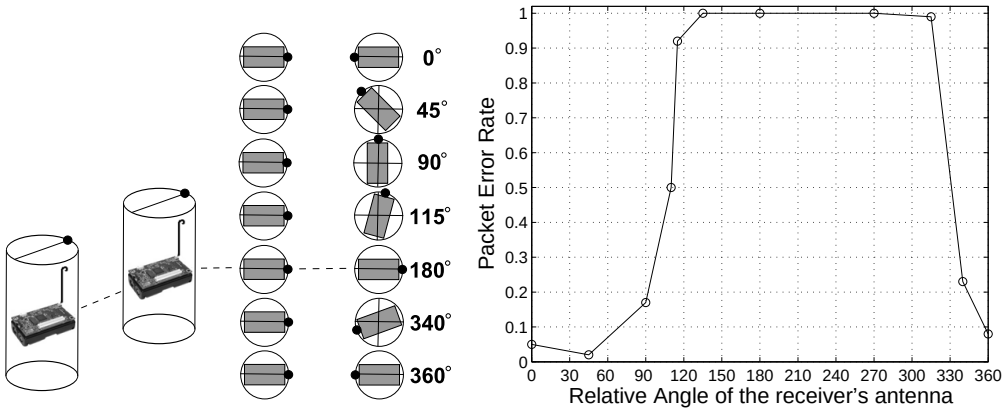

(a) Relative angles for the antenna. (b) PER vs. relative angle for the antenna.

Figure 3.6: The scheme used to test the effects of the antenna orientation in the wireless underground communication [33].

is expected that changes in the antenna orientation causes variations on the signal strength of the receiver node. These variations are specially significant when the underground scenario is considered. The experiments are performed at a *transitional* region, that is, nearby the boundaries of the underground communication range [53].

In Fig. 3.6(b), the packet error rate (PER) is shown as a function of the node orientation. When the relative angle varies from 90^o to 340^o, the PER increases and the orientation of a node has a significant impact on the communication success. When the antenna orientation is between 120^o and 300^o, the communication between the nodes is not possible.

To avoid the interference of the antenna orientation over the experiments results, it is important to choose a unique antenna orientation for all experiments in a WUSN testbed. In our experiments, only the 0^o orientation (Fig. 3.6(a)) is used in order to eliminate the effects of the antenna orientation. Naturally, for every combination of sensor node type and its antenna, different antenna polarizations and orientations can be adopted as the default configuration for all experiments. Accordingly, an experiment

similar to the one shown in Figs. 3.6 must be performed to maintain the accuracy of the results and also to provide the recommendation of the best configuration for the sensor deployment.

3.2.4 Misalignment of RF Measurements

In an ideal wireless testbed, the best accurate tools are selected to be used as the instrumentation for the RF measurements. However, this is not usually the case for WUSN testbeds for two reasons. First, it is a common approach in WUSNs to use the sensor nodes to cooperate and provide the most reliable and efficient communication solution. Therefore, sensor nodes are expected to be also used as network instrumentation. Second, if a special and more accurate instrument, such as a spectrum analyzer, is used at the receiver side of the experiment, the grid idea cannot be applied and multiple tests must be performed one-by-one. The natural consequence is the increase of the time to conclude the experiments.

The grid-based testbed layout involves the measurements from many sensor nodes. Therefore, it is expected that differences between the RF measurements from different sensor nodes cause significant accuracy issues. In the context of a WUSN testbed, this issue is referred as *misalignment problem*. A node is defined to be *aligned* with a given set of nodes, if:

- its PER varies at most 10% from the average PER calculated for the set of nodes and
- its RSSI average varies at most +/-1 dBm from the average RSSI for the set of nodes.

Usually, the nodes present different receiver sensitivities [54]. This fact could cause the mentioned misalignment problem and the accuracy of the experiments can

be compromised. Considering this, a balanced approach adopted in a WUSN testbed is to continue using the sensor nodes as part of the RF instrumentation, but selecting only a subset of the nodes. The selected nodes for an experiment are the ones previously qualified to perform the RSS measurements. Therefore, before using the sensor nodes for the WUSN experiments, they are tested in typical WSN scenarios, using over-the-air tests, in a process called *qualification test*. The reason for this test is explained by the following example.

Suppose that we want to test 3 receiver nodes, all placed in the same hole at different burial depths. The results from this experiment can only be validated if these nodes present similar RSS measurements for an over-the-air test, using the same inter-node distance. If this is the case, the distinct underground measurements provided by the nodes at different burial depths are actually related to the burial depth effects and not a difference caused by their receiver sensitivities.

As an example of a qualification test, one sensor node is assigned with the role of broadcasting (over the air) a total of 200 packets, 30 bytes each, to a set of nodes located in the same physical position and exactly with the same antenna orientation. The transmit power used by the sender node must be small in order to allow the RSS/PER comparison at critical conditions. Usually, we use -10dBm as the transmit power of the sender and 5m as the inter-node distance between the sender and the set of nodes under qualification process. After the test, the results are collected from each node and only the subset of nodes that have similar PER and average RSSI, as previously defined, are selected to participate in the experiment. However, this kind of approach has at least two drawbacks. First, the process is very time-consuming and must be repeated every new day/session of experiments. Second, usually it is not possible to use all the available nodes for the experiment, which means that the grid is constrained by the number of qualified nodes. For instance, in our experiments, using

Mica2 motes, generally only 50% of the available nodes were qualified for each day of experiments. Surprisingly, the qualified nodes are not always the same nodes. The use of sensor nodes as instrumentation for RF measurements requires a huge effort in order to maintain the accuracy of the results. Also, the total number of nodes to be available for a WUSN testbed is significantly higher than the actual number of nodes used in the experiments.

3.2.5 Transitional Region of WUSNs

It is well known that in traditional wireless communication (air channel) there is a region where the reliability of the signal varies, until the point where the communication ceases. It was reported that this issue is highly accentuated in WSNs and this critical region is called the *transitional region* [53]. However, results from preliminary UG2UG experiments show that the underground transitional region is significantly smaller than its air channel counterpart [33]. As already commented, the main problem with wireless underground communication is the very high signal attenuation caused by the soil [1, 2, 22, 33]. At the same time, usually sensor nodes present low-power RF transceivers. The combination of these factors results in a very small width of the transitional region. This fact causes problems in realizing WUSN experiments and it is one of the main reasons for the small number of experiments in this area.

The identification of the transitional region in a WUSN environment, which defines the limits of the communication range, is tied to the burial depth of the nodes, the soil texture, and the WC. For instance, in some of the UG2UG experiments in [33], the transitional region presented a width smaller than 15% of the maximum inter-node distance. More specifically, with a maximum inter-node distance of 100cm and a transmit power level of +5dBm, the transitional region is located between 85 and 95cm. Therefore, such small distance is very critical: an imperceptible slight movement

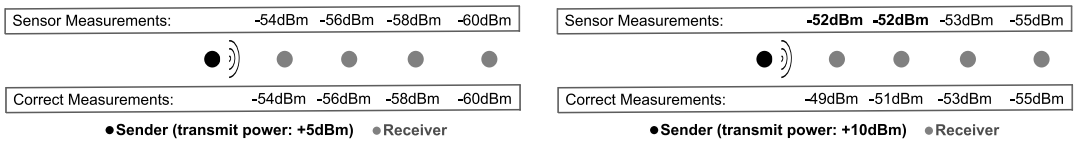

(a) (b)

Figure 3.7: (a) Normal measurements when transmit power level is +5dBm. (b) The clipping effect when transmit power level is +10dBm.

in one direction, when burying the node, causes the change from a good communication region to a transitional region. Therefore, if the tests are being realized very close to the transitional region, a careless manipulation of the sensors can cause significant interferences in the results.

Considering all the presented facts, the recommendation is to limit all the experiments to a *secure* region which is not the transitional region. Restricting the experiments in a secure region is a way to preserve the quality and accuracy of the WUSN experiments. For instance, if WC experiments are realized in the transitional region, it will not be clear if the RSS and PER results uniquely reflect the WC effects or if the results are also affected by the instabilities of the transitional region. On the other hand, for instance, experiments realized at 50% of the maximum inter-node distance present very stable results and the repeatability and comparisons between experiments are feasible in this secure region [33]. Naturally, the exception for this guideline is when the maximum inter-node distance and the transitional region are the aspects under investigation in the experiments.

Many aspects or variables that can potentially interfere with the quality of the WUSN experiments are considered in this section. Guidelines are provided to minimize the issues or completely eliminate the interference of one or multiple variables. The qualification phase is particularly very important due to the well known differences in

the transceiver performances of low-cost sensor nodes. However, even with a qualified set of nodes, the interpretation of the results can still be affected by the way the RF measurements are realized. Guidelines to realize such measurements are provided in the next section.

3.3 Standardized RF Measurements

A WUSN testbed is generally used to provide the infrastructure necessary for the realization of comparisons between experimental results and the predictions made by theoretical models. However, it has been reported that sensor nodes are being used to make RF measurements, generally the RSS [3, 53]. This is usually necessary and desirable because many communication protocols take advantage of the use of the sensor node as an RF measurement tool to make decisions related to multi-hop schemes, topology, localization, etc. However, it is possible to identify some issues related to the use of sensor nodes for such measurements. In this section, a methodology to avoid the issues caused by the limitations of the sensor node receiver circuitry is presented along with guidelines to correctly estimate the path loss exponent.

Clipping Effect. Wireless communication channel models usually use empirically determined parameters, such as path loss exponent (PLE). In a WUSN testbed scenario, the sensor nodes can be used to take RF measurements for the estimation of such parameters. However, these measurements can introduce distortions in the results. The following case involving Mica2 motes was observed in our experiments and illustrates the problem.

Based on the well known Friis free space propagation model [30, 47], it is expected that an increase in the inter-node distance between sender and receiver corresponds to a decrease in the received signal strength. This scenario is illustrated in Fig. 3.7(a),

where RSS are reported for different distances between the sender and the receivers. However, when the transmit power level of the sender node increases from +5dBm to +10dBm, the RSS measurements do not match the 5dB increase, as illustrated in Fig. 3.7(b). We refer to this issue as the *clipping effect*. Consequently, the clipping effect creates distortions in the PLE estimation. The PLE expresses the rate at which the signal power decays as a function of the distance [30] and it is an important input parameter in many WSN/WUSN communication models [53]. This parameter is usually calculated based on many RSS measurements performed by the sensor nodes. If the PLE estimation is not accurate, there will be distortions between the estimations of the communication model and the experimental data provided by the testbed.

The clipping effect is caused by the limitations of the receiver circuitry of the sensor node. In Fig. 3.8, a typical RF circuitry of a sensor node is shown. If a strong signal is received above a certain limit specified by the manufacturer of the sensor, a *limiter circuit* will operate and a maximum RSS will be informed as the RSSI level. Accordingly, different signal levels will correspond to the same informed RSSI and this is the clipping effect.

The clipping effect is challenging because it depends specifically on the hardware. Moreover, the nominal value of the maximum RSS informed by the manufacturer may also vary as already mentioned in Section 3.2. The consequences of the clipping effect on a WSN/WUSN testbed are as follows:

- ***Incorrect interpretation of the testbed data:*** The communication model can predict a RSS value and the experimental data can show a smaller result. If this smaller value is exactly the maximum nominal RSSI of the receiver, probably this is not a model mismatch.

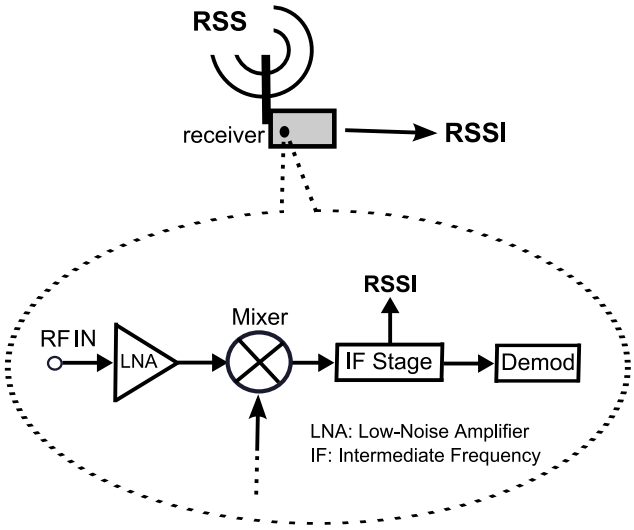

Figure 3.8: Typical receiver circuitry of a sensor node.

- ***Inaccuracy in the model prediction:*** If the communication model is using the testbed to obtain certain empirical parameters, such as PLE, the results of the model will be negatively affected by these incorrect measurements.

Although the first mentioned consequence is not critical because it is only related to the way the experimental data from the testbed is analyzed, the second consequence must be avoided or solved. Therefore, in the case of PLE estimation, only combinations of transmit power levels and inter-node distances that are clearly not affected by the clipping effect can be used. This guideline is specially important when defining the reference distance for PLE measurements [30]. Accordingly, guidelines to calculate PLE are necessary along with a methodology to correctly choose the proper reference distance to avoid the mentioned clipping effect.

Path Loss Exponent Estimation Using Sensor Nodes. The PLE is an essential input parameter in wireless communication models and the following guidelines are

provided in order to increase the accuracy of the PLE's estimation when using sensor nodes to realize the RF measurements:

Select the reference distance d_0: The typical approach to determine the received power from the receiver node's perspective, located a distance d from the sender node, is the use of the well known Friis equation related to the free space propagation model. However, the application of this equation assumes the availability of detailed information about the antennas gain/losses, the overall losses due to transmission line attenuation, filter losses, etc. Another more practical approach to predict the received power at a given distance d from the sender is the use of direct measurements in the radio environment [30]. For this approach, a *reference distance* d_0 from the sender node is chosen. This distance d_0 must be determined considering two simultaneous constraints:

- d_0 ***must lie in the far-field (Fraunhofer) region:*** The far-field region is defined as the region beyond the far-field distance d_f which is defined by [30]:

$$d_f = \frac{2D^2}{\lambda} , \tag{3.3}$$

  where D is the largest physical linear dimension of the antenna and λ is the wavelength of the RF wave in meters. For instance, for the Mica2 node operating at 433MHz, D is approximately 0.17m and, therefore, d_f is 8.3cm. In this case, d_0 must be greater than 8.3cm.

- d_0 ***must be smaller than any distance d used in the deployment of the nodes ($d_0 < d$):*** For instance, for the over-the-air path of the UG2AG/AG2UG links using Mica2, it is usual to consider d_0=1m because the minimum inter-node distance between the sensors is typically higher than 1m.

After selecting a value for the reference distance d_0, the next step is to setup the sender at its minimum transmit power and collect the RSS measurements at the receiver. An additional RSS measurement is taken considering at this time the maximum transmit power. The difference between both measurements must be approximately the nominal difference between the maximum and minimum transmit power levels used. If this goal is not achieved, a higher value for d_0 must be chosen and the above tests must be repeated. In the experiments in [33], the distance d_0 is 10m. Any RSS measurement for inter-nodes distances smaller than 10m will have an error due to the nature of the RF instrumentation used (the sensor node itself). However, if a spectrum analyzer is used, the reference distance d_0=1m could be adopted without any loss of accuracy. Naturally, the value for d_0 will vary for different models of sensor nodes and their antennas. Moreover, the use of multiple receivers will improve the quality of the results in the procedures described in this section.

Take RSS measurements for distances $d>d_0$: Configure the maximum transmit power level at the sender and take many RSS measurements for inter-node distances higher than d_0. For the experiments with Mica2 motes in [33], which used +10dBm for the transmit power, two additional distances are used for the RSS measurements: d_1=15m and d_2=20m.

Apply a linear regression technique to estimate PLE (η): Using the following equation and applying Minimum Mean Square Error (MMSE) technique [30], it is possible to estimate PLE (η) to be used by the wireless communication model.

$$\hat{p}_i = p(d_0) - 10\eta \log_{10}(d_i/d_0) \ , \tag{3.4}$$

where $\hat{p}_i$ is the measured RSS for each measurement instance i.

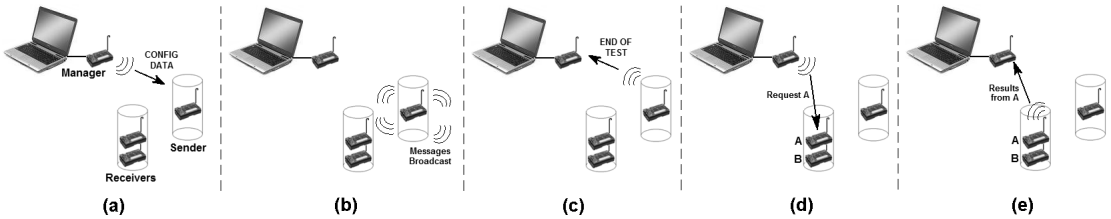

Figure 3.9: Software architecture of the WUSN testbed. (a) The manager sends the configuration to the sender. (b) The sender starts the experiment and (c) informs the conclusion. (d, e) The manager captures the results.

Even if the PLE is not expected to be used, the approach observed in the presented methodology represents the set of best practices for RF measurements using sensor nodes in generic WSNs. In this way, any parameter to be used in a communication model which is based on RSS measurements of sensor nodes must follow a similar approach aiming the accuracy of the investigated model. The guidelines presented in this section can be applied to any WSN experiment. In fact, their relevance with this work is mostly related to the *air path* of the UG2AG and AG2UG experiments.

3.4 WUSN Testbed Software Architecture

A simple and effective software architecture to be used in WUSN testbeds is presented in this section. The software architecture is illustrated in Fig. 3.9. One node, called *manager*, sends the configuration data for the experiment to a node called the *sender*. The configuration data must include the following parameters: transmit power level, delay between the messages, size of each message, and the total number of messages for the experiment. In the Fig. 3.10, a screenshot of our WUSN testbed software running in a laptop is shown.

After receiving the configuration data from the manager, the sender broadcasts the messages. After the broadcasting period, the sender informs the manager node,

via radio channel, that it finished this phase. At this moment, the operator of the experiment can request the results from each *receiver* node via radio channel. It is also possible to select multiple senders to start a transmission contention experiment.

The software in the manager node stores the configuration data for a given experiment, the manual annotations from the operator for that experiment, and the results from each receiver in a local file. If a receiver node receives a request for the results of an experiment but it did not have anything in its buffer, it returns a message to the manager informing *no results*, that is, packet error rate (PER) = 100%. After sending the results to the manager, the receiver erases its buffer. Also, if the receiver receives messages from a new experiment, it automatically erases the previous results which were not requested by the manager.

For the realization of long-term experiments, i.e., experiments that are extended for a longer period of time, such as 24 hours, some modifications in the previous architectural scheme are necessary. First, the operator configures the experiment informing its long-term feature. Then, a special message is sent from the manager to the sender node. This special message informs the sender that it must broadcast messages with a higher interval, e.g., every minute. The message broadcasted by the sender to the receivers also has the information regarding the long-term experiment. Accordingly, the receivers will store the results into their *Flash* memories due to the fact that the RAM memory is not usually large enough to buffer all the results. Finally, the process of capturing the results must also be modified for the long-term experiments. If the radio channel is used for the transfer of long-term results, the process could take hours to finish. The solution is to have each receiver directly connected to the computer acting as the manager to start the dump of the experiment results. In fact, this is the only situation where a cable (usually USB or serial) is necessary in the WUSN testbed.

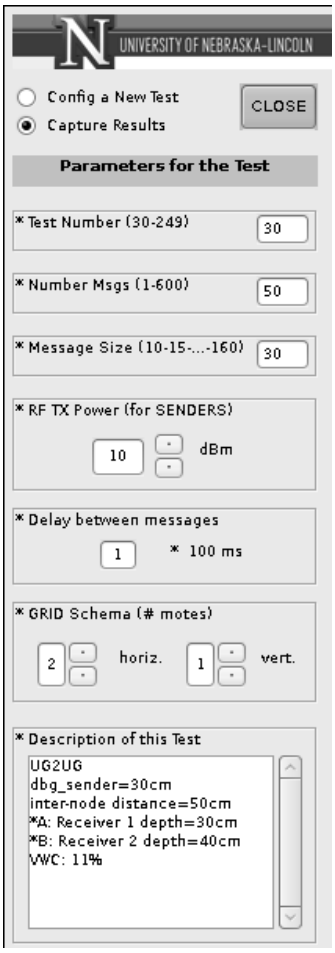

Figure 3.10: A screenshot of the WUSN testbed software running in a laptop.

Each broadcasted message in a given experiment has a sequence number. When the receiver receives that message, it saves in its buffer a summary of the message: its sequence number and the RSSI level related to the reception of the message. The RSSI information is provided by the transceiver of the sensor node as previously discussed in Section 3.3. Therefore, the summary of the message has exactly the same size in the receiver's buffer irrespective of the size of the message. The sequential numbers are used to identify if the loss of packets occur. Therefore, this observation can help to identify if the experiment suffered interference during its realization. If this is the

case, the experiment can be promptly repeated or the source of interference can be identified.

Experiment Setup: final guidelines. Related to the preparation of a WUSN experiment, the following aspects must be known a priori:

- *Soil texture:* This evaluation is realized once, for a given testbed location. The soil texture report must be done for different depths, as shown in Table 3.1.
- *Water content (WC):* This evaluation must be frequently performed. Moreover, it is very important to know the values of WC for different burial depths of the sensors to be tested.
- *Attenuation due to the use of paper/plastic pipes:* This evaluation is realized once, when the WUSN testbed is being built. The fixed average RSS difference between the results with and without the pipes are recorded. If they cannot be neglected, all the RSS results from the experiments must be adjusted accordingly.
- *Default antenna orientation:* This evaluation is realized once, for a given model of sensor node and its antenna. As previously mentioned, once the best antenna orientation is found, all the experiments must use the same antenna scheme.
- *Transitional region:* The range of this value will change as a function of the soil composition, WC, frequency, and transmit power. It is necessary to know, a priori, the different values for this region according to the mentioned parameters. Therefore, experiments in the transitional region must be avoided when trying to analyze a specific aspect of the WUSN communication.

The first step in the preparation for a WUSN experiment is the qualification test, exemplified in Section 3.2.4. After having the set of nodes to be used, the next step is the assignment of the roles for the sensor nodes. Considering that the manager node

does not interfere on the results because it only triggers the start of the experiments and captures the results, the manager node can be elected randomly from the set of available nodes and there is no need to change its role. The node presenting smaller variance in its qualifying results must be selected as the sender. The same sender node can be used for all experiments in a single session. However, the use of the same sender node for different experiments sessions, e.g., different days, is not recommended. Therefore, the remaining qualified nodes can act as receivers. After the preparation phase, the WUSN experiments can be performed.

To conclude, it is clear that the development of an outdoor WUSN testbed and the realization of WUSN experiments are very challenging. In this section, a set of guidelines are provided to achieve a balanced approach between high accuracy and a practical implementation of a WUSN testbed. The basic approach behind the proposed guidelines is the identification and elimination/mitigation of each variable in the testbed.

A WUSN testbed architecture is presented and some aspects, such as the physical layout and software are discussed. The use of paper and plastic pipes are considered in detail, explaining the advantages of these devices in the process of burying and unburying sensor nodes. The influences of the antenna orientation and the soil moisture are highlighted. The importance of the qualification tests and procedures to identify the transitional region in a WUSN are also discussed.

These guidelines are a contribution to the efforts in completely modeling the wireless underground communication and developing simulation environments. To achieve this objective, an accurate outdoor WUSN testbed is essential for the evaluation of the theoretical communication models for WUSNs. The next two sections provide valuable

examples of the relation between the application of the proposed guidelines in this section and the accuracy of empirical WUSN results. In Figs. 3.11-3.14, some pictures of the testbeds used to realize these experiments are shown.

Figure 3.11: Burying a sensor without using paper pipes.

Figure 3.12: Testbed for UG2UG experiments.

Figure 3.13: Testbed for UG2AG and AG2UG experiments.

Figure 3.14: Temporary testbed for UG2AG and AG2UG experiments inside a crop area.

Chapter 4

Empirical Analysis of Underground-to-Underground Communication Channel

In this chapter, the experimental work realized to support the development of the theoretical SSWC underground channel model is discussed [33]. The outdoor experiments were realized during July 2008 to December 2009 period and involved hundreds of hours of very well controlled procedures for different weather conditions, including rainfall and ice. The results of this empirical investigation are summarized here. More specifically, the results of outdoor UG2UG experiments [33] using 45 commodity WSN sensor nodes (operating at 433MHz and 2.4GHz) are presented.

The experiment results show a good agreement with the evaluation of the model proposed in [2, 22] for the 40-cm burial depth. Moreover, the results confirm that the wireless underground channel: (a) exhibits a smaller attenuation at low burial depths, e.g., $<$ 30cm, (b) presents a high degree of temporal stability compared to its air counterpart, and (c) is adversely affected by the volumetric water content (VWC) of the soil. Finally, the results show the potential feasibility of the WUSNs, especially with the use of more powerful RF transceivers at smaller frequencies, e.g., 300-500MHz band. In Section 4.1, the experimental methodology is described and, in Section 4.2, the experiment results for the UG2UG communication link are presented. The results of this section are also used to validate the SSWC channel model described in Chapter 5.

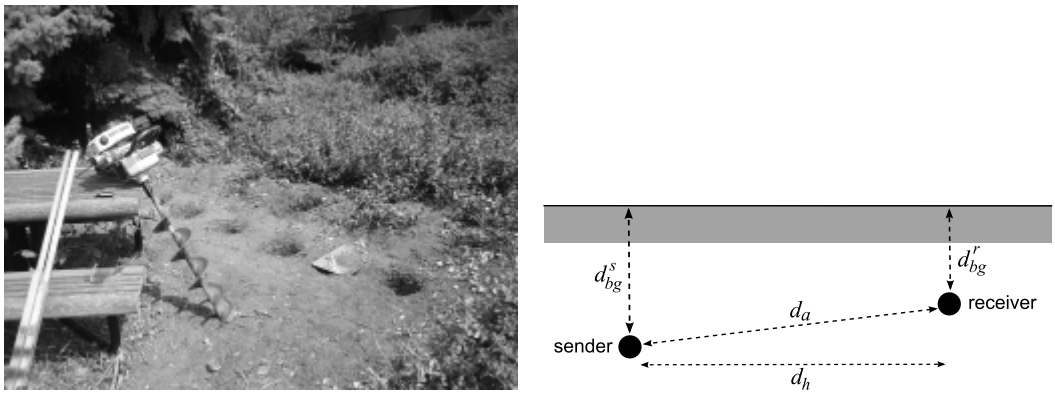

(a) (b)

Figure 4.1: (a) Outdoor environment of the experiments. (b) Symbols used for distances.

4.1 UG2UG Experiment Setup

The underground experiments were carried out in University of Nebraska-Lincoln City Campus on a field provided by the UNL Landscaping Services during August-November 2008 period. The analysis of the soil texture of the experiment site is shown in Table 3.1, according to laboratory analysis [57]. For the majority of the experiments, Mica2 motes [54] operating at 433MHz are used. This frequency range has been theoretically shown to exhibit better propagation characteristics [2]. Additional experiments are realized with MicaZ and IRIS motes [54]. The underground experiments were performed by digging 10 holes of 8 cm-diameter with depths varying from 70 to 100cm with an electric auger. A paper pipe with an attached Mica2 mote is injected to each hole at different depths, following the guidelines described in Chapter 3. The experiment site is shown in Fig. 4.1(a)(a).

For the experiments, a software suite, called S-GriT (Small Grid Testbed for WSN Experiments), is developed to perform long duration experiments without frequent access to the underground nodes [33, 37], as described in Section 3.4. The experiment

setup and the terminology used in representing the results are illustrated in Fig. 4.1(b), where d_{bg} is the burial depth of the node, d_h is the horizontal inter-node distance, and d_a is the actual inter-node distance. The superscripts s and r are also used to indicate sender and receiver. These values, as well as the transmit power, are varied to investigate the packet error rate (PER) and received signal strength (RSS) values of underground communication.

The experiments are realized for 4 transmit power levels, i.e., -3dBm, 0dBm, +5dBm, and +10dBm. 30-byte packets are used with 100ms between each packet. Each experiment in this work is based on a set of 3 experiments with 350 messages or 2 experiments with 500 messages, which result in a total of 1000 packets. The number of packets correctly received by one or more receiver nodes are recorded along with the signal strength for each packet. Accordingly, the packet error rate (PER) and the RSS level from each receiver are collected. To prevent the effects of hardware failures of each individual Mica2 nodes, *qualification tests* have been performed before each experiment. Accordingly, *through-the-air* tests, which consists of 200 packets of 30 bytes, are performed to (1) determine compliant nodes and (2) confirm that the battery level of a node is above a safe limit. A node is labeled compliant with a given set of nodes if (1) its PER varies within 10% of the average PER calculated for the set of nodes and (2) its RSS average varies, at maximum, +/- 1 dBm from the average RSS for the set of nodes. The safe limit for the battery level has been determined as 2.5V. We observed that, in general, only 50% of the 11 nodes used were qualified for each experiment.

4.2 UG2UG Experiment Results

The results are presented considering how some important parameters affect the wireless UG2UG communication: the antenna orientation, the burial depth, the inter-node distance, and the soil moisture. Moreover, the temporal characteristics of the wireless underground communication channel are also discussed.

Antenna Orientation. The details of this experiment result were previously presented in Section 3.2.

Effects of Burial Depth. The effects of the burial depth on the signal strength and PER are investigated. Accordingly, the horizontal inter-node distance between the sender and the receiver is fixed (d_h=50cm), the burial depth of the sender is also fixed (d_{bg}^s=40cm) and the depth of the receiver is varied from 10 to 100cm using different transmit power levels. In Fig. 4.2(a) and 4.2(b), the RSS and PER values are shown, respectively, as a function of the receiver depth. The actual distance, d_a, between the sender and the receiver is also indicated in parenthesis on the x-axis. Each line in the figures shows the results for different transmit power levels. In Fig. 4.2(a), the variance of the RSS is also shown along with the average values for each point.

As shown in Fig.4.2(a), an increase in the actual inter-node distance, d_a, decreases the signal strength. The highest signal strength corresponds to the receiver depth of 30-40cm and the signal strength gradually decreases if the receiver burial depth is smaller than 30cm or higher than 40cm. One exception to this case is $d_{bg}^r = 0$cm, where the signal rays from above the ground impact the received signal strength positively and increase the RSS for each transmit power level. An important observation is the significant difference of RSS values at the same inter-node distances but at different burial depths. As an example, an additional attenuation of 20dB is observed for the

same inter-node distance of d_a=58cm, when the receiver is buried at 70cm compared to the burial depth of 10cm. This behavior occurs mainly due to the reflection of RF signals from the soil surface, which positively affects the RSS when nodes are buried closer to the surface. This result has a fair agreement with the model proposed in [2, 22].

It can be observed in Fig.4.2(b), that for the receiver burial depth of 70cm, the PER increases (0.1<PER<0.2) and an increase in burial depth to 80cm results in a communication loss. Note that this behavior occurs for all transmit power levels, highlighting that the burial depth plays an important role in the connectivity of the WUSN design. It can also be observed in Fig.4.2(a) that the RSS values have a very small variance for all depths and transmit power levels. Accordingly, for a given node deployment, the underground communication channel is very stable as long as the composition of the soil does not change. The only exception is the effect of varying the VWC.

Effects of Inter-node Distance. The effects of the inter-node distance on the signal strength and PER are investigated. Accordingly, the burial depth of the sender and the receiver is fixed (d^s_{bg}=d^r_{bg}=40cm), and the inter-node distance is varied from 10 to 100cm using different transmit power levels. For completeness, the same experiment is repeated for MicaZ and IRIS motes [54], with transmit power levels of 0dBm and +3dBm, respectively. In Fig. 4.3(a) and 4.3(b), the RSS and PER values are shown, respectively, as a function of the depth of the receiver for different transmit power levels. The variance of the RSS values are also shown.

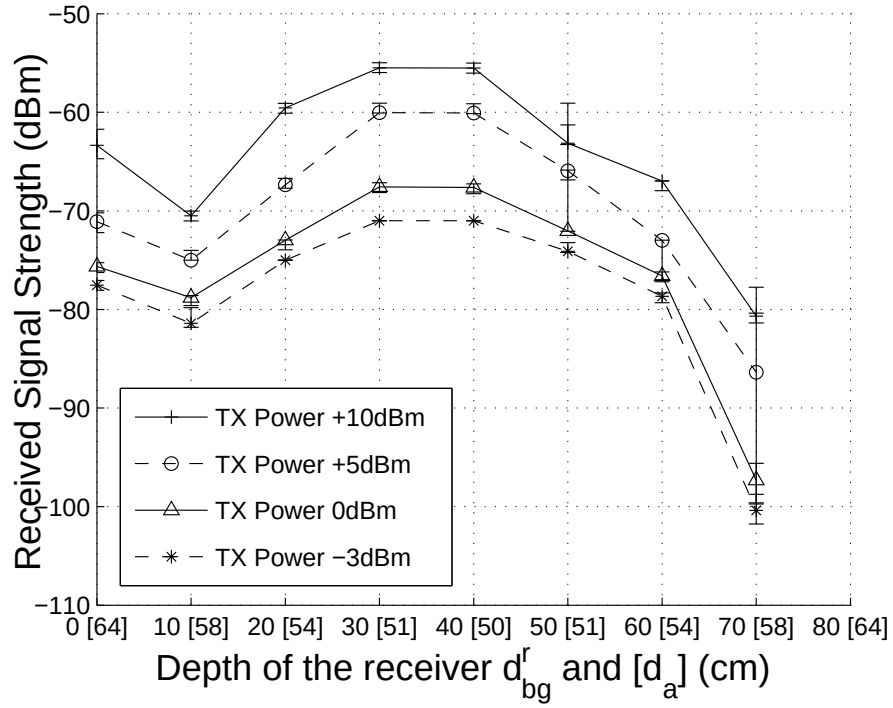

(a)

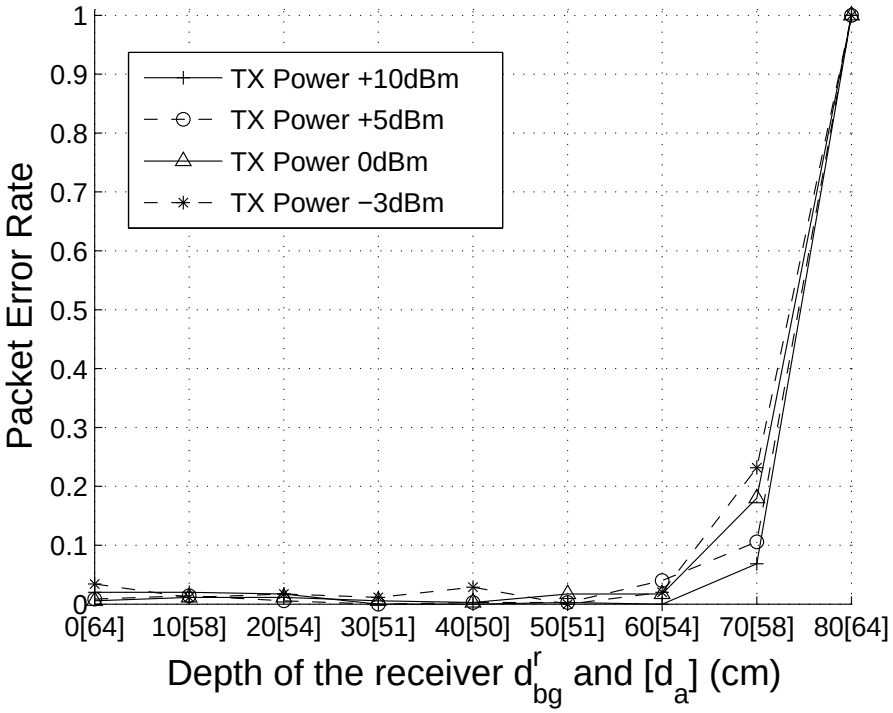

(b)

Figure 4.2: Effects of burial depth on the UG2UG communication performance. (a) RSS vs. depth of the receiver (d^r_{bg}) and actual inter-nodes distance d_a. (b) PER vs. depth of the receiver (d^r_{bg}).

As shown in Fig. 4.3(b), the maximum inter-node distance is found to be between 80 and 90cm for transmit powers of +5 and +10dBm, and 50cm for -3 and 0dBm. For transmit power of -3 and 0dBm, when the inter-node distance varies from 60 to 70cm, the significant decrease of the signal strength can be observed in Fig. 4.3(a), which results in an abrupt PER increase as shown in Fig. 4.3(b). These results reveal the limitations of typical WSN nodes, such as Mica2, considering the use of a low-power transceiver (<+10dBm). In [2, 22], it has been reported that a path loss of about 30dB corresponds to an inter-node distance of 100cm, which is also observed in Fig.4.3(a), where attenuation of almost 30dB for an inter-node distance of 90cm is observed with transmit power of +10dBm.

The performance of the communication using MicaZ (0dBm) and IRIS (+3dBm), for different burial depths and inter-node distances, is shown in Table 4.1. The value, *Yes*, in the column, *Comm. success*, indicates that the communication is possible with a PER$\leq$ 97%. As shown in Table 4.1 and also in Fig. 4.3(b), the use of MicaZ and IRIS, which operate at 2.4 GHz, is limited to an inter-node distance of 10cm for a burial depth d_{bg}^{s}=d_{bg}^{r}=40cm. This result also agrees with previous UG2UG experiment, which presented no communication for MicaZ motes under similar conditions [40]. This experiment also suggests that a lower operating frequency, such as 433MHz used by Mica2, is related to better propagation characteristics than a highe frequency, such as 2.4 GHz used by MicaZ and IRIS. Finally, the results agrees with recent theoretical studies that highlight the need for lower operating frequencies for the feasibility of WUSNs [2, 22].

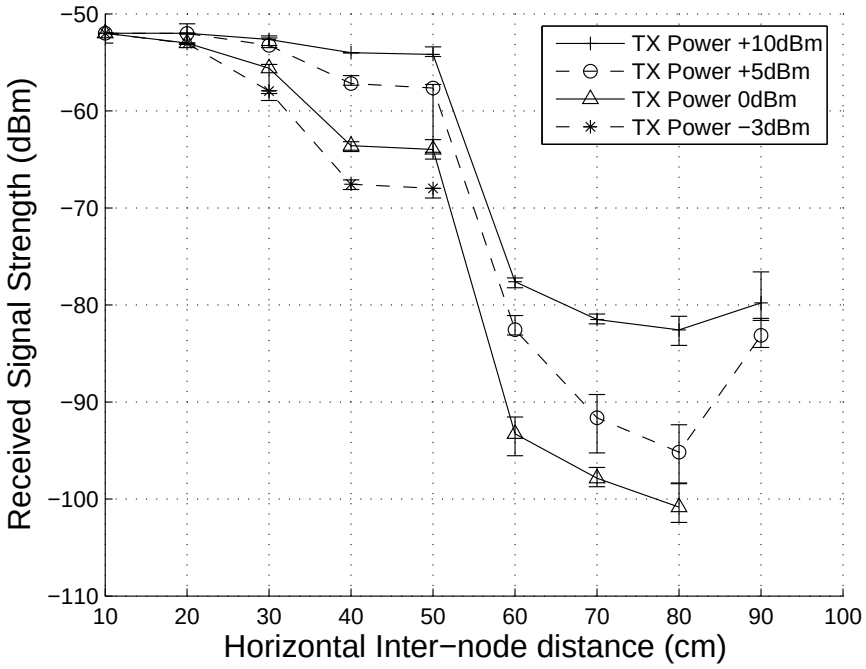

(a)

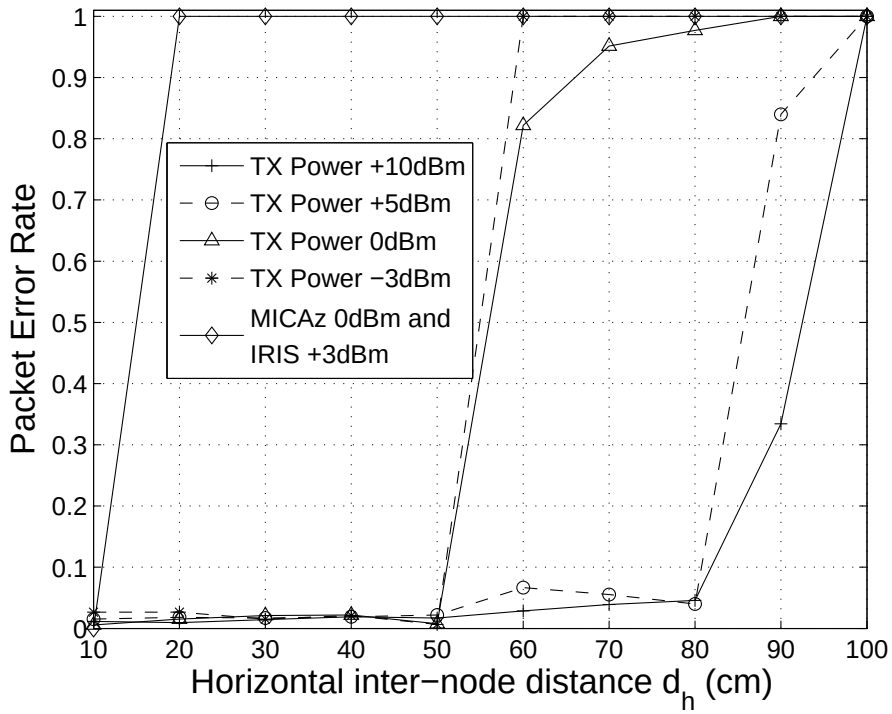

(b)

Figure 4.3: Effects of the inter-node distance on the UG2UG communication performance. (a) RSS vs. horizontal inter-node distance (d_h). (b) PER vs. horizontal inter-node distance (d_h).

Table 4.1: Underground-to-underground communication using MicaZ and IRIS motes

Mote	**Burial depth** (d_{bg}^s=d_{bg}^r)	**Inter-node distance** (d_h)	**Comm. success**
MicaZ	$10-40$cm	10cm	Yes
MicaZ	10cm	20cm	Yes
MicaZ	10cm	$\geq$ 30cm	No
MicaZ	$20-40$cm	$\geq$ 20cm	No
IRIS	$10-40$cm	10cm	Yes
IRIS	$10-20$cm	20cm	Yes
IRIS	$10-20$cm	$\geq$ 30cm	No
IRIS	$30-40$cm	$\geq$ 20cm	No

Temporal Characteristics. The temporal characteristics of the wireless underground channel are investigated. Accordingly, a 24-hour experiment is performed by fixing the horizontal inter-node distance between the sender and the receiver (d_h=50cm), the burial depth of the sender and the receiver (d_{bg}^s=d_{bg}^s=40cm), and the transmit power at +10dBm. For comparison, the same experiment is repeated *over-the-air* in an indoor environment with an inter-node distance of 5m and a transmit power of +10dBm. In Fig. 4.4(a) and 4.4(b), the RSS and PER values are shown, respectively, as a function of time. Each data point shows the average of 30 minutes of RSS or PER information, which corresponds to 150 packets. In Fig. 4.4(a), the confidence intervals of the RSS is also shown along with the average values for each point as well as the results of the over-the-air experiments. In Fig. 4.4(b), the temporal evolution of the cumulative PER is shown for underground communication.

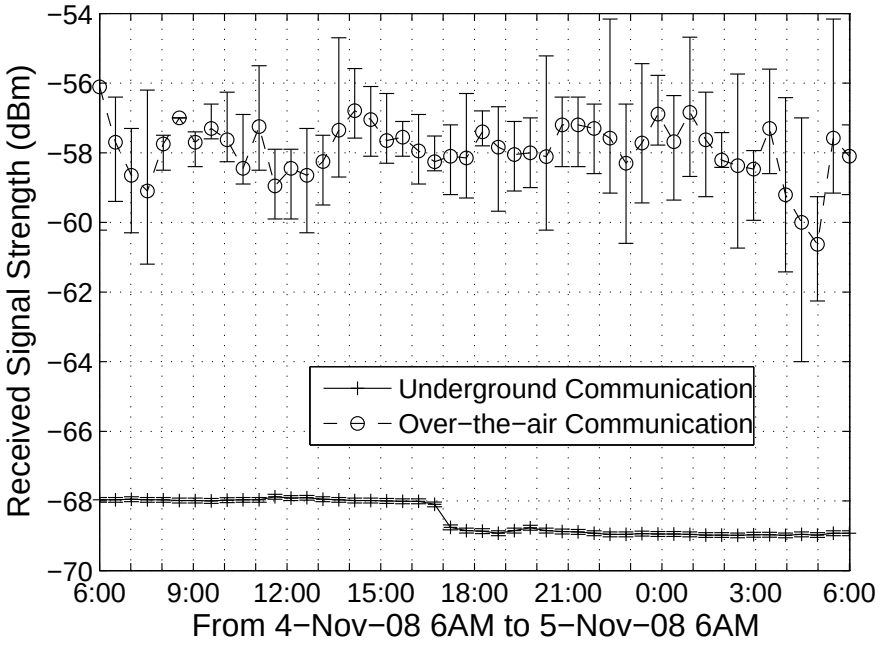

(a)

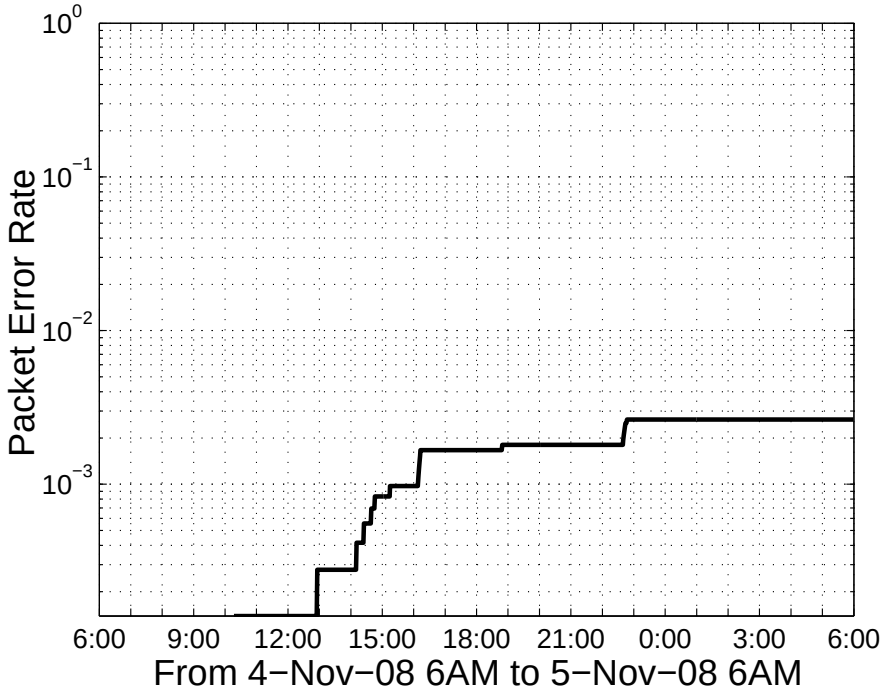

(b)

Figure 4.4: Temporal characteristics of the UG2UG channel compared to the air channel. (a) RSS vs. Time. (b) Historical evolution of PER over the time (PER <1% for all 24h-period).

As shown in Fig. 4.4(a), the maximum variation of the signal strength is only 1 dB. No precipitation event was registered during the period and only a 8^oC variation is observed on the temperature during the experiment. Compared to the over-the-air communication, where both the average and the variance of the RSS vary significantly with time, underground wireless channel exhibits a stable characteristic with time. As shown in Fig.4.4(b), during the same period of time, PER is always smaller than 0.5% with a small variance. This result agrees with the model for wireless underground channel proposed in [2, 22], which points out the high stability of the wireless underground channel. The temporal stability has a stronger impact on the development of routing and topology control protocols for WUSNs.

Effects of Soil Moisture. The effects of the volumetric water content (VWC) on the signal strength and PER are discussed. Accordingly, the burial depth of the sender and the receiver is fixed (d^s_{bg}=d^r_{bg}=40cm), two different inter-node distances (d_h=30cm and 40cm) are used in conjunction with two different VWC levels (dry and wet soil), and the transmit power is varied. The *dry soil* experiments refer to tests realized on Oct 20th, 2008, a sunny day, and the *wet soil* experiments were performed on Oct 22nd, 2008, a rainy day, when 2.5 inches of precipitation was recorded. Based on the *oven drying method* [17], the different VWCs are measured to be 14.6% for dry soil 23.9% for wet soil, which corresponds to an increase of almost 60%in VWC. In Fig. 4.5(a) and 4.5(b), the RSS and PER values are shown, respectively, as a function of the transmit power level of the sender. Each line in the figures shows the results for different VWC and inter-node distances.

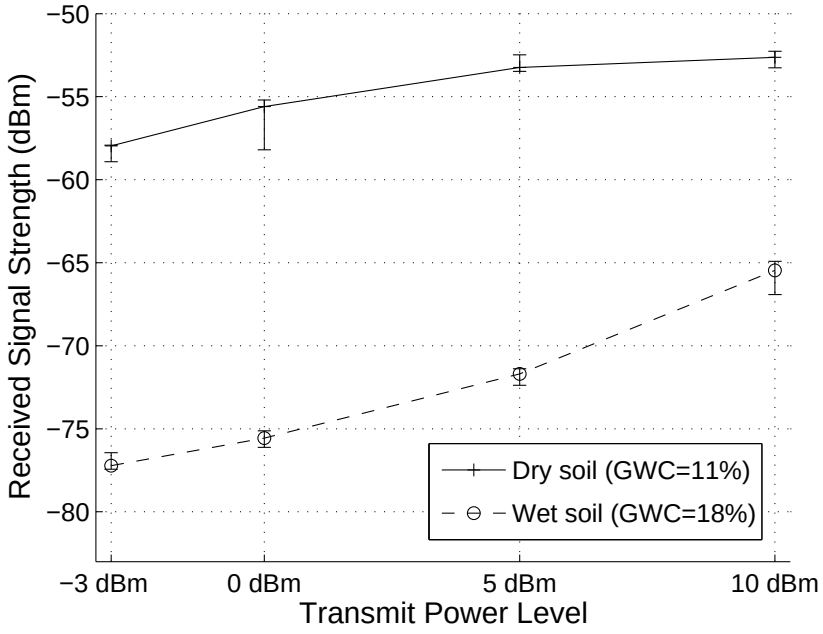

(a)

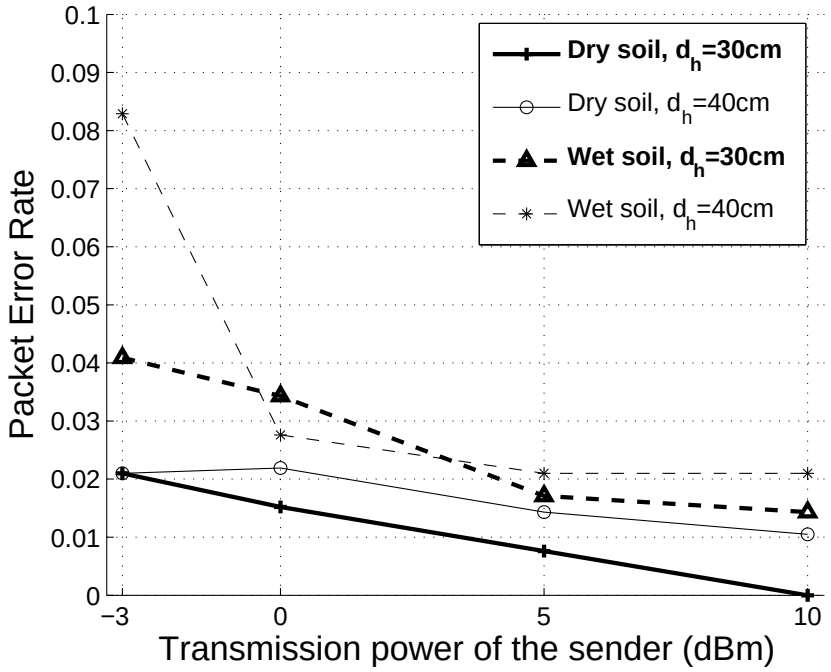

(b)

Figure 4.5: Effects of the volumetric water content (VWC) on the UG2UG communication performance. (a) Comparison of RSS for dry and wet soils. (b) Comparison of PER for dry and wet soils.

As shown in Fig. 4.5(a), for high VWC, i.e., wet soil, the attenuation increases by 12 to 20dB compared to dry soil. The Fig. 4.5(b) also reveals that the increase of VWC implies higher PER. We can also observe, from the Figs. 4.5(a) and 4.5(b), that the negative effect of the VWC over the quality of the communication is reduced when the transmit power is increased. Therefore, for a scenario where the natural or artificial irrigation is expected to occur, the design of the WUSN protocols should carefully consider the variation of the VWC of the soil. For instance, the communication protocol may consider the soil moisture measurements of a physical region to make informed routing decision or even consider to temporarily raise the transmit power of some of the nodes in order to decrease the adverse effects of VWC.

To conclude, the following underground channel aspects are highlighted:

- The orientation of the nodes' antennas plays an important role in the connectivity of WUSNs.
- The burial depth significantly affects the communication performance, with smaller signal attenuation for shallower depths.
- The wireless underground channel has been found to exhibit extreme temporal stability, which is important in the design of routing and topology control protocols.
- For a given deployment and soil composition, there is a minimum transmit power for which the UG2UG communication has the same reliability compared to cases where higher transmit power levels are employed.
- The soil moisture has a very strong effect on the communication performance. However, the negative effects can be mitigated with higher transmit power levels. Therefore, the soil moisture information should be effectively integrated to the design of WUSN networking protocols.

In addition to the characteristics of wireless underground communication, the limitations of the commodity sensor nodes for WUSNs are also observed as a result of these experiments. It can be observed that for this specific Subsoil WUSN scenario, the maximum communication range achieved is smaller than 1m. In terms of signal attenuation, this corresponds to roughly a 1:20 attenuation rate compared to *through-the-air* communication in an outdoor environment [3]. Consequently, a new generation of nodes with more powerful transceivers and/or more efficient antennas are required for the actual deployment of WUSN applications. Moreover, the observed range limitation calls for the investigation of an alternate way of UG2UG communication. This approach is properly investigated with the studies of lateral waves presented in Chapter 5.

Chapter 5

Underground Channel Model for WUSNs

The characterization of the underground channel is essential for the proliferation of communication protocols for WUSNs. However, as observed from the results presented in Chapter 3, the underground channel is significantly different from the air channel. In fact, the underground communication is one of the few fields where the environment has a significant and direct impact on the communication performance. Environmental aspects, such as soil moisture and texture, potentially change the dielectric properties of the soil and affect the wireless communication [2]. Moreover, deployment parameters, such as the burial depth and the frequency, also have strong impact on the communication [2, 33]. Therefore, an underground communication channel must capture these aspects related to the environment and nodes deployment.

After empirical studies [33, 35, 36, 37], the analysis of the empirical results leads to the realization of a comprehensive characterization of the underground channel for UG2UG links in WUSNs. Accordingly, the Soil Subsurface Wireless Channel (SSWC) model is proposed for WUSNs. The SSWC model provides a way to predict the signal attenuation and bit error rate (BER) for the UG2UG link. The model is composed of five components, as follows:

1. **Dielectric properties model.** The dielectric properties of the soil are captured based on the assumption that the volumetric water content (VWC) data, a dynamic environmental parameter, is available. The remaining parameters, such as the soil texture and bulk density, must be measured just one time because they usually do not present temporal variability [16]. Accordingly, with these

environmental parameters and the operating frequency, this model can predict the soil permittivity and conductivity for the 300-1300MHz frequency range.

2. **Direct wave model.** This model estimates the attenuation suffered by the signal that propagates in a direct path between the nodes, i.e., the direct wave (DW). Observe that although the SSWC is developed specifically for UG2UG links, the first two mentioned models are fundamental parts of future UG2AG and AG2UG channel models.

3. **Reflected wave model.** This model estimates the attenuation suffered by the signal that is reflected at the soil surface and reaches the receiver, i.e., the reflected wave (RW).

4. **Lateral wave model.** This model estimates the attenuation model suffered by the lateral wave (LW). The lateral wave propagation is also known as *up-over-and-down* propagation [21].

5. **Signal superposition model.** This model estimates the resulted signal strength from the superposition of DW, RW, and LW waves, given the transmit power level of the transmitted signal. Therefore, the total signal attenuation and BER are calculated and represent the outputs of the SSWC model. Therefore, depending on multiple factors, such as the burial depth and the inter-node distance, one of these signals can potentially dominate the signal superposition at the receiver node. In practice, if one of the signals is higher than 10dB in relation to the others, the resulted signal is essentially the higher signal with negligible effects from the others.

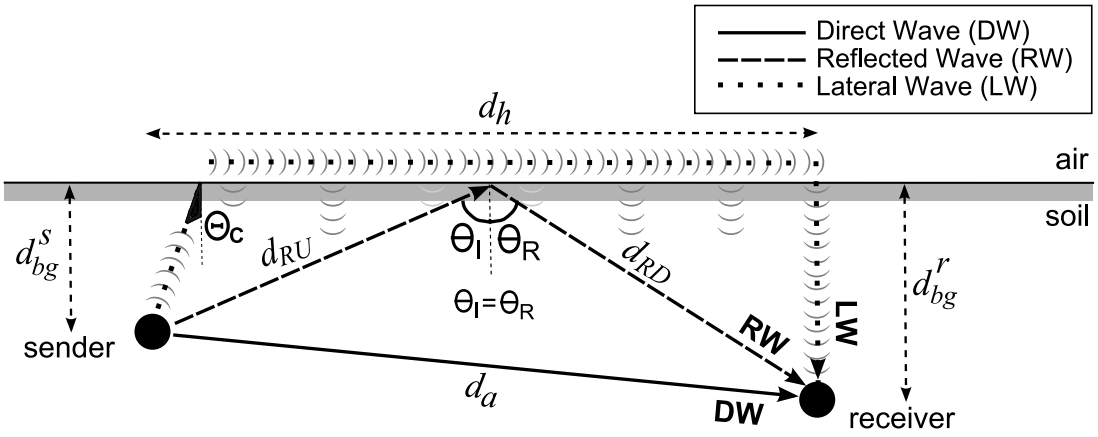

Figure 5.1: The received signal is a superposition of direct wave (DW), reflected wave (RW), and lateral wave (LW).

This chapter is organized as follows: In Section 5.1, an overview of the model and its assumptions are provided. In Section 5.2, the model which predicts the dielectric soil properties is presented. The direct wave (DW) and reflected wave (RW) attenuation models are developed in Sections 5.3 and 5.4, respectively. In Section 5.5, the lateral wave (LW) attenuation model is presented along with an introductory about the lateral-waves theory. In Section 5.6, the process of signal superposition at the receiver node is described. This last component provides the estimation of the total signal attenuation and BER for a transmitted signal with a known transmit power level.

5.1 SSWC Channel Model: Overview

In this section, an overview of the SSWC attenuation model for the UG2UG communication in the soil subsurface region is provided. The contribution of each signal, DW, RW, and LW, and the terminology used in this section are illustrated in Fig. 5.1, where d_{bg} is the burial depth of the node, d_h is the horizontal inter-node distance, and d_a is the actual inter-node distance. The superscripts s and r are also used to indicate

sender and receiver. Related to the reflected wave (RW), d_{RU} is the distance between the sender and the reflection point at the soil surface and d_{RD} is the distance between this point and the receiver node. Defined with respect to the normal to the soil surface, the angles of incidence and reflection are respectively, θ_I and θ_R. Due to the Snell's law of reflection [47], $\theta_I = \theta_R$.

As shown in Fig. 5.1, the received signal is potentially a superposition of 3 waves that follow different paths. The model for the direct wave (DW) signal attenuation is the simplest one and basically counts for the attenuation due to the soil propagation. The reflected wave (RW) attenuation model incorporates an additional loss caused by the reflection at the soil surface. The permittivity of the soil, the orientation of the antennas (polarization of the plane wave), and the distances d_{bg}^{s}, d_{bg}^{r}, and d_h are determinant factors to affect the reflection loss.

The third component for the received signal is the lateral wave (LW). As shown in Fig. 5.1, the path followed by the LW explains why the lateral wave propagation is also called *up-over-and-down* transmission [10, 21]. However, a detailed investigation on this topic [10], reveals that this phenomenon is maximum at the *critical angle*, Θ_c, but also involves a wide range of values for θ_I. Typically, Θ_c varies from 10^o to 20^o and it is exclusively a function of the dielectric properties of soil and air. The LW model is one of the most complex components of the SSWC model because the analytical solution for the integration of the expressions for determining the electric fields of lateral waves has not been achieved so far [21]. Therefore, the feasible way to obtain the value corresponding to the contribution of the LW component is by numerical methods [21], which is also the approach adopted in the SSWC model.

Finally, the last component of the model, the signal superposition model, calculates the positive or negative contribution among the signals due to their magnitude and also phase shifting.

As previously highlighted, the SSWC model presented in this work does not completely address all possible antenna schemes (types and orientations). More specifically, for the sake of reducing the overall model complexity, the LW model assumes the use of an isotropic dipole in the horizontal orientation (parallel to the soil surface). Therefore, the adoption of a different antenna scheme implies the introduction of a distortion in the SSWC model. To reduce the impact of this issue, the SSWC model provides distinct antenna factors for each type of signal (DW, RW, LW). These factors are input parameters of the model, as explained in Section 5.6. However, to obtain the values of these factors, further analytical or empirical investigation is necessary. Fortunately, in practice, the latter option may be sufficient without highly compromising the accuracy of the model.

A second assumption of the SSWC model is the use of insulated antennas. In practice, this assumption does not have serious implications for antennas with small size. For instance, the original antennas of the Mica2 motes are already insulated. A third model assumption is that the antenna is not in a container. For instance, if the antenna is enclosed in a plastic box filled with air, the electromagnetic model is significantly altered. More specifically, related to the LW model, this new form of node deployment would require modifications in this model to extend its application for a stratified media (air/soil/air).

Another model assumption is a non-magnetic soil, which is usually is the case. Finally, the dielectric model is based on an existing model [28] which is constrained to the $300 - 1300$ MHz frequency range. Naturally, different dielectric models can be used for other frequency ranges. However, previous studies reveal that this frequency range is a balanced option for WUSNs [2, 33]. This conclusion is also confirmed in the model evaluation discussed in Section 5.8.

5.2 Dielectric Soil Properties Model

The soil is a *dielectric material*, characterized by a specific *relative permittivity* or dielectric constant. The propagation of EM waves is directly affected by the permittivity of the material. More specifically, a smaller value of the relative permittivity basically implies better conditions for the propagation of EM waves. The soil medium behaves as a dielectric material composed of air, *bound* water, *free* water, and bulk soil. Additionally, if the soil presents a smaller bulk density, it means that the soil has a higher porosity. In this case, the attenuation of the EM waves is smaller due the higher quantity of air in the medium. On the other hand, the presence of water in soil has a strong adverse effect on the signal attenuation. In fact, the quantity of water in the soil, e.g., the volumetric water content (VWC) is the main attenuation factor for the propagation of EM waves in soil [1, 2, 33, 35, 36].

The volume of water in the soil (VWC) is composed of two parts, the *bound water* and the *free water*. The *bound water* corresponds to water molecules tightly held to the surface of the soil particles. The *free water* corresponds to water molecules *free* of action of soil particles [6], i.e., located in the voids between the soil particles. Therefore, for the same VWC value, a soil sample can contain more free water than other sample due to differences on the soil texture of the samples. More specifically, the quantity and also the type of clay particles determine the amount of bound water in the soil [6, 16]. This fact will be demonstrated in the Section 5.8, where a variation of the more than 20dB is observed for the same VWC and different soil textures. The explanation for this is the fact that the dielectric properties of the bound water are different from the free water. Therefore, in the dielectric model, different weights are expected for bound and free water. This is exactly what it is observed in equation 5.1, which is discussed latter.

A soil where clay particles are predominant, such as the one classified as *clay* in Fig. 2.3, is typically worse for underground communication than a *sand* soil. From the physics of soils [16], it is well known that a gram of clay absorbs much more water than a gram of silt or sand. The water absorption is a direct function of the surface area of the soil particle and clay particles have higher surface areas than silt and sand particles. Observe that the surface area is inversely proportional to the size of the particles. Since clay particles are very small compared to sand particles, e.g., more than 25 times, they absorb more water in the form of bound water, as previously explained.

Besides the VWC, the frequency of the signal also affects the relative soil permittivity and, thus, the level of attenuation suffered by the EM wave. The soil permittivity is a non-linear function of the frequency [6]. Moreover, depending on the frequency, the soil *conductivity* dominates the attenuation function [6, 21]. Therefore, contrary to the general belief, a smaller frequency is not always related to a smaller signal attenuation [6, 28]. In general, the mentioned statement is true, but there are several exceptions according to the frequency range under analysis. Consequently, even if all the soil parameters values are promptly available, including the VWC, there is no direct formula to calculate the value of the soil permittivity for an unrestricted range of frequencies. Therefore, without the soil permittivity value, further estimation of the signal attenuation in soil is not possible.

To mitigate the above problem, many distinct soil dielectric models were developed for specific frequency bands [6, 13]. Naturally, these models are used by distinct applications which have different frequency requirements. With a constrained frequency range, many assumptions and simplifications are possible to be considered in these models, significantly reducing the complexity of the model without sacrificing accuracy. Accordingly, during the analysis of the dielectric model to be used by SSWC, the first aspect to be evaluated is the frequency range to be used in WUSNs.

Frequency values around 1GHz are usually associated with smaller soil permittivity values, compatible with the wireless communication and microwave remote sensing applications [2, 18, 28]. Furthermore, frequencies below 300MHz can also result in smaller attenuation rates. However, when the frequency decreases, the wavelength of the signal increases and the antennas also increase in size. Hence, the use of frequency smaller than 300MHz is typically not practical for WUSN scenarios. Based on these facts, in the SSWC model is adopted a balanced approach between accuracy and practical factors in WUSNs. Accordingly, the semi-empirical soil dielectric model in [28], which is constrained to the $300 - 1300$MHz frequency range [28], is selected as the soil dielectric model for the SSWC.

The input parameters of the SSWC dielectric model are the operating frequency and the soil parameters, such as texture, bulk density, and VWC. The outputs of the dielectric model are the relative complex permittivity and conductivity of the soil, which are required by the RW, DW, and LW models. With the support of this dielectric model, it is possible to predict the value of the soil permittivity when, for instance, rainfall or artificial irrigation occurs. The permittivity value is essential for predicting the resulted attenuation suffered by the signal while propagating in soil. As observed in this example, besides the use of the SSWC model for protocol design purposes, the model can actually be embedded in cross-layer protocols for WUSNs to provide a way to dynamically adapt the behavior of these protocols to environmental parameters.

Using the Peplinski's dielectric model [28], the dielectric properties of soil can be calculated as follows:

$$\begin{aligned}
\epsilon &= \epsilon' - j\epsilon'', \\
\epsilon' &= 1.15[1 + \frac{\rho_b}{\rho_s}(\epsilon_s^{\alpha'} - 1) + m_v^{\beta'}\epsilon_{f_w}'^{\alpha'} - m_v]^{1/\alpha'} - 0.68, \\
\epsilon'' &= [m_v^{\beta''}\epsilon_{f_w}''^{\alpha'}]^{1/\alpha'},
\end{aligned} \tag{5.1}$$

where ϵ is the relative complex permittivity of the soil-water mixture, m_v is the VWC of the mixture, ρ_b is the bulk density in grams per cubic centimeter, $\rho_s = 2.66g/cm^3$ is the specific density of the solid soil particles, $\alpha' = 0.65$ is an empirically determined constant, and β' and β'' are also empirically determined constants, dependent on soil-type and given by:

$$\begin{aligned} \beta' &= 1.2748 - 0.519S - 0.152C, \\ \beta'' &= 1.33797 - 0.603S - 0.166C, \end{aligned} \tag{5.2}$$

where S and C represent the mass fractions of sand and clay, respectively. The quantities ϵ'_{f_w} and ϵ''_{f_w} are the real and imaginary parts of the relative permittivity of free water [6, 28]. Note that the influences of free water and bounded water are both considered in the above formula. The mass fractions of sand and clay considered in (5.2) and also the volumetric water content m_v are used to determine the amount of free water and bounded water in the soil. This distinction is important because the amount of free water causes a stronger attenuation effect for EM waves propagation when compared with the effects of the bounded water.

The analysis of the above equations shows that the value of the soil permittivity ϵ is especially dependent on the following factors:

- *Operating frequency*, f, of the sensor nodes. For this specific $300 - 1300$MHz range, typically, a higher frequency is associated with a higher ϵ.

- *Composition of soil* in terms of sand and clay fractions, S and C. This factor depends on the deployment region of the sensor nodes.

- *Bulk density,* ρ_b, indirectly expresses the amount of air in the soil. Again, this factor depends on the deployment region of the sensor nodes.

- *Soil moisture or volumetric water content (VWC)*, m_v. A higher VWC value is associated with a higher ϵ. This factor depends on the deployment region as well as time (e.g., occurrence of rainfall or artificial irrigation).

5.3 Direct Wave (DW) Model

The direct wave (DW) propagation mode is the basic form of propagation of EM waves through soil. The DW model starts with the well known Friis equation for the over-the-air (ota) attenuation. Assuming that the antennas are oriented in the direction of the maximum power transfer, the following Friis transmission formula [47] can be applied. The over-the-air path loss, PL_{ota}, is the relation between the received signal strength (RSS) and the transmit power level:

$$PL_{ota} = \frac{P_r}{P_t} = G_t G_r \left(\frac{\lambda_0}{4\pi d_a} \right)^2, \tag{5.3}$$

where P_r is the RSS at the receiver, P_t is the transmit power level, G_t and G_r are the gains of the transmitting and receiving antennas, λ_0 is the wavelength of the signal in free space, and d_a is the actual inter-node distance between the transmitter and receiver (λ_0 and d_a have the same unit).

For the underground settings, the equation (5.3), which represents the attenuation for the signal propagating in free space for a distance d_a, must be modified. First, λ_0 must be converted to the wavelength of the signal in the soil, λ_{soil}. Also, a soil path loss factor, L_{soil} (≤ 1), must be added to the original attenuation equation (5.3). Therefore, the soil path loss, PL_{soil}, is given by:

$$\frac{P_r}{P_t} = G_t G_r \left(\frac{\lambda_s}{4\pi d_a} \right)^2 L_s, \tag{5.4}$$

(5.4) expresses exactly the attenuation suffered by the direct wave (DW). Therefore, the total attenuation for DW, L_{DW}, in dB, is given by:

$$\begin{aligned} L_{DW} &= G_t + G_r - L_s + 10log\left(\frac{\lambda_s}{4\pi d_a}\right)^2, \\ &= G_t + G_r - L_s + 20log\lambda_s - 22 - 20logd_a, \end{aligned} \tag{5.5}$$

where L_{DW} is the total attenuation in dB suffered by the direct wave (DW). λ_s and d_a are in centimeters and the value of λ_s is given by:

$$\lambda_s[cm] = 100\frac{2\pi}{\beta}, \tag{5.6}$$

where β is the *phase constant*, in rad/m.

In (5.5), the L_s is the dominant attenuation factor and correctly reflects how lossy is the soil medium. L_s is given by [47]:

$$L_s = \frac{8.68}{100}d_a\alpha, \tag{5.7}$$

where α is the *attenuation constant* in Np/m and d_a is the inter-node distance in centimeters.

The attenuation constant, α, and the phase constant β are part of the complex propagation constant of EM waves in lossy medium, which is given as $\gamma = \alpha + j\beta$ [47]. Therefore, the actual values of the attenuation constant α and the phase constant β are expressed in terms of the real and imaginary parts of the complex relative soil permittivity ϵ [47]:

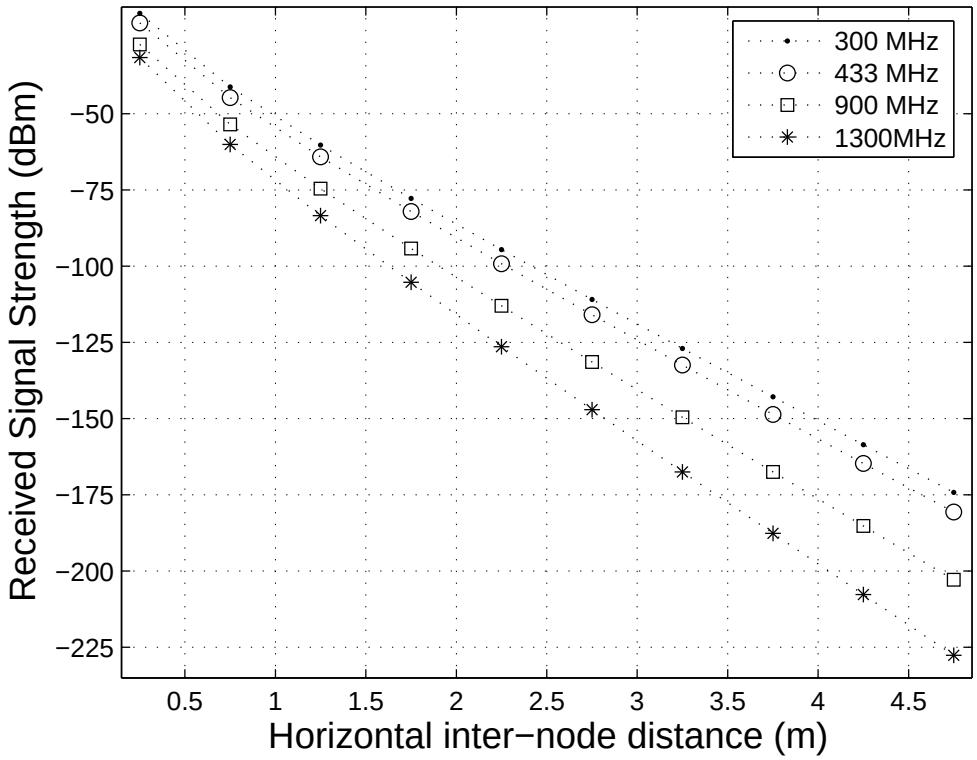

Figure 5.2: Direct wave (DW) attenuation model. Effects of the inter-node distance (d_h) on the RSS for different frequencies (+10dBm transmit power level).

$$\begin{aligned} \alpha &= \omega \sqrt{\frac{\mu\epsilon'}{2}\left[\sqrt{1+\left(\frac{\epsilon''}{\epsilon'}\right)^2}-1\right]}, \\ \beta &= \omega \sqrt{\frac{\mu\epsilon'}{2}\left[\sqrt{1+\left(\frac{\epsilon''}{\epsilon'}\right)^2}+1\right]}, \end{aligned} \tag{5.8}$$

where $\omega = 2\pi f$ is the angular frequency, μ is the magnetic permeability constant ($4\pi 10^{-7}$H/m), and ϵ' and ϵ'' are the real and imaginary parts of the soil permittivity, as given in (5.1), respectively. It is assumed that soil is non-magnetic, which is usually the case.

Next, 5.5 is evaluated with simulations to investigate the effects of the inter-node distance on the signal strength of DW. Accordingly, the parameters of the simulation as configured as follows. The burial depth of the sender and the receiver is fixed (d^s_{bg}=d^r_{bg}=40cm), and the inter-node distance is varied from 0.1 to 5m using different frequencies. A +10dBm transmit power level is adopted in conjunction with a parallel polarization for the antennas, e.g., monopole antennas in vertical orientation. The remaining parameters, including VWC, are exactly the same of the testbed site described in Section 4. If not stated, these parameters and the 433MHz frequency are the default input parameters for all model simulations in this document. The simulation results are shown in Fig. 5.2. Observe that the *antenna problem* is not included in these results. More specifically, usually the DW attenuation will be higher or smaller considering the merit factor of the antenna when sender and receiver are at the same burial depth. A deeper analysis of these results will be provided in Section 5.8.

The total attenuation suffered by the EM waves which travel directly to the receiver (DW) is given by (5.5). Besides the natural dependence on the inter-node distance d_a, the DW attenuation model is clearly dependent on the value of the soil permittivity ϵ. The real and imaginary parts of ϵ are provided by the dielectric soil properties model in (5.1), as discussed in Section 5.2. For higher depths, e.g. $>$ 1m, only the DW component is usually considered because RW and LW are strongly attenuated. Therefore, for such scenarios, the SSWC model is basically the application of the first 2 models. For instance, if the transmit power level is +10dBm, d_{bg}=100cm, and the estimated value of the L_{DW} provided by the model is $-$90dB, it means that the expected RSS at the receiver is $-$80dBm. However, for shallower depths, the RW and LW components must also be evaluated. Accordingly, the next sections are necessary in the model.

5.4 Reflected Wave (RW) Model

The RW model is an extension of the DW model with three modifications. First, as illustrated in Fig. 5.1, the soil path length must change from d_a to $d_{RU} + d_{RD}$. Second, an additional attenuation factor due to the reflection loss at the soil-air boundary is considered. Finally, the RW model provides an additional output, the shifting angle Φ caused by the reflection of the signal at the soil surface. The angle Φ is not actually used by the RW model considered in this section and must not be confused with θ_I or Θ_c. However, Φ will be considered in the last step of the SSWC model, the signal superposition process described in Section 5.6.

The total attenuation, in dB, suffered by the reflected wave (RW), L_{RW}, is given by:

$$\begin{aligned} L_{RW} &= G_t + G_r - L_{s'} + 10log\left(\frac{\lambda_s}{4\pi d_a}\right)^2 - L_r, \\ &= G_t + G_r - L'_s + 20log\lambda_s - 22 - 20logd_a - L_r, \end{aligned} \tag{5.9}$$

where L_{RW} is the total attenuation in dB suffered by the reflected wave (RW), L'_s is the soil path loss factor, and L_r is the attenuation due to the reflection.

In (5.9), L'_s is not the same in (5.7) because a new path using d_{RU} and d_{RD} must be considered in the RW case:

$$L'_s = \frac{8.68}{100}(d_{RU} + d_{RD})\alpha, \tag{5.10}$$

where α is the *attenuation constant* in Np/m. d_{RU} and d_{RD} are the distances, in cm, between the sender and receiver to the reflection point at the soil surface, respectively.

In (5.9), L_r is calculated based on the complex Fresnel reflection coefficient, $\Gamma = Ae^{j\Phi}$, and depends on the polarization of the antenna (perpendicular or parallel), and

is given as follows [47]:

$$\begin{aligned} L_r &= -20logA, \\ Ae^{j\Phi} &= \Gamma, \\ \Gamma_\perp &= \frac{\eta_{air}\cos\theta_I - \eta_{soil}\cos\theta_T}{\eta_{air}\cos\theta_I + \eta_{soil}\cos\theta_T}, \\ &= \frac{\sqrt{\frac{\mu_{air}}{\epsilon_{air}}}\cos\theta_I - \sqrt{\frac{\mu_{soil}}{\epsilon_{soil}}}\cos\theta_T}{\sqrt{\frac{\mu_{air}}{\epsilon_{air}}}\cos\theta_I + \sqrt{\frac{\mu_{soil}}{\epsilon_{soil}}}\cos\theta_T}, \\ \Gamma_\parallel &= \frac{\eta_{air}\cos\theta_T - \eta_{soil}\cos\theta_I}{\eta_{air}\cos\theta_T + \eta_{soil}\cos\theta_I}, \\ &= \frac{\sqrt{\frac{\mu_{air}}{\epsilon_{air}}}\cos\theta_T - \sqrt{\frac{\mu_{soil}}{\epsilon_{soil}}}\cos\theta_I}{\sqrt{\frac{\mu_{air}}{\epsilon_{air}}}\cos\theta_T + \sqrt{\frac{\mu_{soil}}{\epsilon_{soil}}}\cos\theta_I}, \end{aligned} \tag{5.11}$$

where L_r is the attenuation in dB due to the reflection, $Ae^{j\Phi}$ is the phasor representation of the complex reflection coefficient Γ, A is the magnitude of Γ, Φ is the shifting phase of Γ, $\Gamma_\perp$ and $\Gamma_\parallel$ are the equations of Γ for the perpendicular and parallel polarization cases, respectively. θ_I and θ_T are the incident and transmission (or refraction) angles, respectively. η_{air}, η_{soil}, μ_{air}, μ_{soil}, ϵ_{air}, and ϵ_{soil} are the intrinsic impedance, relative permeability, and relative permittivity of air and soil, respectively.

For non-magnetic soil, the values of the angles θ_I and θ_T are given by:

$$\theta_I = \arctan\left(\frac{d_h}{d^s_{bg}+d^r_{bg}}\right), \theta_T = \arcsin\left(\frac{\sqrt{\epsilon_{soil}}}{\sqrt{\epsilon_{air}}}\sin\theta_I\right), \tag{5.12}$$

where d_h is the horizontal inter-node distance, d^s_{bg} is the burial depth of the sender, and d^r_{bg} is the burial depth of the receiver, as shown in Fig. 5.1.

The total attenuation suffered by the EM waves (RW) which are reflected by the soil surface before reaching the receiver is given by (5.9). The model is highly dependent on the physical distances between the nodes and in relation to the soil surface. Again,

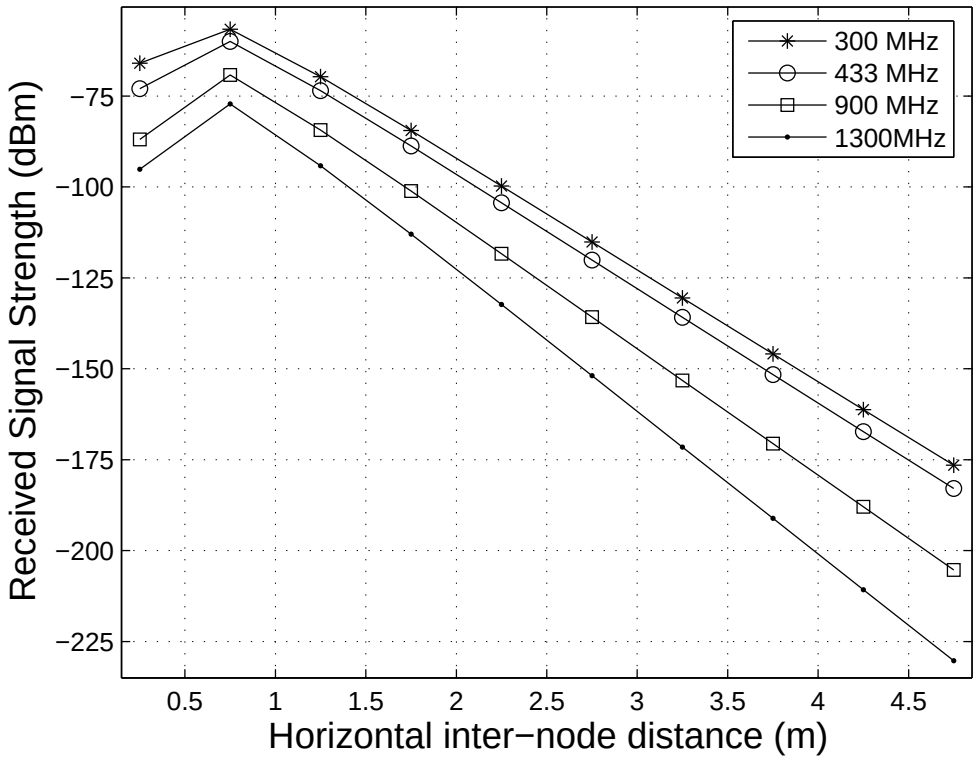

Figure 5.3: Reflected wave (RW) attenuation model. Effects of the inter-node distance (d_h) on the RSS for different frequencies (+10dBm transmit power level).

this attenuation model is dependent on the value of the soil permittivity ϵ provided in (5.1).

Next, the effects of the inter-node distance on the signal strength of RW are investigated. Accordingly, the burial depth of the sender and the receiver is fixed (d^s_{bg}=d^r_{bg}=40cm), and the inter-node distance is varied from 0.1 to 5m using different frequencies. The simulation results are shown in Fig. 5.3. A quick comparison with the results in Fig. 5.2 reveals a higher attenuation of RW compared to DW. This is expected since the soil path is higher for RW. Also, an additional attenuation which occurs when the wave is reflected is considered. Moreover, for this scenario, there is an inter-node distance where the attenuation is smaller due to the smallest value for Γ.

As previously mentioned, the *antenna problem* is not included in these results. In other words, it is possible to have antennas with particular radiation patterns and better directivity for RW than DW. Again, a deeper analysis of these results will be provided in Section 5.8.

5.5 Lateral Wave (LW) Model

The lateral waves are waves that reached the soil surface with a critical angle Θ_C. Instead of being reflected or refracted, these waves travel along the surface continuously diffusing downward and eventually these waves reach the receiver, as illustrated in Fig. 5.1. The main advantage of such type of transmission is the fact that the soil attenuation is restricted to the sum of the depths of sender and receiver. For shallower depths, this up-over-and-down transmission can significantly increase the communication range for the same transmit power level [19, 21, 48].

The radial component of the electric field, E_ρ, is the one with the best range of distances and it is usually the one used for communication purposes. This is the reason why the recommended orientation for buried dipoles is the horizontal, that is, the dipole antennas parallel to the soil surface [19, 21, 48]. This assumption of the SSWC model significantly reduces the complexity of the LW model because the three remaining dipoles, i.e., magnetic vertical, magnetic horizontal, and electric vertical, are not included in the SSWC model.

The radial component of the electric field, E_{d_h}, due to a unit electric moment, for an inter-node distance d_h and d^s_{bg}=d^s_{bg}=d_{bg}, is given by [21]:

$$E_{d_h} = -\frac{\omega\mu_0}{4\pi k_1^2}\cos\phi\Bigg(\int_0^\infty \{k_1^2 J_0(\lambda d_h) - (\lambda^2/2)[J_0(\lambda d_h) - J_2(\lambda d_h)]\}\gamma_1^{-1}\lambda\, d\lambda + \int_0^\infty \Bigg\{\frac{\gamma_1(k_1^2\gamma_2 - k_2^2\gamma_1)}{2(k_1^2\gamma_2 + k_2^2\gamma_1)}[J_0(\lambda d_h) - J_2(\lambda d_h)] - \frac{k_1^2(\gamma_2 - \gamma_1)}{2\gamma_1(\gamma_2 + \gamma_1)}[J_0(\lambda d_h) + J_2(\lambda d_h)]\Bigg\} e^{i2\gamma d_{bg}}\lambda\, d\lambda\Bigg), \tag{5.13}$$

where d_h is the radial or horizontal inter-node distance, d_{bg} is the burial depth of sender and receiver, ω is the angular frequency, ϕ is radial cylindrical coordinate of the electric field, μ_0 is the permeability of free space, and k_1 and k_2 are the complex wave numbers for regions 1 (soil) and 2 (air), respectively. λ, which is the radial transform variable (not the wavelength), J_n are integral representations of the Bessel functions, and γ_1 and γ_2 are given by [21]:

$$\gamma_1 = \sqrt(k_1^2 - \lambda^2), \gamma_2 = \sqrt(k_2^2 - \lambda^2). \tag{5.14}$$

The closed form solution to (5.13) has not been found yet [21, 48]. Therefore, a practical approach is to analyze (5.13) numerically. In [48], numerical techniques are developed to evaluate the electromagnetic field components of the 4 types of dipoles: magnetic or electric, horizontal or vertical. A similar approach is found in [21], where tables for different values of horizontal inter-node distances, conductivity σ, permittivity ϵ, and frequencies are provided for horizontal electric dipole. The values in these tables express the total signal attenuation (in dB) of the lateral wave. The expression (5.13) used in the LW attenuation model is based on the numerical evaluation in [21] and applying the value of the conductivity σ given by:

$$\sigma = \epsilon'' \epsilon_0 \omega, \tag{5.15}$$

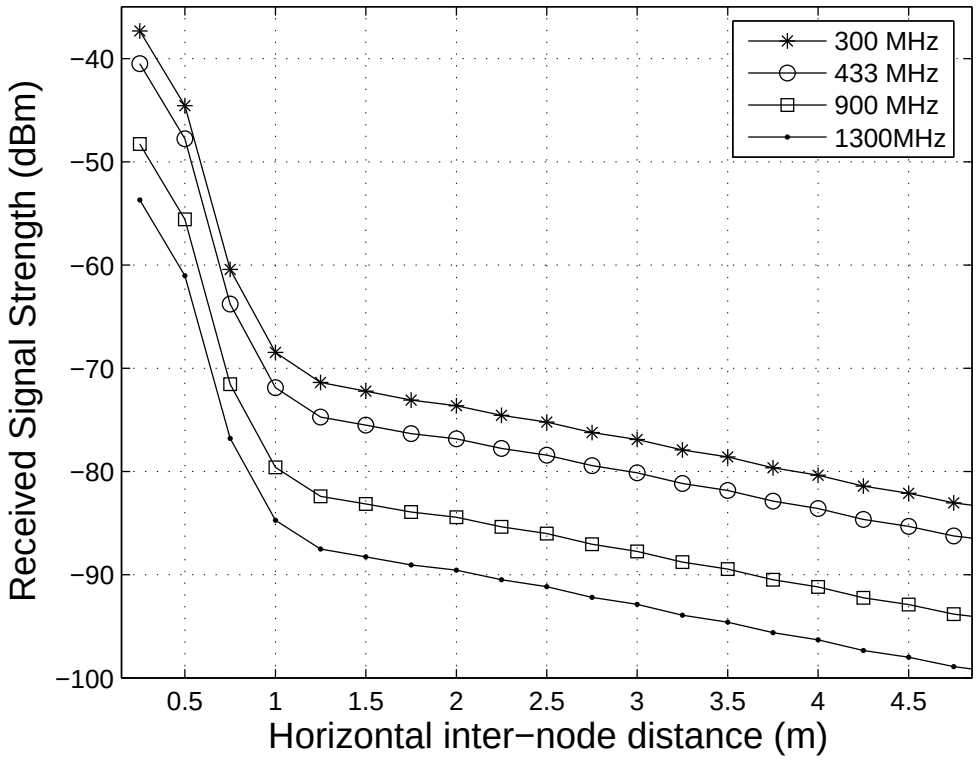

Figure 5.4: Lateral wave (LW) attenuation model. Effects of the inter-node distance (d_h) on the RSS for different frequencies (+10dBm transmit power level).

where σ is the conductivity of soil in S/m, ϵ'' is the imaginary part of the relative permittivity of soil, given by (5.1), ϵ_0=8.85 $*$ 10$^-$12 F/m is the permittivity of free space, and ω=2πf is the angular frequency with f in Hz.

The total attenuation, in dB, suffered by the lateral wave (LW), L_{LW}, is given by:

$$L_{LW} \quad = \quad G_t + G_r - L_{s''} - E'_{d_h}, \tag{5.16}$$

where L_{LW} is the total attenuation in dB suffered by the lateral wave (LW) in dB, E'_{d_h} is the normalized value of E_{d_h}, the attenuation suffered by the radial component of the electric field of the lateral wave, given by (5.13). $L_{s''}$ is the correction value of

soil path loss for the case where d_{bg}^{s} is different from d_{bg}^{r}. In this case, d_{bg} in (5.13) is the smallest value between d_{bg}^{s} and d_{bg}^{r} and $L_{s''}$ is given by (5.7), substituting d_a by the absolute difference between d_{bg}^{s} and d_{bg}^{r}.

Next, the effects of the inter-node distance on the signal strength of LW are investigated. Accordingly, the burial depth of the sender and the receiver is fixed (d_{bg}^{s}=d_{bg}^{r}=40cm), and the inter-node distance is varied from 0.1 to 5m using different frequencies. The simulation results are shown in Fig. 5.4. A quick comparison with the results in Figs. 5.2 and 5.3 reveals the better performance of LW for longer communication ranges. This is expected since the propagation path is mainly formed by the over-the-air part for high inter-node distances. Again, as previously mentioned, the *antenna problem* is not included in these results. Therefore, an antenna with poor performance for the *up* direction can strongly minimize the advantages of the LW propagation. Also, the soil surface is assumed to be free of obstacles. A deeper analysis of these results and the practical use of LWs for 10m or higher UG2UG communication ranges will be discussed in Section 5.8 and Chapter 6, respectively.

One important aspect of the lateral wave, which also explains its better performance for underground communication, is the fact that a LW is generated by "a bundle of rays or a beam of bounded extent at an angle Θ close to Θ_c, [7]" the critical angle for internal reflection. Therefore, what is represented by a line for the LW path in Fig. 5.1 is actually a non-negligible region. Therefore, if a very efficient directional antenna is used targeting the region close to Θ_c, an additional significant gain is achieved and can be represented as G_t and G_r at the equation (5.16).

Assuming $\mu_{air} = \mu_{soil}$, the critical angle, Θ_c, is given by [47]:

$$\Theta_c = \arcsin\left(\frac{\sqrt{\epsilon_{air}}}{\epsilon_{soil}}\right), \tag{5.17}$$

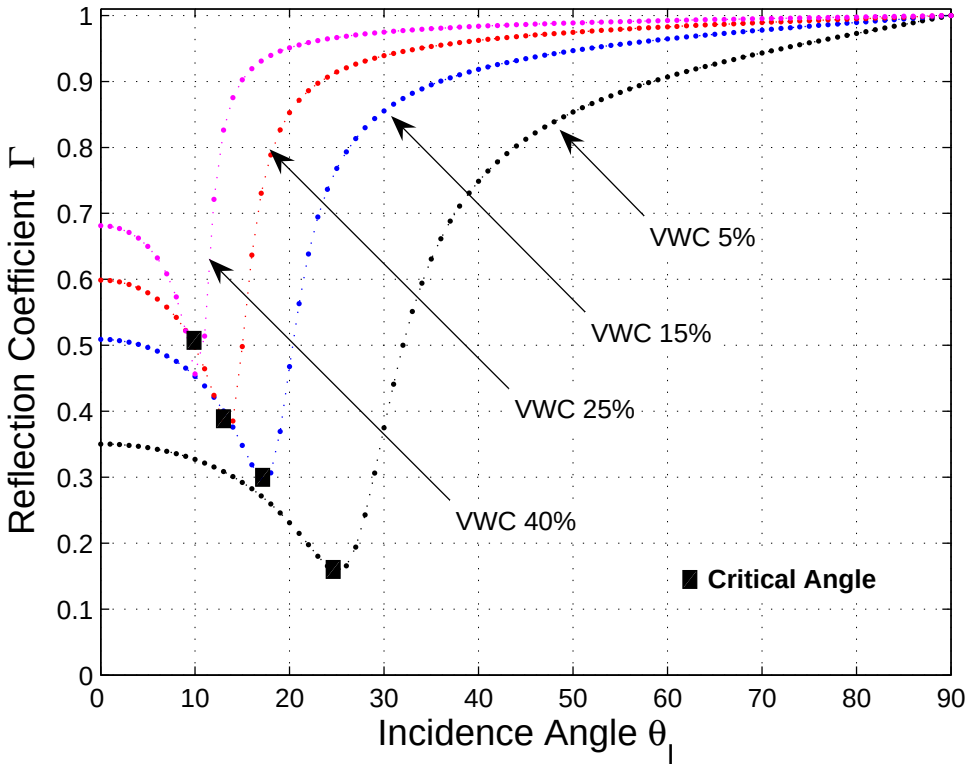

Figure 5.5: The critical angle Θ_c depends on the soil permittivity which is strongly affected by the volumetric water content (VWC).

For instance, for the parameters of the testbed discussed in Section 4, the value of Θ_c is 15^o and 19.4^o, for the dry (VWC=14.6%) and wet soil (VWC=23.9%), respectively. Additional simulation results for different values of VWC and the default testbed parameters are shown in Fig. 5.5. The value of Θ_c does not depend on the deployment parameters. However, it strongly depends on the soil parameters, specially the VWC which is constantly changing in an outdoor environment. These results present an additional reason why the *antenna problem* is so difficult to be modeled. Different variations of a dipole antenna can have different radiation patterns which affect the directivity in relation to the region nearby Θ_c.

5.6 Signal superposition

In this section, the process of the superposition of the signals DW, RW, and LW that eventually reach the receiver is investigated. The superposition of these signals is not a trivial algebraic sum of signals for three important reasons. First, the sum must be realized in dB. Second, the differences between the lengths of the each signal propagation path, DW, RW, and LW, can cause significant phase shifting among these signals. Therefore, positive or negative contributions in the signal superposition can occur depending on the value of this phase shift between two or more signals. Finally, to provide a certain degree of support for different types of antennas, distinct antenna factors must be applied to each signal, thus representing distinct weight factors for each signal in the superposition process.

Although a generic antenna gain factor is also available as an input of the model, the outdoor experiments [33, 35, 36] reveal that this parameter alone is not sufficient. Usually, the employed antennas do not have the same performance compared to ideal dipoles with isotropic radiation pattern, similar to what occurs with the antennas used in the experiments in Chapter 3. Therefore, some level of directivity of the antenna will eventually increase the signal strength of one of the signals (DW, RW, LW) in detriment of the others. To reduce the impact of this problem, antenna factors are introduced in the SSWC model, which is a novel approach in the research area of WSNs, including WUSNs. The usual approach is to consider antenna gains in conjunction with an initial signal decay (Chapter 3.3). With the signal superposition, such naive approach may cause distortions in the model.

To exemplify how critical is the use of a generic antenna factor, a global gain (or attenuation) factor, instead of a distinct antenna factor for each type of signal (DW, RW, LW), a real case is discussed. In the experiments in [19, 48], a terminated travelling-wave antenna is adopted. This antenna has a strong directivity in the direction of the

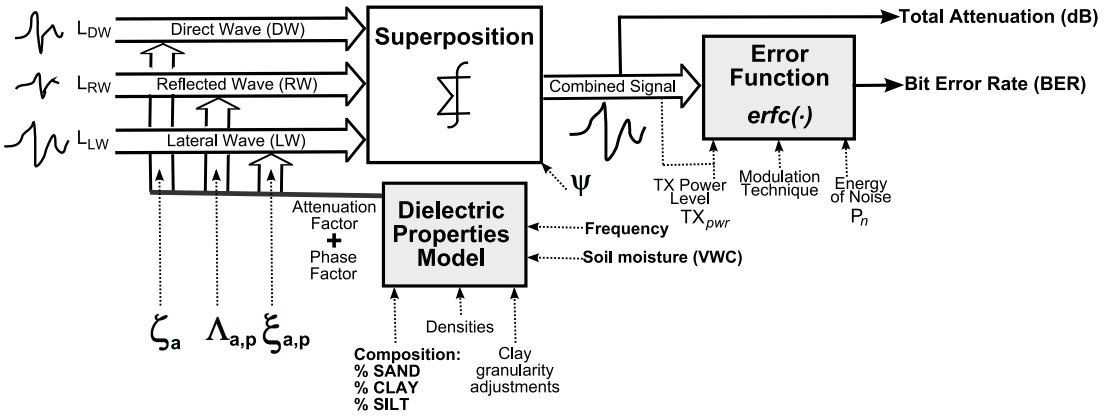

Figure 5.6: Signal superposition model.

soil surface, just above the sensor node, thus targeting the Θ_c angle. For this antenna scenario, DW is practically eliminated and RW is also strongly attenuated. Therefore, the LW dominates the signal superposition and DW and RW may be neglected. To represent this scenario in the SSWC model, individual antenna factors are required in order to produce the correct attenuation and BER estimations.

When an antenna presents a radiation pattern closer to an ideal isotropic antenna, all these antenna factors are essentially the same, recapitulating the original concept of generic antenna gain which is represented as G_t and G_r in (5.5), (5.9), and (5.16). However, for all remaining scenarios, individual antenna factors are desirable and G_t and G_r values in the mentioned equations can be properly set to 0.

As illustrated in Fig. 5.6, the superposition model produces two output estimations, the total attenuation in dB and the BER, based on 11 input parameters, explained as follows:

1. L_{DW}. Expected signal strength, in dBm, of the direct wave. This value is provided by the DW model using the equation (5.5) and the transmit power level of the sender node.

2. L_{RW}. Expected signal strength, in dBm, of the direct wave. This value is provided by the RW model using the equation (5.9) and the transmit power level of the sender node.

3. L_{LW}. Expected signal strength, in dBm, of the lateral wave. This value is provided by the LW model using the equation (5.16) and the transmit power level of the sender node.

4. ζ_a. Antenna factor for the direct wave, in dB. This value is empirically or analytically evaluated when a non-isotropic antenna is used.

5. λ_a. Antenna factor for the reflected direct wave, in dB.

6. ξ_a. Antenna factor for the lateral wave, in dB.

7. ξ_p. Phase of the complex reflection coefficient, Γ, given by (5.11).

8. ψ. Phase shifting set of parameters used to realize the superposition of the signals considering positive and negative contributions due to the phase shifting. These parameters are the following: λ_s (5.6), d_h, d^s_{bg}, d^r_{bg}, d_a, d_{RU}, and d_{RD} (Fig. 5.1).

9. *Modulation Technique.* This parameter, e.g. ASK, FSL, PSK, 2PSK, is used by the error function, $erfc(\cdot)$, to estimate the BER.

10. TX_{pwr}. The transmit power level, in dBm, is also used by the error function, $erfc(\cdot)$, to estimate the BER.

11. P_n. The energy of noise, in dBm, is empirically determined and is also used by the error function, $erfc(\cdot)$, to estimate the BER.

The superposition process first discover which is the stronger signal among DW, RW, and LW. The two weaker signals are combined and, then, the result is combined with the original stronger signal. Let TX_{pwr} denote the transmit power level and P_A the

signal strength, in dBm, of the superposition related to the weaker signals. Similarly, P_B denotes the signal strength, in dBm, related to the superposition of P_A and the stronger signal. P_A and P_B are given by:

$$\begin{aligned}
\tau = &\quad \cos\left[\pi + \tfrac{2\pi}{\lambda_{air}} d_h + \tfrac{2\pi}{\lambda_{soil}}(d_{bg}^{s} + d_{bg}^{r} - d_a)\right], \\
\upsilon = &\quad \cos\left[\pi - \Theta + \tfrac{2\pi}{\lambda_{soil}}(d_{RU} + d_{RD} - d_a)\right], \\
P_{DW} = &\quad TX_{pwr} - \zeta_a - L_{DW}, \\
P_{RW} = &\quad TX_{pwr} - \lambda_a - L_{RW}, \\
P_{LW} = &\quad TX_{pwr} - \xi_a - L_{LW}, \\
P_{max} = &\quad max(P_{DW}, P_{RW}, P_{LW}), \\
P_{min1} = &\quad min_1(P_{DW}, P_{RW}, P_{LW}), \\
P_{min2} = &\quad min_2(P_{DW}, P_{RW}, P_{LW}), \\
P_A = &\quad 20log\left(\Delta 10^{\frac{P_{min1}}{20}} + \Delta 10^{\frac{P_{min2}}{20}}\right), \\
P_B = &\quad 20log\left(\Delta 10^{\frac{P_{max}}{20}} + \Delta 10^{\frac{P_A}{20}}\right),
\end{aligned} \tag{5.18}$$

where ζ_a, λ_a, ξ_a are empirically or analytically determined parameters for the DW, RW, and LW antenna factors, respectively. Δ is a placeholder variable which can assume one these three values: (a) 1, if the related signal if DW or the calculated P_A, (b) τ if the related signal is LW, and (c) υ if the related signal is RW.

Finally, the total attenuation, L_{total}, in dB, estimated by the SSWC model is given by:

$$L_{total} = \quad TX_{pwr} - P_B. \tag{5.19}$$

The numerically evaluation of (5.18) shows that when one of the signals is higher than almost 10dB in relation to the others, the strongest signal dominates the superposition. In practice, any of these signals, DW, RW, and LW, can dominate the signal superposition depending on deployment and environmental factors. For instance, when high depths are employed ($d_{bg} > 1$m), the RW and LW are strongly attenuated and DW dominates. On the other hand, for shallower depths, LW can easily dominate the superposition. In fact, for longer communication ranges, DW and LW are strongly attenuated and LW always dominates, provided that obstacles at the soil surface do not refract the lateral wave. The prevalence of RW is unique non usual scenario and this scenario will only occur if the radiation pattern and/or obstacles in soil significantly attenuate LW in relation to RW.

Besides, the total attenuation L_{total} given in (5.19), the SSWC model also estimates the bit error rate (BER). The BER of a digital communication system depends on 3 factors [43]:(a) the signal attenuation estimated by the channel model, (b) the digital modulation technique, and (c) the signal to noise ratio (SNR). Assuming 2PSK as a reasonable representative for the modulation in the presented scenario where Mica2 motes are employed in this work [2], the BER is given by [43]:

$$\begin{aligned} SNR = &\quad TX_{pwr} - L_{total} - P_n, \\ BER = &\quad \tfrac{1}{2} erfc(\sqrt{SNR}), \end{aligned} \tag{5.20}$$

where TX_{pwr} is the transmit power level, in dBm, L_{total} is the total estimated attenuation given by (5.19), in dB, P_n is the energy of noise, and $erfc(\cdot)$ is the error function. P_n is usually empirically determined. For instance, in [22], the measured noise strength at 30cm-depth is -103 dBm.

5.7 Model Validation

In this section, the empirical results shown in Section 4 are compared with the predictions from the SSWC to validate the model. The deployment and environmental parameters used in the simulations in this section are exactly the same provided in Section 4, related to the UG2UG testbed site. The determination of the so-called *initial decay* [30] and its relation with the model parameters G_t, G_r, ζ_a, λ_a, ξ_a, ξ_p are discussed in Section 5.7.1. In Section 5.7.2, the validation of the SSWC channel model is realized by the comparison between empirical and simulated results, followed by a discussion.

5.7.1 Initial Decay and Antenna Factors

As explained in Section 3.3, the use of sensor nodes as RF measurements tools deserves special attention in order to preserve the accuracy of the results. Therefore, in this section, the guidelines provided in Section 3.3 are applied and discussed. Moreover, the determination of the antenna factors G_t, G_r, ζ_a, λ_a, ξ_a, ξ_p, parameters of the SSWC model, is discussed in detail. First, these empirical determined values capture the *antenna problem* and are necessary for the accuracy of the model's prediction. Alternatively, one may also develop a theoretical model for each antenna scheme to be eventually employed in WUSNs, which is a topic of discussion in Chapter 6.

To this end, two sets of additional and independent experiments are realized in different sites. The outdoor underground experiments with 433MHz Mica2 [54] sensor nodes are carried out in South Central Agricultural Laboratory (SCAL) of the University of Nebraska-Lincoln, located at Clay Center, NE. The outdoor over-the-air experiments for determination of the initial decay of the sensor nodes are carried out in Schorr Center, at the City Campus of the University of Nebraska-Lincoln, located at Lincoln, NE.

Following the guidelines in Section 3.3, the initial decay for over-the-air experiments with Mica2 motes at 433MHz is found to be 42dB for d_0=10m and +10dBm of transmit power level. This value is not directly plugged in the model, however, it provides a lower bound for the sum of G_t, G_r, ζ_a, λ_a, ξ_a, ξ_p. Considering the fact that the initial decay reflects the overall loss caused the RF circuitry, transmission line, and antenna directivity (positive or negative contribution), it is expected that part of initial decay be a common factor to all waves, DW, RW, and LW. Therefore, for an ideal isotropic antenna, a practical and valid approach is to plug the value of the initial decay as the sum $G_t + G_r$ in the equations (5.5), (5.9), and (5.16), with all the values ζ_a, λ_a, and ξ_a set to 0. For a real scenario, however, the mentioned procedure is just the first step for determining the real values for ζ_a, λ_a, and ξ_a.

The second and third steps for determining the antenna factors involve underground experiments. The second step is the realization of experiments in a scenario where only DW dominates. The third step is the realization of experiments where the superposition of DW, RW, and LW occurs. An additional step, not employed in this work, is the realization of experiments where only LW dominates. This is the case when higher power transceivers, or directional antennas, or a combination of both are employed. An example of this scenario, with the use of eccentrically insulated traveling-waves antennas, is found in [19, 48].

The experiments for the second and third steps are realized using high and low depths, respectively. To this end, an experiment is realized where the burial depth of the sender is fixed at 80cm and the depth of the receiver is varied. In Fig. 5.7, the RSS is shown as a function of the burial depth of the receiver (d^r_{bg}), which varies from 40 to 130cm. Also, the actual inter-node distance, d_a is represented between parentheses. The following parameters are used: horizontal inter-node distance d_h=80cm, the transmit power level TX_{pwr}=−3dBm, fraction of sand S=16%, fraction of clay C=38%,

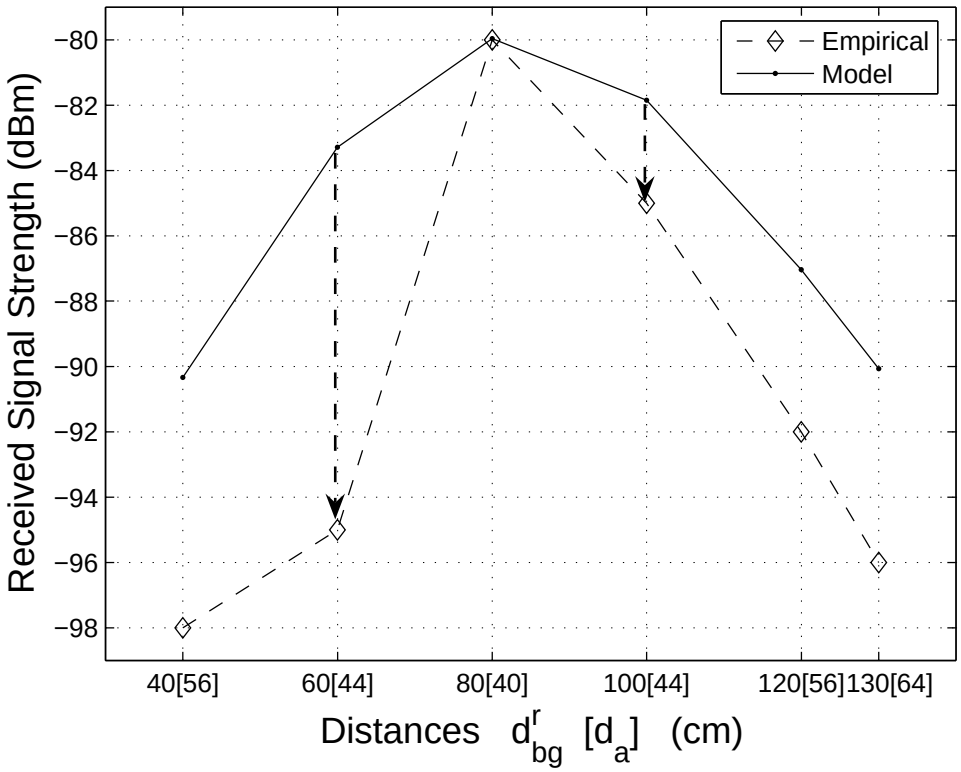

Figure 5.7: Determining the initial decay for the underground setting.

volumetric water content VWC=14.16%, and the remaining parameters are the default values for the experiments in this work. The distances and transmit power level are carefully selected to define a scenario where DW dominates, that is, the soil surface effects are negligible. Observe that the model is adjusted to have a perfect match for the burial depth where both sender and receiver are at the same level (d_{bg}=80cm). A value of ζ_a=35.5dB is found to be the one necessary to achievehave the mentioned matching. This value is relatively close to the over-the-air initial decay of 42dB, previously determined.

The next step is to indirectly obtain information about the antenna directivity which can favor or not the RW and LW. As shown in Fig. 5.7, for distances d_a higher

than 40cm the RSS decreases. However, a significant asymmetry is observed for the same d_a values and different depths of the receiver. For instance, comparing the RSS values for d^r_{bg}=100 and d^r_{bg}=60, a difference of 10dB is observed, although the d_a is the same (44cm). The results suggest a significant deformation of the typical radiation pattern of the default antenna of Mica2 when the mote is buried. Accordingly, another experiment is necessary at shallower depth (third step) to determine the values of the antenna factor for RW and LW, Λ_a and ξ_a, respectively.

The next experiment, representing the third step of this procedure, is realized using 40cm-depth for sender and receiver and varying the horizontal inter-node distance d_h. The transmit power level TX_{pwr}=+10dBm and VWC=9.1% are the only different parameters in relation to the last experiment. In Fig. 5.8, the RSS is shown as a function of the horizontal inter-node distance (d_h), which varies from 10 to 80cm. The values of Λ_a and ξ_a are adjusted to reach the best possible matching for this new experiment scenario, which is represented in Fig. 5.8. The values of Λ_a and ξ_a are found to be 17 and 16 dB, respectively. This assignment of values suggests that DW, for this specific antenna scheme, has a worse performance than RW and LW due to the improved directivity to the up and down direction. A theoretical explanation to this observation is provided in Chapter 6.

After the empirical determination of the antenna factors realized in this section, all the necessary parameters to validate the SSWC channel model are available. The validation of the model is realized in the next section.

5.7.2 Comparison of Empirical Results and the SSWC Model

Simulations based on the SSWC model are realized with the parameters of the experiment site mentioned in Section 4. The results are compared with the empirical results and a fair matching is observed related to the effects of the inter-node distance

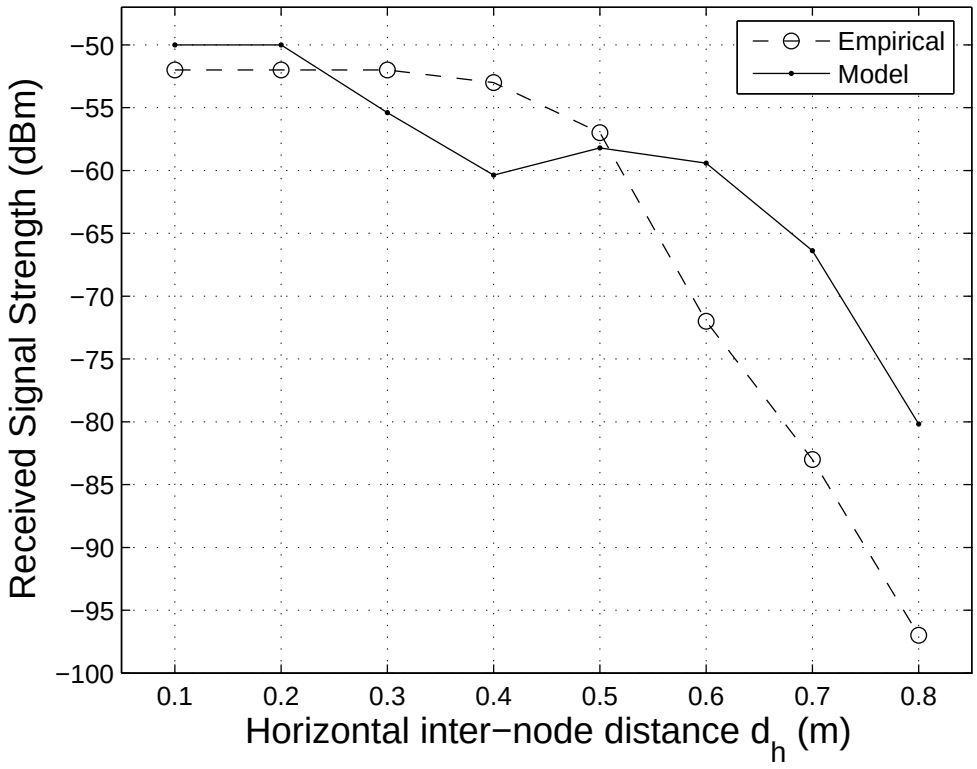

Figure 5.8: Empirical data used to determine the antenna factors (different outdoor site).

and soil moisture (VWC) on the UG2UG communication performance. However, a complete validation of the model is only possible when the LW-dominant scenarios for long-range ranges are empirically exploited. This experimental work is part of the future work discussed in Chapter 7.

In Fig. 5.9, the RSS is shown as a function of the horizontal inter-node distance d_h which varies from 10 to 90cm. Empirical and model results are compared. The burial depth both sender and receiver is d_{bg}=40cm, TX_{pwr}=0dBm, and VWC=14.1%. As shown in Fig. 5.9, there is a good matching from 10 to 40cm and a fair matching in the remaining distances. At the time when the experiments were realized, we did not know about the existence of lateral waves. Therefore, one possible reason to explain the

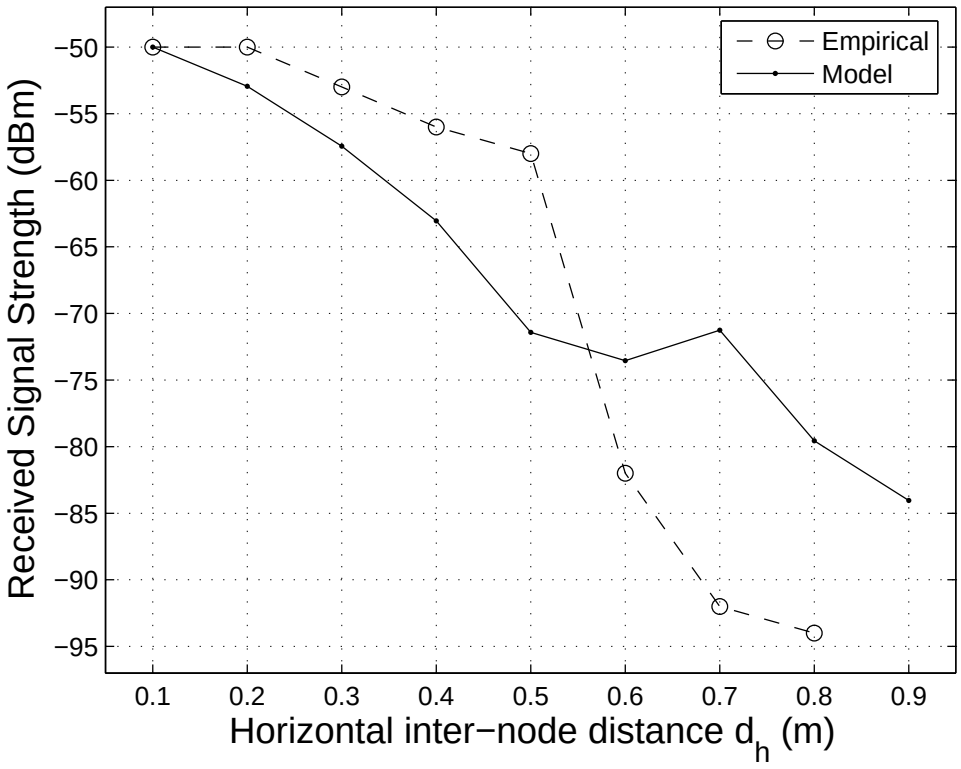

Figure 5.9: Effects of the inter-node distance. Comparison between empirical and simulated results.

mismatch around d_h=70cm, with a difference of 19dB, is the fact that the experiments were realized without a special attention to the existence of obstacles in the air path between the holes where the nodes were located. The constant use of bags containing soil above the holes, as discussed in Chapter 3, can significantly minimize the LW. A second possible cause for the mentioned mismatch is the error due to the inclusion of the antenna factors. However, the overall behavior of the empirical and simulated curves are in good agreement.

An additional comparison is realized to verify the accuracy of the model in relation to the effects of the VWC. In Fig. 5.10, the RSS is shown as a function of the transmit power level for two values of VWC: dry (14.6%) and wet (23.9%) soil. The burial depth

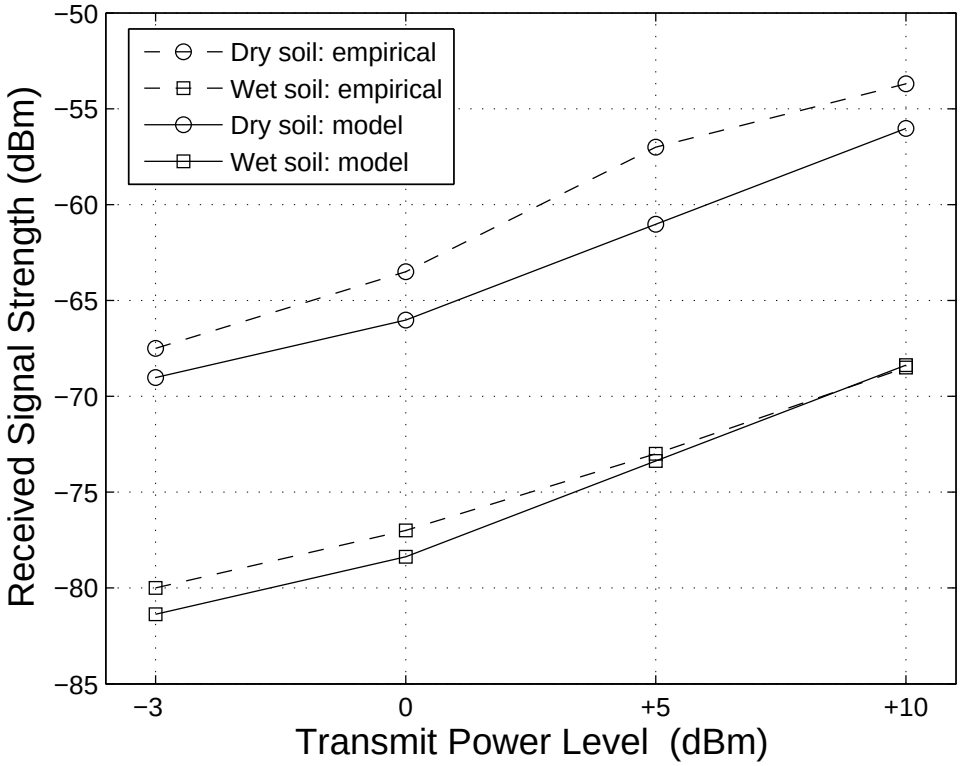

Figure 5.10: Effects of the volumetric water content (VWC). Comparison between empirical and simulated results.

is fixed d^s_{bg}=d^s_{bg}=40cm and also the horizontal inter-node distance d_h=40cm. Empirical and model results are compared and present a good matching, validating the model for this aspect. However, as previously stated, the complete validation of the SSWC model depends on the realization of experiments for long communication ranges using high power transceivers, special antennas to enhance the LW propagation performance, or a combination of both.

Table 5.1: Parameters used in the model evaluation.

Symbol	Description	Value
ρ_b	Bulk density	1.33 g/cm^3
ρ_s	Particle density	2.66 g/cm^3
ρ_s	Particle density	2.66 g/cm^3
S	Sand fraction	35%
C	Clay fraction	30%
-	Silt fraction	35%
m_v	Volumetric water content (VWC)	14.6%
f	Operating frequency	433MHz
-	Antenna polarization	Parallel
d_{bg}	Burial depth	40cm
-	Modulation scheme	2PSK
ζ_a	DW antenna factor	35.5dB
λ_a	RW antenna factor	17.0dB
ξ_a	LW antenna factor	16.0dB
G_t	Antenna gain (sender)	0dB
G_r	Antenna gain (receiver)	0dB
$TXpwr$	Transmit power level	+10dBm
P_n	Energy of noise	-103dBm

5.8 Analytical Results

In this section, the results from the simulations based on the SSWC channel model are presented and discussed. If not specifically informed in the simulation, the parameters for the simulations correspond to the parameters of the testbed for the empirical experiments reported in Section 4. Some of these parameters and additional ones particularly used in the model are listed in Table 5.1.

In Fig. 5.11, the RSS is shown as a function of the inter-node distance where each line corresponds to one signal: DW, RW, LW, and the final combined signal. It is observed that the superposition among signals occurs up to d_h=1.5m. After this inter-node distance, the DW and RW signals quickly decreases in relation to LW. Therefore, from that point, LW becomes the dominant signal and the combined signal is essentially

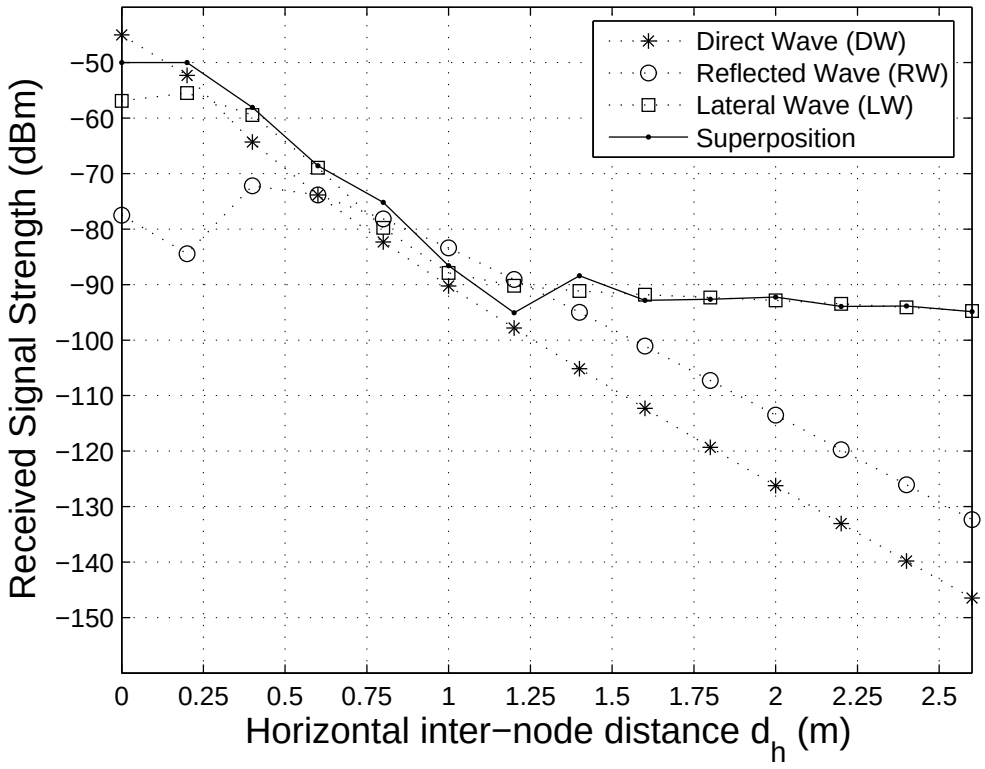

Figure 5.11: Contributions of DW, RW, and LW for the final RSS for different horizontal inter-node distances.

LW. This results indicate that the contribution to DW and RW are limited to small communication ranges. Naturally, for different parameters, such as the TX_pwr, VWC and depth, this range can be extended.

The effects of the horizontal inter-node distance and the burial depth on the RSS and BER are evaluated with simulations based on the SSWC model and the results are shown in Figs. 5.12 and 5.13. In Fig. 5.12, the RSS is shown as a function of d_h and the d_{bg}. For all burial depths, the RSS decreases when d_h increases. The irregular portions of the curves correspond exactly to the inter-node distances of up to 1.5m, as previously highlighted. From that point, the behavior of the curves are strongly monotonic. Another important aspect observed in Fig. 5.12 is the strong effect of the

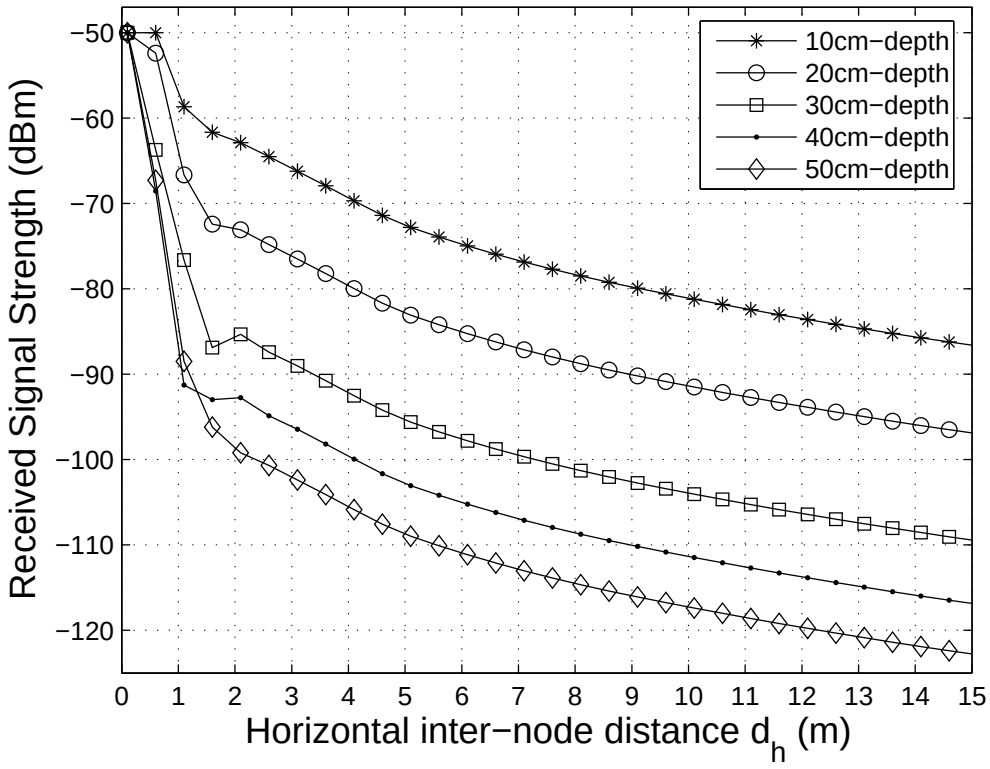

Figure 5.12: Effects of the horizontal inter-node distance and burial depth on the RSS.

burial depth on the RSS. A higher burial depth is always associated with a significant increase in the signal attenuation. For instance, for d_h=2m, the difference on the RSS between the cases where the depths are 10 and 50cm is 37dB. This result highlights the importance of employing the smallest possible burial depth, subject to the restrictions of the WUSN application.

In Fig. 5.13, the BER is shown as a function of d_h and the d_{bg}. The overall results clearly suggest that the BER operational limit for WUSNs is far from $10^{-}3$ or $10^{-}4$ error rates. In practice, error rates from $10^{-}2$ to $10^{-}1$ are expected to be usual for underground links. As already reported in [33], the problem is not related to the channel noise, but to the constant existence of very attenuated signals. Considering

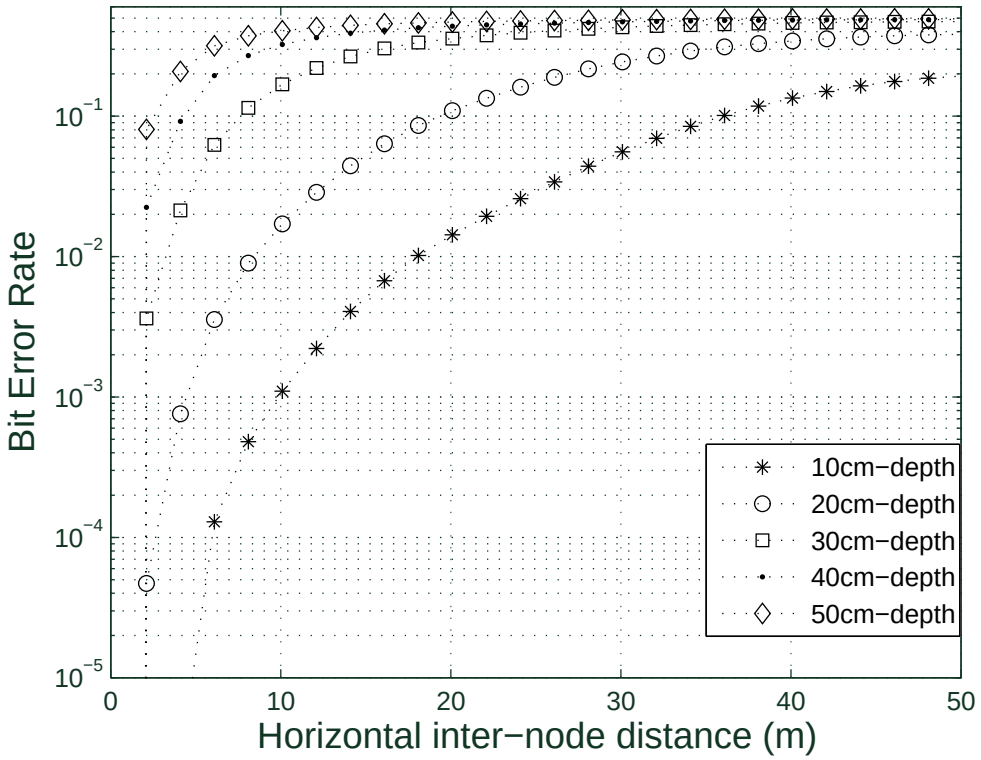

Figure 5.13: Effects of the inter-node distance and burial depth on the BER.

that WUSN applications usually demand small quantity of data and also are very infrequent, such impact of this elevated error rate in WUSNs is mitigated. As shown in Fig. 5.13, in order to achieve a BER <10% for an inter-node distance of 10m, burial depths of 20cm and smaller must be employed.

The effects of the horizontal inter-node distance and the VWC on the RSS and BER are evaluated with simulations based on the SSWC model and the results are shown in Figs. 5.14 and 5.15. In Fig. 5.14, the RSS is shown as a function of d_h and the VWC. For all VWC values, the RSS decreases when d_h increases. The small number of exceptions occur in the irregular portions of the curves due to the intense superposition of signals. Another important aspect observed in Fig. 5.14 is the strong

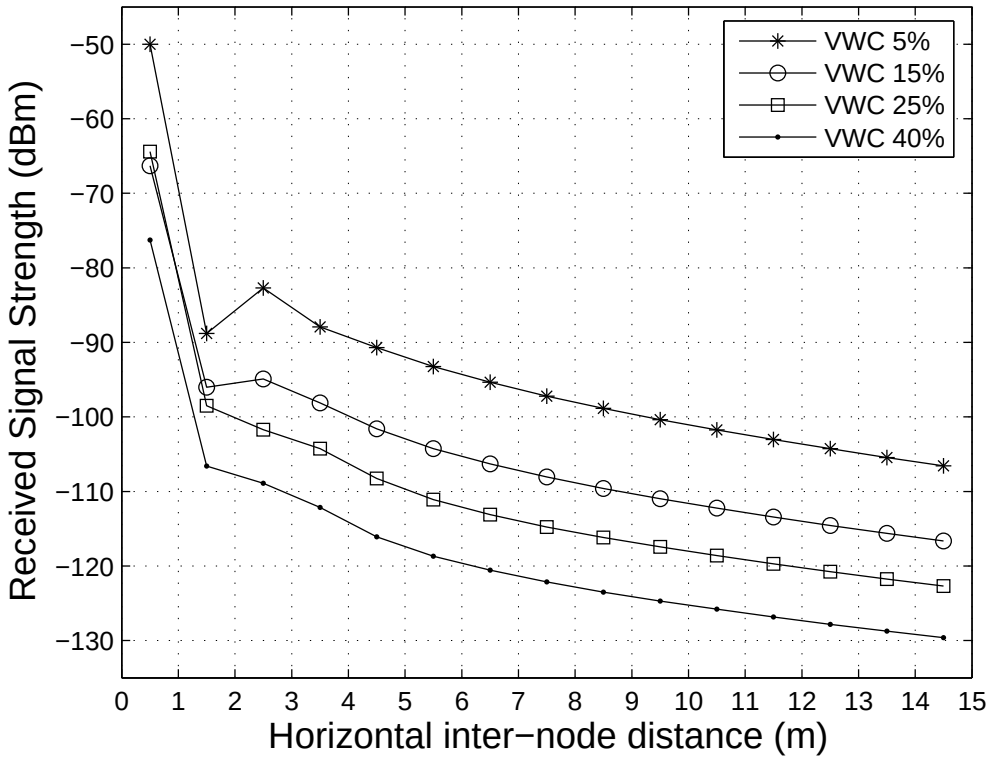

Figure 5.14: Effects of the inter-node distance and VWC on the RSS.

effect of the VWC on the RSS. A soil with higher VWC is generally associated with a significant increase on the signal attenuation. For instance, for d_h=2.5m, the difference in the RSS between a 5%-VWC (very dry soil) and a 40%-VWC (saturated soil) is 22dB. This result highlights the importance of having protocols in WUSNs which are environment-aware. In this way, the communication can be automatically avoided when the VWC reaches a prohibitive value. Alternatively, higher transmit power levels can be automatically configured to face the temporal issue related to the VWC increase [33].

In Fig. 5.15, the BER is shown as a function of d_h and VWC. As already highlighted, the overall results suggest that the usual BER for WUSNs is around 10^{-2} to

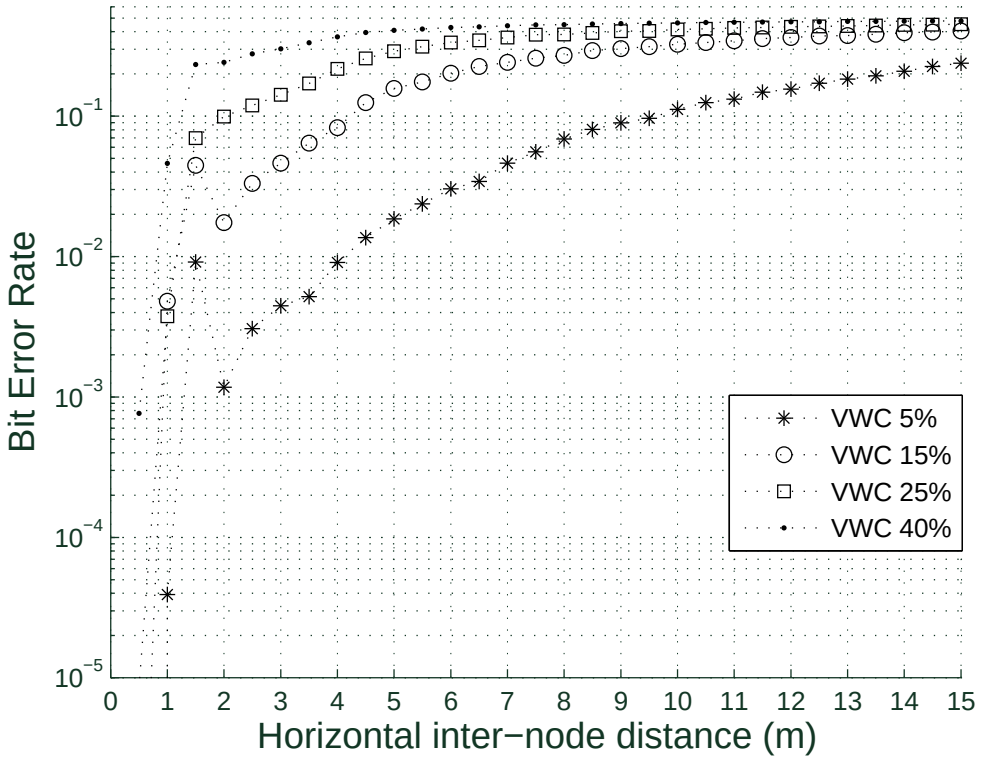

Figure 5.15: Effects of the inter-node distance and burial depth on the BER.

10^{-1}. As shown in Fig. 5.15, for this specific scenario, in order to achieve a BER $< 10\%$ the inter-node distances must be 1m or $9m$, for 40%-VWC and 5%-VWC, respectively. This significant range reduction of almost one order clearly confirms how the VWC impacts the underground communication.

The effects of the horizontal inter-node distance and the frequency on the RSS are evaluated with simulations based on the SSWC model and the results are shown in Fig. 5.16. In Fig. 5.16, the RSS is shown as a function of d_h and the frequency. For all frequencies, the RSS decreases when d_h increases. The irregular portions of the curves occur for inter-node distances of up to 1.5m. Another important aspect observed in Fig. 5.12 is the impact of the frequency on the RSS. Although this impact is not so

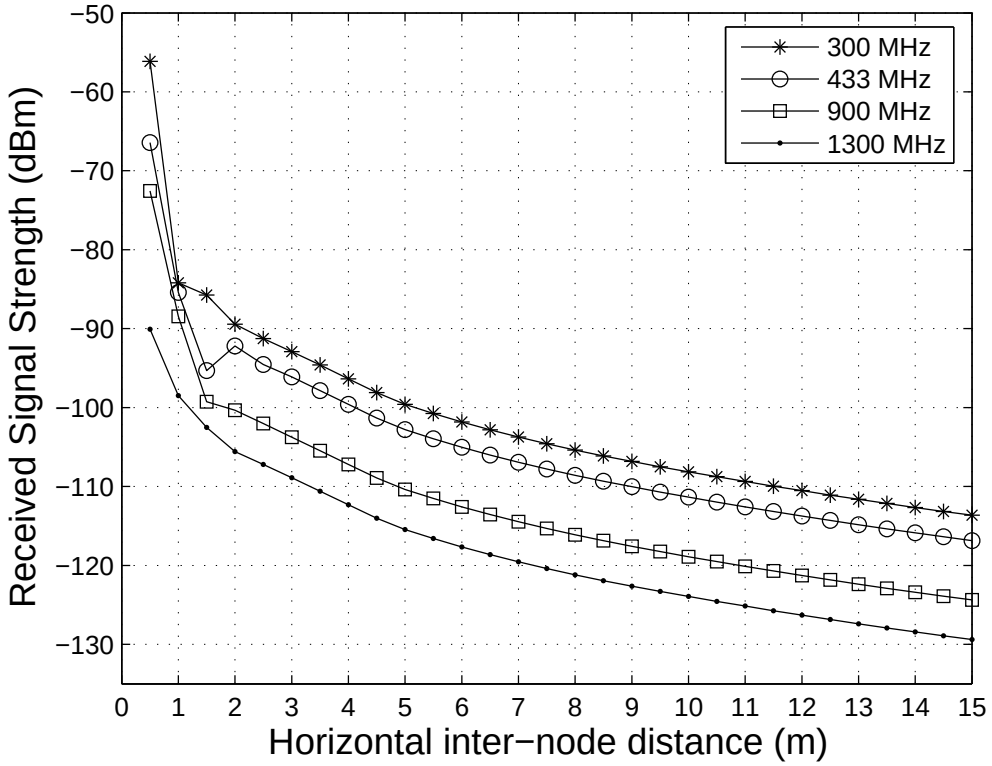

Figure 5.16: Effects of the inter-node distance and frequency on the RSS.

high compared to the burial depth or the VWC, the reduction of the frequency can still represent a way to decrease the attenuation. For instance, for d_h=2m, the difference on the RSS between the cases where the frequencies are 300 and 1300MHz is 16dB, not a negligible value. This result highlights the importance of employing the smallest possible frequency in the 300-1300MHz range, constrained only by communication regulations and practical sizes of antennas.

The effects of the VWC and the soil composition, especially related to the fraction of clay particles, are evaluated with simulations based on the SSWC model and the results are shown in Fig. 5.17. In this simulation, the fractions of sand and silt are exactly the same. In Fig. 5.17, the RSS is shown as a function of fraction of clay

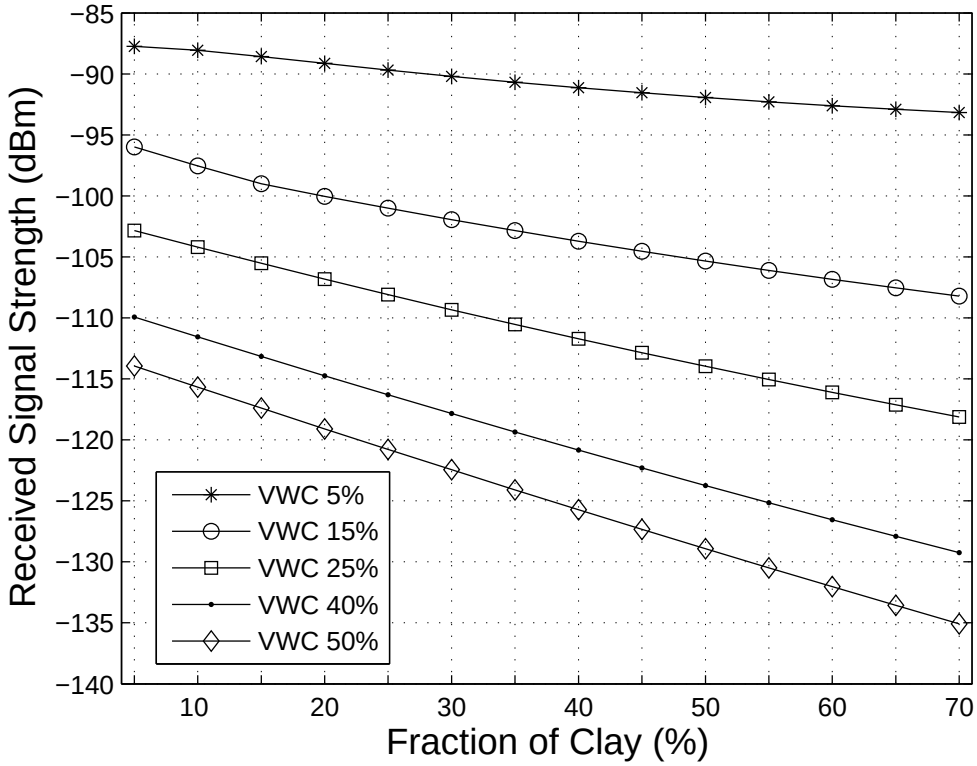

Figure 5.17: Effects of the soil composition and VWC on the RSS.

present in the soil for different values of VWC. One can observe that for the same value of VWC, its impact depends on the soil texture, as previously discussed in Section 5.2. For instance, for the most critical case of 50%-VWC, the difference in RSS between the cases where the fractions of clay are 5% and 70% is 21dB. Therefore, a clayey soil aggravates the VWC problem.

Chapter 6

Research Challenges in WUSNs

As observed from the empirical and analytical results, for the proliferation of WUSNs, a significant number of research challenges must be properly investigated. Currently, there is a trend of the use of centralized networking solutions for WUSNs basically in two types of architectures. The first approach is the use of buried sensors that communicate to an aboveground device with long-range distances [9, 46]. In this kind of architecture, basically the UG2AG links are used. Some current commercial solutions for sports field irrigation use this approach [56]. A second kind of architecture is also mainly based on the use of aboveground devices, but these devices may include mobile aboveground nodes [36]. In [1], such approach is called *Hybrid WUSNs* because over-the-air (ota) links are also used intensively in the overall solution. Besides the ota links, UG2AG and AG2UG links are also intensively used. Therefore, it is clear that the multi-hop networking involving UG2UG links has not been deeply investigated.

In this thesis, a comprehensive analysis of the underground-to-underground communication is performed. Naturally, due to the complexity of the underground environment, this work cannot address all the existing challenges. Nevertheless, the clear identification of the challenges and possible solutions is an important contribution of this work to this research area. To this end, the main identified research challenges are properly discussed.

Antenna problem. The theoretical analysis of any radio communication system is divided into two parts: the propagation problem and the antenna problem. The SSWC model is a model for the propagation problem in the underground settings. If the antenna is a dipole with an ideal isotropic radiation pattern, the use of generic antenna

gains and initial decays may be sufficient for the high accuracy of the model. However, as discussed in Section 5.6, the introduction of distinct antenna factors for DW, RW, and LW, is a valid and practical approach to mitigate the inaccuracy issues due to the existence of non-ideal antennas. It is expected that the empirical investigation with a significant number of VWC values, burial depths, and transmit power levels, would address the antenna problem more accurately.

The inclusion of the antenna problem in the underground channel model is not a simple task to be realized. For instance, consider the complexity related to just one of the components of the antenna problem: the radiation pattern of the antenna and its implied directivity gain. In Figs. 6.1 and 6.2, the effects of the VWC on the radiation pattern of the antenna are shown. First, the a variation of the VWC changes the wavelength of the signal is soil. Because the buried antenna has a fixed length (17.3cm), the ratio between this length and the wavelength also varies, as shown in Fig. 6.1. The presented values are related to the original antenna of Mica2 mote, a 1/4-wave monopole antenna operating at 433MHz. The values for the ratio $antenna's\ length/wavelength$ considers the actual size of the Mica2 antenna multiplied by 2, e.g. 34.6cm, and divided by the wavelength of the signal in the medium, air or soil. The mentioned multiplication by 2 is necessary because, for this scenario, a 1/4 monopole antenna is basically a 1/2 dipole with half of the antenna represented by the ground structure of the device. For comparison, the obvious 1/2 ratio for a half-wave dipole is also shown. When the VWC increases, the wavelength decreases, causing the increase of the ratio $antenna's\ length/wavelength$, as shown in Fig. 6.1.

In Fig. 6.2, the elevation pattern of a vertically oriented linear dipole antenna is shown as a function of its physical length measured in wavelengths units [47]. The variation of ratio $antenna's\ length/wavelength$ shown in Fig. 6.1 are represented as different radiation patterns shown in Fig. Fig. 6.2. When the VWC increases, the

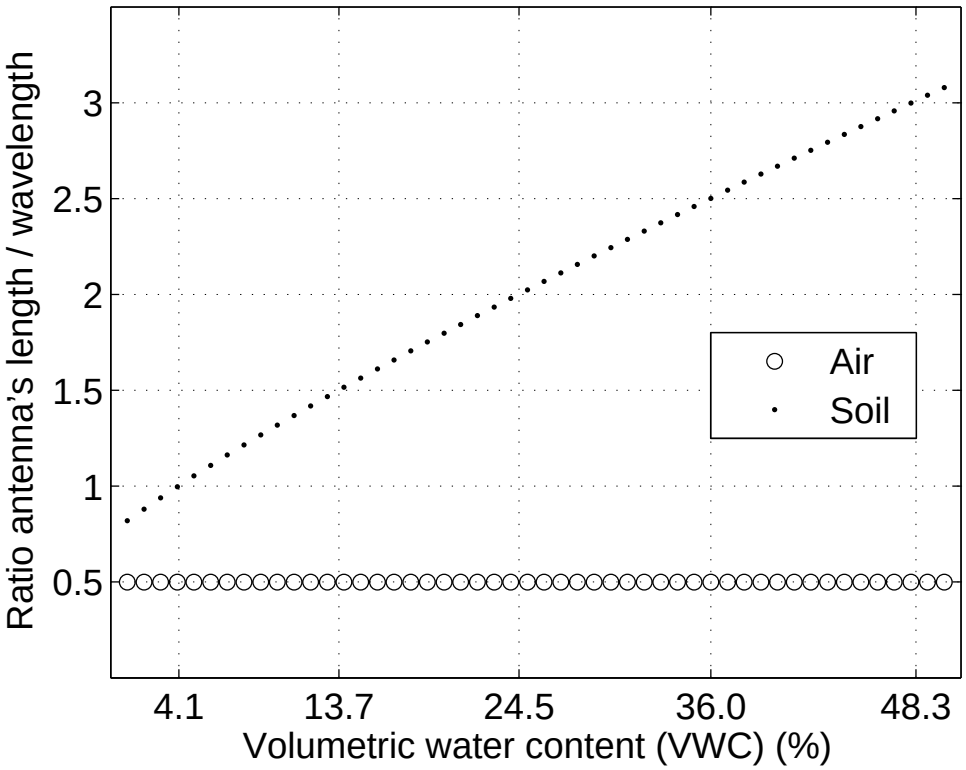

Figure 6.1: Effects of the VWC on the ratio between antenna's length and wavelength of the signal.

ratio *antenna's length/wavelength* also increases, causing non-monotonic behavior of the radiation pattern.

As observed, the antenna problem must be addressed specifically for each kind of antenna and its orientation. However, not all antenna schemes are feasible or provide advantages for underground communication. Therefore, the identification of the specific set of antenna schemes which provide the best communication performance for UG2UG, UG2AG, and AG2UG links must be deeply investigated in order to support a further development of antenna models to be attached to the SSWC channel model. One potential solution suggested by the results in [19, 21, 35, 36, 46, 48] is the use of an

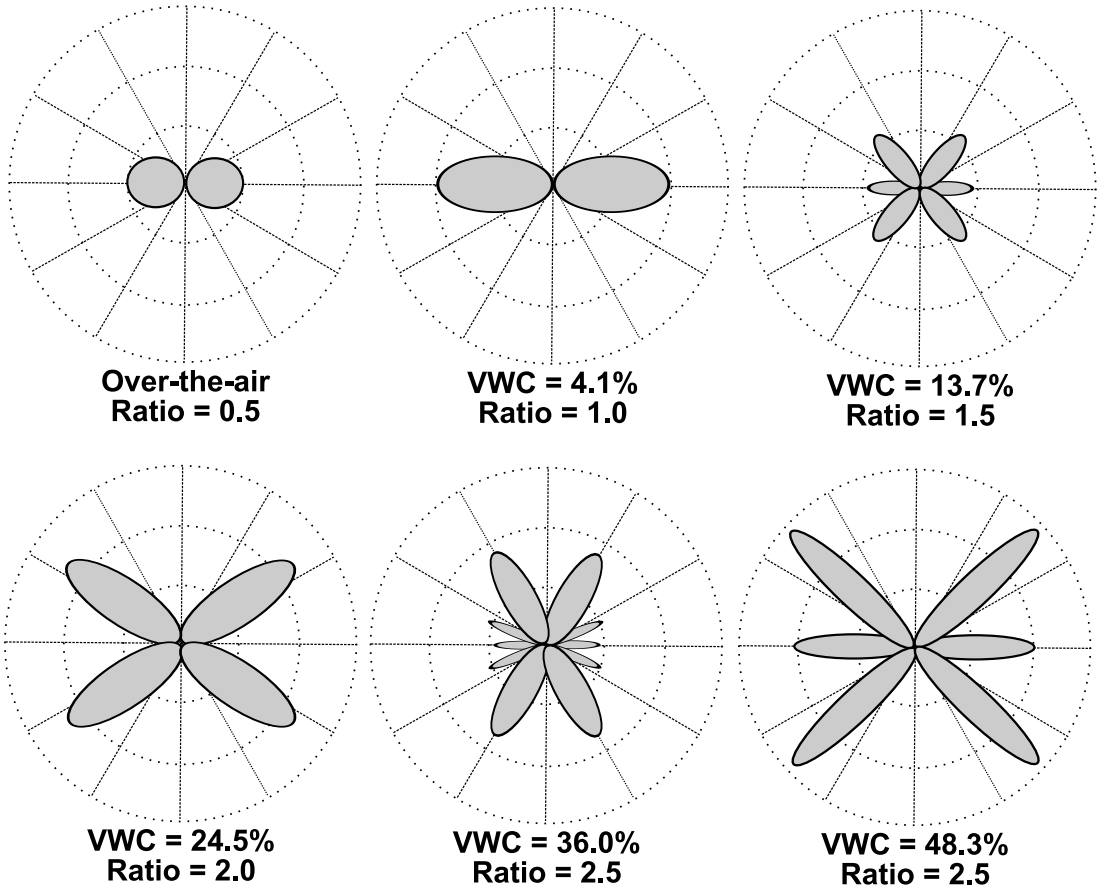

Figure 6.2: Effects of the VWC on the radiation pattern of an one-quarter wave monopole.

ultra-wide band antenna for UG2AG and AG2UG links and a terminated travelling-wave antenna for lateral wave propagation in UG2UG links. Extensive empirical studies must be realized to investigate the feasibility of such solutions for different levels of transmit power and depths.

Burial depth. The theoretical and empirical results show a strong relation between burial depth and communication performance. Therefore, from all the architectural options, the depth is the parameter which can significantly extend the communication range without the use of high-power transceivers. The initial discussion

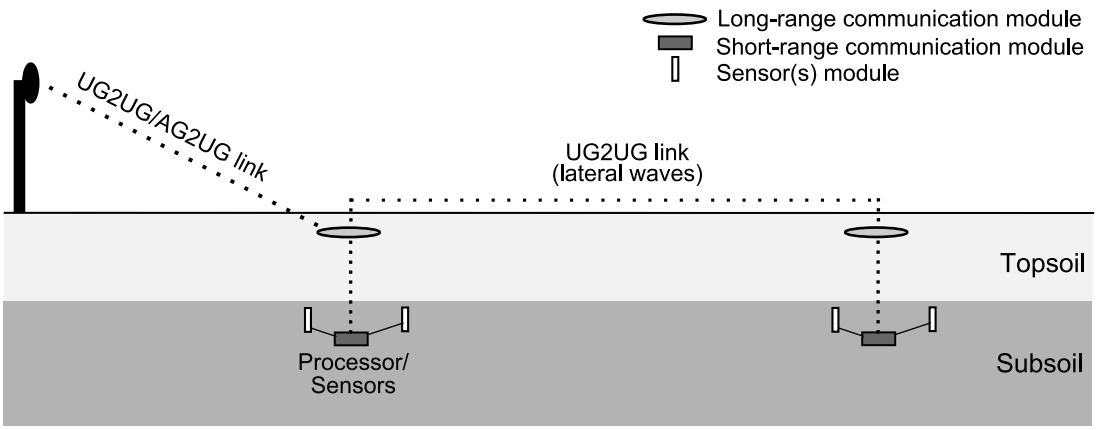

Figure 6.3: A different approach WUSN not yet investigated.

related to this aspect in [33], highlights that many WUSN applications impose a design constraint which cannot be violated. For instance, for a crop irrigation application, it is expected to have the nodes below the topsoil region where plowing and similar activities occur. However, other possibilities had not been investigated so far.

From the viewpoint of the SSWC model, the burial depth parameter is the distance between the center of the antenna and the soil surface. In other words, the burial depths of the sensor(s) and the radio/communication modules do not affect the model, only the antenna's depth. Therefore, the challenge is to achieve a way to deploy antennas at the topsoil that are resilient to mechanical activities at this region. One possibility, for some applications, is the installation and removal of the nodes. Besides the costs of this approach, the real main issue is the installation of the soil *sensors*, an activity that takes time and requires calibration. However, in a scenario where the processor and sensor(s) modules are permanently installed at the subsoil, it is still possible to easily install and remove long-range communication modules buried very close to the soil surface, as illustrated in Fig. 6.3. In this case, the sensors are permanently installed and the only module that is *removable* is the long-range communication module, fortunately

the module which consumes more energy. Naturally, this module would require 2 independent transceivers, one for short-range communication with the deeply installed sensor node and other transceiver with the communication with aboveground devices and other long-range modules. The best burial depth for this long-range module, including d_{bg}=0, must be also investigated.

Housing for the sensor nodes. Some WUSN applications do not require high depths, but the concealment of the sensor nodes is the main issue. One possibility is the use of plastic boxes where the processor/communication module and also the antenna are installed. However, this practical way of the deployment was not properly investigated related to UG2UG communication. We realized preliminary experiments and observed a completely different behavior on the communication performance. Therefore, the stratified media scenario, e.g. air/soil/air, must be investigated for UG2UG links in WUSNs.

Direct and reflected waves. The results presented in this work highlight the lateral waves as the feasible low-power solution for long-range UG2UG communication. Based on this, the SSWC model could be simplified to the LW model. However, such simplification is not desirable for many reasons. For instance, in Fig. 6.3, the short-range communication mainly is mainly based on DW. Also, for the development of UG2AG/AG2UG channel models, part of the SSWC model can be promptly used. Finally, the use of directional antennas and high-power transceivers can increase the inter-node distance where DW, RW, and also LW will be combined. In this scenario, the complete SSWC can be used to model the communication performance.

Lateral waves. An intensive theoretical and empirical investigations related to the lateral wave propagation for UG2UG links in WUSNs must be realized. The results in this work is highly constrained by the low-power transceiver and antennas

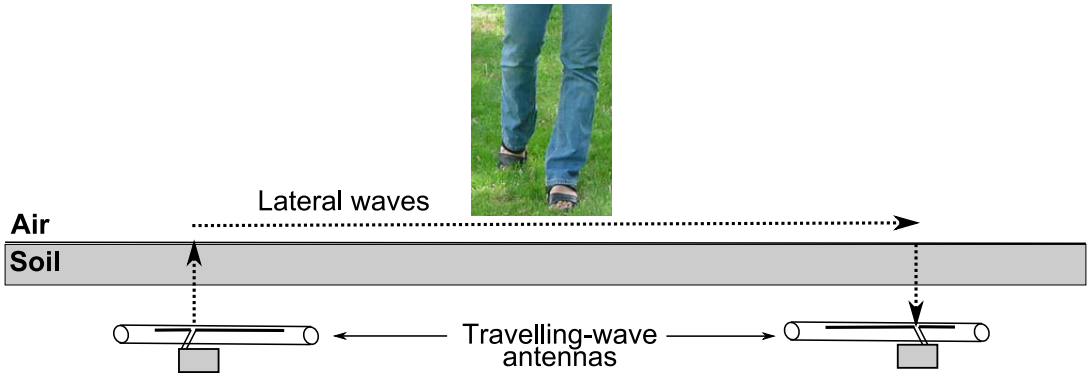

Figure 6.4: Lateral waves can potentially be applied in security applications for WUSNs.

employed. To achieve long-range communication ranges, special antennas and high-power transceivers may be employed. In this way, a complete validation of the SSWC channel model will be possible.

One promising line of investigation is the use of terminated travelling-wave antennas which were previously tested for the underground communication [19, 21, 48]. Therefore, these studies must be extended to typical WUSN scenarios, with different set of deployment parameters. Finally, the power budgets related to the centralized one-hop UG2AG/AG2UG and multi-hop LW/UG2UG approaches can be properly investigated providing extremely important guidelines for the development of WUSNs.

Another aspect to be investigated related to the use of lateral waves for UG2UG links is the effect of obstacles, water, and snow on the soil surface. These aspects are not covered in the this work and is also very important to complement the SSWC model. Surprisingly, this investigation can be strategically used for final application purposed. For instance, for security applications, such as border patrol, the lateral waves can be used to detect intruders. The detecting process in this case is based on perturbations of the wireless channel, as illustrated in Fig. 6.4.

UG2AG and AG2UG channel models. Despites the fact that the SSWC channel is essential for WUSNs, it is only part of the overall communication model for WUSNs. To this end, comprehensive channel models for the UG2AG and AG2UG links must also be developed. As previously mentioned in Section 2.4, the current related models present limitations for their applicability in generic WUSNs. An initial empirical investigation is realized in [35, 36], however a deeper theoretical analysis is not reported.

Besides the channel model for UG2AG and AG2UG links, the power budget of such solutions must be properly investigated. With the promising application of the lateral waves propagation to UG2UG links, comparison between the power budgets of centralized one-hop UG2AG/AG2UG and multi-hop LW/UG2UG approaches are expected. Naturally, the investigations of the options for UG2AG and AG2UG links will also be oriented in function of the UG2UG achievements.

Chapter 7

Conclusions

The characteristics of the wireless channel for the underground-to-underground communication in Wireless Underground Sensor Networks (WUSNs) are discussed based on an extensive empirical study realized in a large agriculture field. According to the empirical results, the Soil Subsurface Wireless Communication (SSWC) channel model is developed. The model has a comprehensive set of features and estimates the total signal attenuation and bit error rate (BER) based on environmental parameters, such as the soil texture and moisture, and on deployment aspects, such as the frequency and the depth of the sensor nodes.

The SSWC channel model considers the potential contribution of three distinct waves which propagate using different paths. The direct wave propagates directly to the receiver. The reflected wave reflects at the soil surface before reaching the receiver. Finally, the lateral wave follows a quasi-vertical path in the direction of the surface (up), propagates over the air very close to the soil surface and returns to soil (down), eventually reaching the receiver. The three waves have different characteristics and, therefore, distinct models are developed for each wave. In addition to these models, the SSWC also has the Dielectric Soil Properties model. This component estimates the soil permittivity and conductivity based on the operating frequency and soil parameters. These parameters are used by the three mentioned wave models to estimate the signal attenuation for each kind of wave. Finally, the last component of the SSWC model, the Signal Superposition model, estimates the overall contributions of the three waves to compose the signal perceived by the receiver.

The empirical results are compared with the results from the model and a good agreement is observed. Also, the main characteristics of the underground channel,

previously confirmed with the experimental work, are also captured by the model. The analytical results show that the soil moisture and the burial depth are the most critical parameters. For instance, an additional 37dB of attenuation occurs when the depth changes from 10 to 50cm. Such result confirms that low-power underground communication is only feasible when the sensor nodes are buried in the soil subsurface region, which is defined as the top few meters of the soil. More specifically, for low-power operation, the burial depth must be smaller than 50cm.

The soil moisture, measured by the volumetric water content (VWC), also has a stronger impact on the communication performance. However, the degree of this impact is also associated with the fraction of clay particles in soil. Comparing the simulated results between a clayey soil with 40%-VWC (worst scenario) and a sandy soil with 5%-VWC (best scenario), an additional 66dB of attenuation is observed. This result shows that networking protocols for WUSNs must be developed considering the dynamic adaptation according to VWC variations.

The operating frequency is another parameter which significantly affects the communication performance. For instance, the analytical results show an additional 16dB of attenuation when the frequency changes from 300MHz to 1.3GHz. These results justify the employment of low frequencies for WUSNs. However, due to practical issues related to the size of the antennas, frequencies below 300MHz are usually not acceptable.

The SSWC channel model is fundamental for the development of cross-layer communication solutions for WUSNs and for the development of underground-to-aboveground (UG2AG) and aboveground-to-underground (AG2UG) channel models for WUSNs. However, for the proliferation of WUSNs, several research challenges must be properly investigated. In this thesis, some of these challenges are highlighted and novel design aspects are proposed for deeper investigation.

The most important research challenge is the realization of long-range experiments with the lateral waves propagation. Based on the analytical simulations with the SSWC model, the lateral waves promise to significantly enhance the communication range without sacrificing energy. This analytical result agrees with the fact that, for long-range distances, the propagation path of lateral waves is mainly formed by the over-the-air path. However, the impact of the existence of irregularities, water, ice, and obstacles at the soil surface has not been investigated so far. Moreover, directional antennas designed for lateral waves propagation will significantly enhance the communication performance and this research topic must be investigated specifically considering the typical WUSN scenarios.

The realization of low-power and long-range ($>$ 10m) multi-hop underground-to-underground (UG2UG) communication will eventually intersect the current trend in WUSNs of using centralized one-hop solutions involving aboveground devices and UG2AG/AG2UG links. Therefore, the major research topic in WUSN will be eventually the design of networks that efficiently minimize the energy costs and maximize the communication performance in WUSNs by mixing both approaches.

Bibliography

[1] I. F. Akyildiz and E. P. Stuntebeck. Wireless underground sensor networks: Research challenges. *Ad Hoc Networks Journal (Elsevier)*, 4:669–686, July 2006.

[2] I. F. Akyildiz, Z. Sun, and M. C. Vuran. Signal propagation techniques for wireless underground communication networks. *Physical Communication Journal (Elsevier)*, 2(3):167–183, Sept. 2009.

[3] C. Alippi and G. Vanini. Wireless sensor networks and radio localization: a metrological analysis of the mica2 received signal strength indicator. In *Proc. IEEE Workshop on Embedded Networked Sensors*, Florida, USA, November 2004.

[4] L.K. Bandyopadhyay, S. K. Chaulya, and P. K. Mishra. *Wireless Communication in Underground Mines: RFID-based Sensor Networking*. Springer, 2010.

[5] A. Banos. *Dipole Radiation in the Presence of a Conducting Half-Space*. Pergamon Press, 1966.

[6] J. Behari. *Microwave Dielectric Behavior of Wet Soils*. Springer, 2005.

[7] A. D. Boardman, editor. *Electromagnetic Surface Modes*. John Wiley & Sons, 1982.

[8] H. R. Bogena, J. A. Huisman, C. Oberdorster, and H. Vereecken. Evaluation of a low-cost soil water content sensor for wireless network applications. *Journal of Hydrology*, 344(1-2):32–42, September 2007.

[9] H. R. Bogena, J. A. Huismana, H. Meierb, U. Rosenbauma, and A. Weuthena. Hybrid wireless underground sensor networks: Quantification of signal attenuation in soil. *Vadose Zone Journal*, 8(3):755–761, August 2009.

[10] L. M. Brekhovskikh. *Waves in Layered Media*. Academic Press, New York, 2 edition, 1980.

[11] A. Chehri, P. Fortier, and P. M. Tardif. Application of ad-hoc sensor networks for localization in underground mines. In *Proc. Wireless and Microwave Technology Conference 2006 (WAMICON '06)*, Florida, USA, December 2006.

[12] A. Chehri, P. Fortier, and P. M. Tardif. Security monitoring using wireless sensor networks. In *Proc. Communication Networks and Services Research, 2007 - CNSR '07*, New Brunswick, Canada, May 2007.

[13] A. Chukhlantsev. *Microwave Radiometry of Vegetation Canopies*. Springer, 2006.

[14] D. J. Daniels. Surface-penetrating radar. *Communication Engineering Journal*, 8(4):165–182, August 1996.

[15] N. Elkmann, H. Althoff, S. Kutzner, T. Stuerze, J. Saenz, and B. Reimann. Development of fully automatic inspection systems for large underground concrete pipes partially filled with wastewater. In *Proc. 2007 IEEE International Conference on Robotics and Automation*, volume 1, pages 130–135, Roma, Italy, April 2007.

[16] H. D. Foth. *Fundamentals of Soil Science*. John Wiley & Sons, 8 edition, 1990.

[17] W. H. Gardner. *Water Content, in: Klute, A. (Ed.), Methods of Soil Analysis - Part 1.* American Society of Agronomy - Soil Science Society of America, Madison, WI, 2 edition, 1986. Physical and Mineralogical Methods.

[18] T. R. H. Holmes. Measuring surface soil parameters using passive microwave remote sensing. the elbara field campaign 2003. Master's thesis, Vrije Universiteit Amsterdam, 2003.

[19] S. Huang. An antenna for underground radio communication. Master's thesis, Univeristy of Houston, 1979.

[20] G. A. Kennedy and P. J. Foster. High resilience networks and microwave propagation in underground mines. In *Proc. European Conference on Wireless Technology 2006*, Manchester, UK, September 2006.

[21] R. King, G. S. Smith, M. Owens, and T. T. Wu. *Antennas in Matter - Fundamentals, Theory, and Applications*. MIT Press, 1981.

[22] L. Li, M. C. Vuran, and I. F. Akyildiz. Characteristics of underground channel for wireless underground sensor networks. In *Proc. Med-Hoc-Net 07*, Corfu, Greece, June 2007.

[23] K. Martinez, R. Ong, and J. Hart. Glacsweb, a sensor network for hostile environments. In *IEEE SECON '04*, pages 81–87, Santa Clara, CA, October 2004.

[24] J. F. Mastarone and W. J. Chappell. Urban sensor networking using thick slots in manhole covers. In *Proc. Antennas and Propagation Society International Symposium 2006*, New Mexico, USA, July 2006.

[25] T.W. Miller, B. Borchers, J. M. H. Hendrickx, S. Hong, L. W. Dekker, and C. J. Ritsema. Effects of soil physical properties on gpr for landmine detection. In *Fifth International Symposium on Technology and the Mine Problem*, Monterey, CA, April 2002.

[26] J. Paek, K. Chintalapudi, R. Govindan, and S. Masri. A wireless sensor network for structural health monitoring: Performance and experience. In *Proc. IEEE Workshop on Embedded Networked Sensors (EmNetS-II)*, Sydney, Australia, May 2005.

[27] C. Park, Q. Xie, P. Chou, and M. Shinozuka. Duranode: Wireless networked sensor for structural health monitoring. In *Proc. IEEE Sensors 2005*, pages 277–280, Irvine, CA, November 2005.

[28] N. Peplinski, F. Ulaby, and M. Dobson. Dielectric properties of soils in the 0.3-1.3-ghz range. *IEEE Trans. Geoscience and Remote Sensing*, 33(3):803–807, May 1995.

[29] J. Powell and A. Chandrakasan. Differential and single ended elliptical antennas for 3.1-10.6 Ghz ultra wideband communication. In *Antennas and Propagation Society International Symposium*, volume 2, Sendai, Japan, August 2004.

[30] T. S. Rappaport. *Wireless Communications - Principles and Practice*. Prentice Hall PTR, 1 edition, 1996.

[31] C. J. Ritsema, H. Kuipers, L. Kleiboer, E. Elsen, K. Oostindie, J. G. Wesseling, J. Wolthuis, and P. Havinga. A new wireless underground network system for continuous monitoring of soil water contents. *Water Resources Research Journal*, 45:1–9, May 2009.

[32] A. Sheth, K. Tejaswi, P. Mehta, C. Parekh, R. Bansal, S. Merchant, T. Singh, U.B.Desai, C.A.Thekkath, and K. Toyama. Senslide: a sensor network based landslide prediction system. In *Proc. SenSys'05*, pages 280–281, San Diego, CA, November 2005.

[33] A. R. Silva and M. C. Vuran. Empirical evaluation of wireless underground-to-underground communication in wireless underground sensor networks. In *Proc. IEEE DCOSS '09*, Marina Del Rey, CA, June 2009.

[34] A. R. Silva and M. C. Vuran. Channel contention in wireless underground sensor networks. In *to appear in Proc. III Intl. Conf. on Wireless Communications in Underground and Confined Areas (ICWCUCA' 10)*, Val-dOr, Canada, August 2010.

[35] A. R. Silva and M. C. Vuran. Communication with aboveground devices in wireless underground sensor networks: An empirical study. In *to appear in Proc. IEEE ICC '10*, Cape Town, South Africa, May 2010.

[36] A. R. Silva and M. C. Vuran. CPS^2: Integration of center pivot systems with wireless underground sensor networks for autonomous precision agriculture. In *to appear in Proc. ACM/IEEE First International Conference on Cyber-Physical Systems (ICCPS' 10)*, Stockholm, Sweden, April 2010.

[37] A. R. Silva and M. C. Vuran. Development of a Testbed for Wireless Underground Sensor Networks. *EURASIP Journal on Wireless Communications and Networking*, 2010.

[38] A. Sommerfeld. Uber die ausbreitung der wellen in der drahtlosen telegraphie ((about the propagation of waves in wireless telegraphy)). *Ann. Physik*, 28:665–737, 1909.

[39] A. Sommerfeld. Uber die ausbreitung der wellen in der drahtlosen telegraphie (about the propagation of waves in wireless telegraphy). *Ann. Physik*, 81:1135–1153, 1926.

[40] E. Stuntebeck, D. Pompili, and T. Melodia. Underground wireless sensor networks using commodity terrestrial motes. In *poster presentation at IEEE SECON 2006*, Reston, USA, September 2006.

[41] C. T. Tai. Radiation of a Hertzian dipole immersed in a dissipative medium. Cruft Laboratory Technical Report 21, Harvard University, 1947.

[42] C. T. Tai and Robert Collin. Radiation of a hertzian dipole immersed in a dissipative medium. *IEEE Transactions on Antennas and Propagation*, 48(10):1501–1506, October 2000.

[43] Herbert Taub. *Principles of communication systems*. McGraw-Hill, New York, 1970.

[44] M. J. Tiusanen. Attenuation of a Soil Scout radio signal. *Biosystems Engineering*, 90(2):127–133, January 2005.

[45] M. J. Tiusanen. Wideband antenna for underground Soil Scout transmission. *IEEE Antennas and Wireless Propagation Letters*, 5(1):517–519, December 2006.

[46] M. J. Tiusanen. Wireless Soil Scout prototype radio signal reception compared to the attenuation model. *Precision Agriculture*, 10(5):372–381, November 2008.

[47] F. T. Ulaby. *Fundamentals of Applied Electromagnetics*. Pearson Prentice Hall, 5 edition, 2007.

[48] F. Vaziri, S. C. F. Huang, S. A. Long, and L. C. Shen. Measurement of the radiated fields of a buried antenna at vhf. *Radio Science*, 15(4):743–747, August 1980.

[49] J. Wait and J. Fuller. On radio propagation through earth: Antennas and propagation. *IEEE Trans. Antennas and Propagation*, 19(6):796–798, November 1971.

[50] T. P. Weldon and A. Y. Rathore. Wave propagation model and simulations for landmine detection. Technical report, Univ. of N. Carolina at Charlotte, 1999.

[51] G. Werner-Allen, K. Lorincz, M. Welsh, O. Marcillo, J. Johnson, M. Ruiz, and J. Lees. Deploying a wireless sensor network on an active volcano. *IEEE Internet Computing*, 10(2):18–25, 2006.

[52] N. Xu, S. Rangalwala, K. Chintalapudi, D. Ganeshan, A. Broad, R. Govindan, and D. Estrin. A wireless sensor network for structural monitoring. In *Proc. ACM SenSys '04*, Baltimore, MD, November 2004.

[53] M. Zuniga and B. Krishnamachari. Analyzing the transitional region in low power wireless links. In *Proc. IEEE SECON '04*, Santa Clara, CA, October 2004.

[54] Crossbow Mica2, Micaz, and IRIS motes. http://www.xbow.com.

[55] Decagon devices. EC-5 sensor. http://www.decagon.com /ag_research/soil/ec5.php.

[56] Turf Guard Wireless Soil Monitoring System. http://www.turfguard.net/index.php.

[57] Ward Laboratories. http://wardlab.com.